Reconstitution and localisation studies of a type IV secretion system

Reconstitution and Localisation Studies of a Type IV Secretion System

*Thesis submitted to the **University of London** for the degree of **Doctor of Philosophy**, 2013/14*

Sarah Connery

Department of Biological Sciences, Birkbeck College, London

Declaration

I, Sarah Connery, hereby declare that the work presented in this thesis is my own. Where information has been derived from other sources, I confirm that this has been indicated in the thesis.

_____

Sarah Connery, September 2013

"In science, we must be interested in things, not in persons."

Marie Curie

Abstract

Bacterial conjugation is the transport of a DNA molecule from a donor cell to a recipient. Since bacteria do not reproduce sexually, conjugation is a major contributor to prokaryotic genome plasticity and the spread of antibiotic resistance genes.

A Type IV Secretion System (T4SS) mediates the DNA transport during conjugation. T4SSs are large macromolecular assemblies embedded in the membrane of bacteria, and are associated with pathogenesis, bacterial conjugation and natural transformation. They are a versatile family of secretion systems, who transport a wide variety of substrates, such as virulence proteins, DNA—protein complexes as well as only DNA.

Here, we investigate the minimal requirements for conjugation, and the T4SS's localisation within the cell. We show that the conjugative T4SS of the plasmid pR388 requires a total of 14 genes to efficiently mobilise DNA from a donor cell to a recipient cell and is arranged around the cell circumfence in a helical array.

Our study of two reconstituted and fully functional conjugative T4SSs opens doors for further structural and functional analysis.

Table of Contents

Acknowledgements

First and foremost, I would like to thank my supervisor Professor Gabriel Waksman, whose support and encouragement got me through the endeavour of my PhD. He always believed in me, even after yet another conjugation assay with no transconjugants. Further, I would like to thank him for giving me the amazing opportunity to work in his lab, and for helping me on the way to become and independent scientist. I would also like to thank the members of my Thesis Committee, my second supervisor Dr Maya Topf and Professor Helen Saibil, for reading endless reposts about cloning and their support and advice during our meetings.

My thanks also go to Dr Richard Hayward, Dr Maud Dumoux and Susan Andrew who supported me with my fluorescence microscopy experiments. Your support was invaluable and I couldn't have done that extra step without you.

Very special thanks go to my fantastic lab mates. You are a crazy and fantastic bunch and I had a whale of a time with you! Especially, I would like to thank Dr Harry Low for teaching me so much in the lab, as well as in project design. Also, I would like to thank Dr Adam Redzej, Dr Danai Papaioannou and Sofie Vonlanthen for endless conversations about my life and my project, their honest opinions and for always having an ear for my complaints and worries.

My friends Vanessa Krug, Rebecca Sulzmann, Kristin Basjmeleh, Aylin Türer-Strzelczyk, Zlata Bayar and Diana Conners have made the most wonderful

impact on my life and I want to thank them for being my second family, even though they are far away.

My family are most important to me, and I would like to thank my parents for their love and support during my education and my choices in life. My sister, I would like to thank for being my best friend. My grandma, I want to thank for being my great inspiration. Her life experience is precious to me.

The person who has walked through my PhD with me every step of the way and supported my every single day of it, and therefore deserves my utmost gratitude, is my wonderful husband Andrew Connery. Every day, I feel so lucky to have you in my life and this is why I would like to dedicate this work to you.

To my wonderful husband

Abbreviations

Å	Ångström
ADP	Adenosine Diphosphate
Amp	Ampicillin
approx.	Approximately
ATP	Adenosine Triphosphate
ATPase	Adenosine Triphosphatase
bp	Base Pair
Cam	Chloramphenicol
D	Donors
Da	Dalton
DIC	Differential Interference Contrast
DNA	Deoxyribonucleic Acid
DR	Direct Repeat
ds	Double Stranded
e.g.	Example Given
EDTA	Ethylenediamine Trifluoroacetic Acid
EM	Electron Microscopy
et al.	Et Alii (and others)
g	Gram
h	Hour
i.e.	In Effect

ICE	Integrative and Conjugative Element
Inc	Incompatibility Group
IPTG	Isopropyl Thiogalactoside
IR	Inverted Repeat
k	Kilo
Kan	Kanamycin
kbp	Kilo Base Pairs
kDa	Kilodalton
KoriT	pKM101 *orign-of-transfer* sequence
l	Liter
m	Minute
M	Molar (mol/liter)
m	Milli
mDa	Megadalton
mRNA	Messenger Ribonucleic Acid
n	Nano
n.d.	Not Determined
Nal	Nalidixic Acid
nr.	Number
nt	Nucleotide
NTP	Nucleotide Triphosphate
oriT	*Origin-of-transfer*
PCR	Polymerase Chain Reaction
R	Recipients

RoriT	pR388 *origin-of-transfer* sequence
rpm	Revolutions Per Minute
RT	Room Temperature
s	Second
SDS-PAGE	Sodium Dodecyl Sulfate Polyacrylamide Gel Electrophoresis
Spec	Spectinomycin
ss	Single Stranded
T-strand	Transfer Strand
T3SS	Type III Secretion System
T4CP	Type IV Secretion System Coupling Protein
T4SS	Type IV Secretion System
TC	Transconjugants
Tyr	Tyrosine
V	Voltage
xg	Times Gravitational Force
μ	Micro

Table of Figures

Table of Tables

1 Introduction on Bacterial Conjugation

Bacterial conjugation was first described by Joshua Lederberg and Edward L Tatum in 1953 as bacterial sexual reproduction (Lederberg & Tatum, 1953); however, the term describes the transfer process of deoxyribonucleic acid (DNA) from a bacterial donor cell to a recipient cell. Conjugation systems mediate DNA transfer between cells of the same species (Lawley et al., 2003); however, it has also been shown to occur between cells of different species and even into eukaryotic cells (Kienesberger et al., 2011; Fernández-González et al., 2011). In this context, conjugation is implied to contribute significantly to horizontal gene transfer and bacterial genome plasticity. Particularly the rise of multidrug resistant bacteria generated by the spread of resistance genes to commonly used antibiotics via conjugation machineries poses a major threat to human health (Douard et al., 2010).

1.1 Overview of the process of bacterial conjugation

The process of conjugation can be divided into three distinct biochemical processes: (i) substrate processing, (ii) substrate recruitment and (iii) substrate transfer. The nature of substrate processing is a highly conserved biochemical process among all types of conjugative elements. The conjugative DNA is recognised at a specific sequence termed *origin-of-transfer* (*oriT*), and enzymatically converted from a supercoiled state to a “relaxed” open–circular state. The enzyme catalysing this process is termed relaxase. The relaxase nicks

the DNA at a specific nic-site within *oriT* and remains covalently bound to the transfer (T)-strand of the DNA throughout the translocation. Varying auxiliary proteins may be necessary for efficient recognition of *oriT*, and together with the relaxase, the complex formed is termed relaxosome. A coupling protein (T4CP) then recruits the relaxase–DNA complex to a Type IV Secretion System (T4SS). The T4SS is responsible for the translocation of the conjugative DNA from the donor to the recipient cell; a process also highly conserved among all conjugation systems. Figure 1 provides an overview of the process of conjugation.

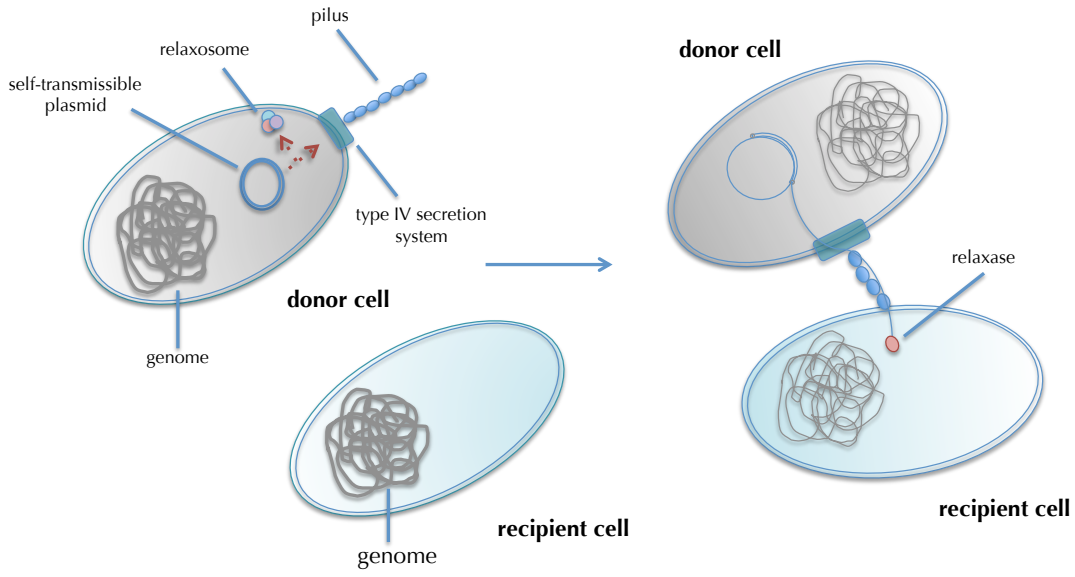

Figure 1. An overview of the process of conjugation. In the donor cell, the self-transmissible plasmid encodes all genes necessary for it's own transfer. The Relaxosome processes the DNA, and the relaxase stays covalently bound to the single stranded DNA. The Type IV Secretion System elaborates the pilus and transports the DNA relaxase complex into the recipient cell, which then becomes a donor cell itself.

1.2 Bacterial conjugation systems may be divided into two categories

Conjugative systems may be divided into two categories according to the nature of the transferred DNA. The most intensely studied systems are the self-transmissible plasmids.

The term self-transmissible describes the property that all genes necessary to mediate the conjugative transfer of the plasmid are encoded on the plasmid itself. Within this category, the plasmids pKM101 of the IncN, R388 (IncW), RP4 (IncP) and F (IncF) are the most intensely studied systems.

Self-transmissible plasmids usually prevent other conjugative plasmids from entering the cell by a mechanism termed entry exclusion, where proteins are presented on the cell surface that prevent entry plasmids from similar backgrounds (Garcillán-Barcia & de la Cruz, 2008). According to their exclusivity, plasmids can be grouped in so called incompatibility groups (Inc), a term first coined by Hedges & Datta (1971). Incompatibility in this case means that plasmids fall in the same group if they cannot co-exist in the same cell.

The second class termed as integrative and conjugative elements (ICEs) follows a similar secretion pathway; however, these genetic elements form a part of the genome and have to be excised by a recombinase/excisionase complex prior to undergoing the relaxase-mediated nicking reaction and transport via the T4SS. ICEs then integrate into the recipient-genome by homologous recombination or via ICE-encoded integrases. Please refer to Wozniak & Waldor (2010) for a more in-depth discussion of ICEs, since the text presented here will focus on

the conjugation systems of the self-transmissible plasmids pKM101 and pR388 occurring in the Gram-negative enterobacteria *Escherichia coli* and *Salmonella typhimurium*.

1.3 The nomenclature of Gram-negative conjugation systems

Conjugation systems and especially the T4SS are related to the Ti-plasmid transfer system of *Agrobacterium tumefaciens*. This plasmid confers phytopathogenicity to *A. tumefaciens* and causes crown-gall disease in plants. The Ti-plasmid encodes all genes necessary for its own transfer, as do conjugative self-transmissible plasmids. Further, they show similar operon organization. In *A. tumefaciens*, the proteins VirD1 and VirD2 are involved in substrate processing, and the T4CP VirD4 mediates substrate recruitment. The proteins named VirB1-11 form the T4SS (see Figure 2). Since the Ti system is the archetype for T4SSs, this text will use the *A. tumefaciens* nomenclature in conjunction with its plasmid's protein names in order to simplify the nomenclature and underline the homology of the systems.

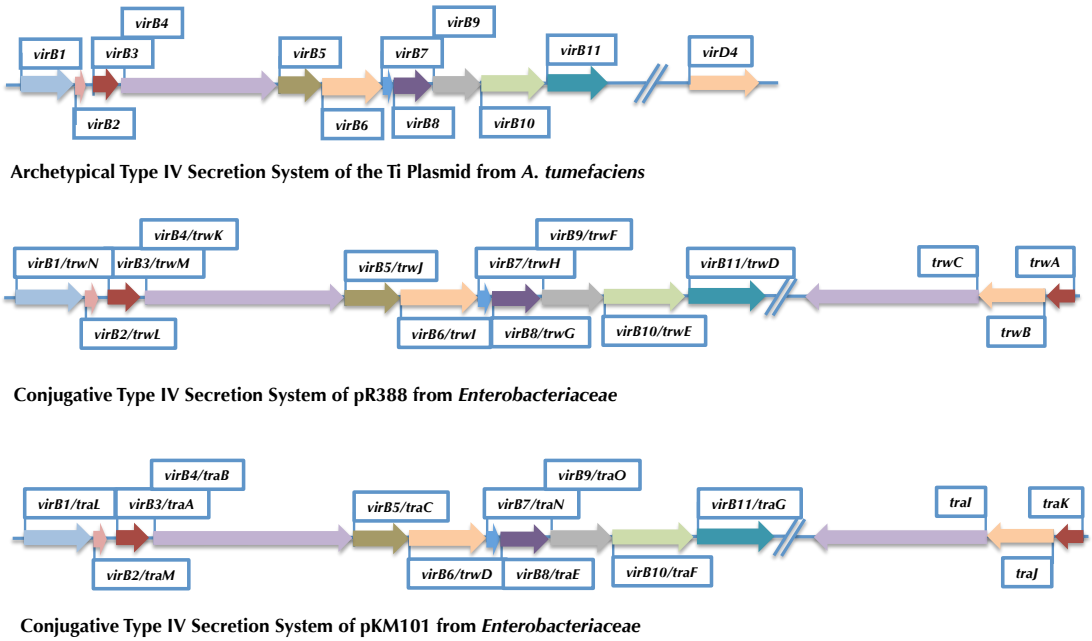

Figure 2. The relationship between Type IV Secretion Systems of conjugative systems pKM101 and R388 to the arechetypical *Agrobacterium tumefaciens* Ti-system. Homologous genes are coloured in similarly.

1.4 Substrate recognition and processing in bacterial conjugation systems

The best-studied conjugative relaxosome is that of the plasmid pR388 (IncW) and will be used here to illustrate proceedings of conjugative substrate recognition and processing. The components of the relaxosome are encoded in an operon structure encoding the genes *trwA* (relaxase enhancer protein), *trwB* (T4CP) and *trwC* (relaxase). The *oriT* sequence immediately precedes the *trwA* gene. A complex of relaxase enhancer and relaxase was first observed by negative-stain electron microscopy (EM), formed by the relaxosome components of the conjugative system RP4 (Pansegrau et al., 1990a). In this system, a third protein (TraH) was necessary to stabilize the relaxosome complex on the DNA.

1.4.1 The relaxase enhancer protein contains dual function

Substrate recognition is partly achieved by specific binding of the auxiliary protein TrwA to *oriT*. However, the relaxase TrwC can recognise and perform the nicking reaction without TrwA being present (Llosa et al., 1995). The *oriT* of plasmid pR388 is approximately 400 base pairs (bp) long and contains four inverted repeats (IRs) and one direct repeat (DR), which are important for recognition by the relaxosome components. TrwA specifically binds two regions within *oriT*, but exhibits different binding affinities for these regions. DNA footprinting experiments showed that with low amounts of protein from 0.25 µg, TrwA binds efficiently to the single DR within *oriT*, whereas the second binding site located at IR4 was only protected from DNaseI digestion at concentration higher than 1 µg (Moncalián et al., 1997). TrwA has been shown to be tetrameric and to significantly enhance conjugation efficiency, as well as relaxase-mediated nicking efficiency (Moncalián et al., 1997; Moncalián & de la Cruz, 2004). It further displays regulatory effects by suppressing the expression of the *trwABC* operon (Moncalián & de la Cruz, 2004). Similar effects have been described for the TrwC homologue TraY of the F plasmid conjugation system (Lum et al., 2002). Its enhancing effect on the relaxase-mediated nicking reaction led to TrwA's description as the relaxase enhancer protein.

1.4.2 The relaxase initiates the conjugation process

Relaxases are large proteins and most of them display phosphodiesterase and helicase activity, which are located on two distinct domains: an N-terminal "relaxase" domain and a C-terminal helicase domain (Llosa et al., 1996). The C-terminally located helicase domain, however, may be absent in some relaxases and additional domains can also be present in this family of proteins (Garcillán-Barcia et al., 2009). The relaxase TrwC specifically recognises the *oriT* nic-site. The x-ray crystal structure of the TrwC relaxase domain in complex with a 25mer oligonucleotide corresponding to IR_2 of the pR388 *oriT* (*RoriT*) upstream of the nic-site, and additional affinity studies, showed the importance of a hairpin secondary structure for efficient binding of TrwC to *oriT* (Guasch et al., 2003). However, *in vitro* cleavage also occurs when IR_2 is not present, indicating a distinct specificity of TrwC for specific recognition and cleavage of the DNA at nic (Lucas et al., 2010). Upon recognition, cleavage of the DNA is achieved by a nucleophilic attack of the catalytic tyrosine residue (Tyr18), which remains covalently attached to the 5'-end of the T-strand throughout DNA transfer, while the 3'-end is released (Pansegrau et al., 1990b; Draper et al., 2005). The helicase domain then unwinds the double-stranded (ds) DNA in an adenosine triphosphate (ATP)-dependent manner in the direction 5' → 3', moving along the single stranded T-strand (Llosa et al., 1996). The remaining circular strand is used as template for DNA replication in the donor cell, according to the rolling circle principle (Kingsman & Willetts, 1978). A second catalytic tyrosine residue in TrwC (Tyr26) is thought to be responsible for re-circularization of the T-strand in the recipient cell (Gonzalez-

Perez et al., 2007).

1.4.3 The T4CP shuttles the substrate to the T4SS

The T4CP is responsible for connecting the relaxase–DNA complex to the T4SS for transport to the recipient cell. The gene for the T4CP, *trwB* in the pR388 system, is located within the same operon as the relaxosome components. The T4CP is an integral membrane ATPase, and the x-ray crystal structure of the soluble moiety of TrwB, lacking the N-terminal transmembrane helix, showed a nucleotide binding domain of RecA-like fold, which also displays similarity to DNA helicases (Gomis-Rüth et al., 2001). A second all-α domain was also present. Its ATPase activity is DNA-dependent, but not sequence specific, and higher oligomers are formed when ATPase activity can be detected *in vitro* (Tato et al., 2005). In the x-ray crystal structure, the TrwB monomers formed an almost spherical homohexamer with a 20 Å wide channel protruding though the centre of the hexamer (Gomis-Rüth et al., 2001). It displays striking resemblance to F1-ATPases, which leads to the assumption that TrwB-like proteins could function as pumps to facilitate DNA translocation from the donor to the recipient cell. Conformational changes observed in the TrwB homohexamer upon binding of different ATP analogues, and in the apo protein underline these expectations (Gomis-Rüth et al., 2002).

TrwB exhibits specificity for interaction with its cognate relaxosome; in pull-down assays, immobilized TrwB retained the R388 relaxosome components TrwA and TrwC (Llosa et al., 2003). The pKM101 T4CP, however, could not

retain TrwA. Results from bacterial two-hybrid studies indicate that the interaction of TrwB with the T4SS is mediated through contact with VirB10-like proteins, which form an integral part of the T4SS and insert into the inner and outer membrane of Gram-negative bacteria (Llosa et al., 2003; Chandran et al., 2009). The membrane-associated domains of both proteins mediate this interaction; on deletion of the N-terminal trans-membrane segments of either TrwB or TrwE/VirB10, no *in vivo* interaction could be observed (Llosa et al., 2003). These studies further showed that TrwC also interacts with VirB10-like proteins of other conjugative systems, such as pKM101 and R6K. Overall, the assumption was made that T4CPs exhibit strong specificity for their cognate relaxosome, but weaker specificity for their cognate T4SS. The interaction of TrwB with TrwA was stronger than TrwB's interaction with the relaxase TrwC, which indicates that TrwB recognises its cognate relaxosome via interaction with TrwA. This potentially explains TrwA's enhancing effect on conjugation efficiency. However, in the relaxase TraI of the conjugative plasmid R1, certain domains within the protein were determined to be important for recognition of the relaxosome by its T4CP TraD (Lang et al., 2010; Redzej et al., 2013).

1.5 Substrate transfer is dependent on a Type IV Secretion System

Conjugative transfer is mediated by a large macromolecular complex embedded in the cell envelope named Type IV Secretion System (T4SS). T4SSs are highly versatile, double-membrane spanning protein complexes (Fronzes et al., 2009b). They display a wide substrate range that includes DNA, proteins

and DNA–protein complexes and occur in both Gram-negative and Gram-positive bacteria, as well as in the archaeal phylum *Crenachaeota*.

All occurring T4SSs can be divided into three categories according to their function. First, they mediate conjugative DNA transfer, as has been described previously. Secondly, T4SSs mediate the uptake (natural transformation) and release of DNA from or to the extracellular milieu (Chen & Dubnau, 2004). Apart from conjugation, the occurrence of naturally competent bacteria through T4SSs further contributes to bacterial genome plasticity. Thirdly, T4SSs are involved in effector translocation of plant and animal pathogens. Type IV secretion also contributes to virulence in human pathogens such as *Helicobacter pylori*, *Legionella pneumophila* and *Brucella suis*, where T4SSs are utilized to translocate virulence factors into eukaryotic cells (Juhas et al., 2008). The best-studied system in this context is the VirB/VirD4 system of *A. tumefaciens* that injects DNA into plant cells and thereby causes Crown Gall disease (Bomhoff et al., 1976). Figure 3 illustrates the three types of T4SSs.

The most intensely studied T4SS are those of the conjugative plasmid pKM101, the archetypical *A. tumefaciens* Ti-plasmid, and to some extent the T4SS of plasmid pR388 (Winans & Walker, 1985b; Bolland et al., 1990). The further discussion will focus on the conjugative T4SSs. As previously mentioned, the components of these T4SS are closely related to those of the archetypal *A. tumefaciens* T4SS. Therefore, the nomenclatures will be jointly in this text (for example, TraD/VirB6 for pKM101 components or TrwI/VirB6 for pR388 components).

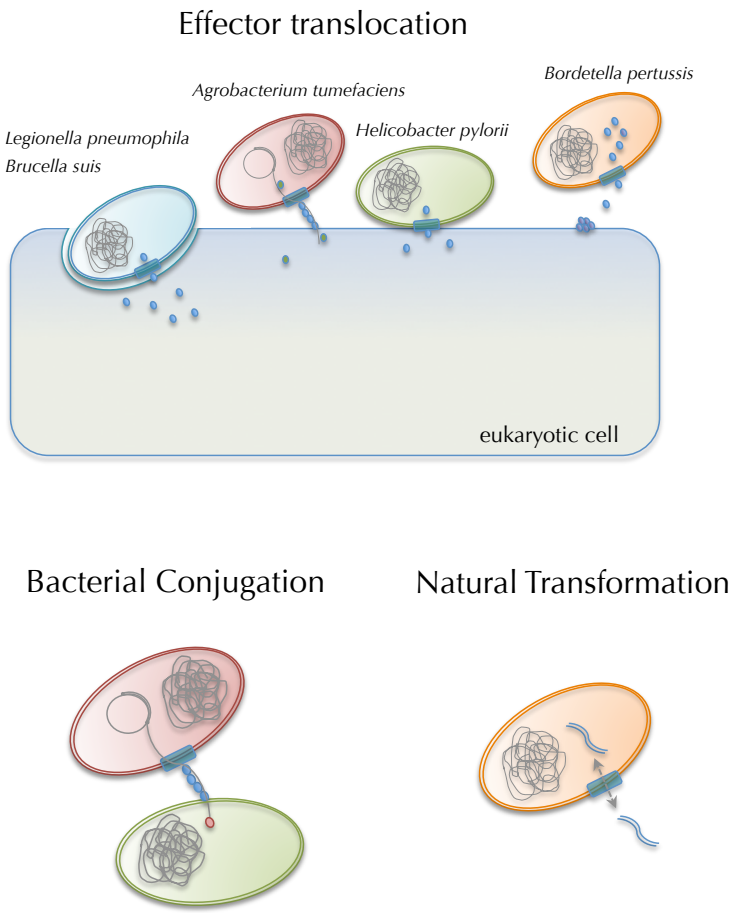

Figure 3. Type IV secretion Systems can be categorised into three distinct types according to their function. First, effector-translocation T4SSs translocate virulence proteins to eukaryotic host cells. Second, conjugative T4SSs translocate DNA—protein substrates from a donor cell to a recipient cell. Third, T4SSs facilitate natural transformation by either secreting DNA into the extracellular milieu, or mediating the uptake of free DNA. Figure re-drawn from Fronzes et al. (2009a).

The Vir-like conjugative T4SSs comprise 11 proteins; however, other systems may present additional components or lack homologues for some modules. In the pKM101 conjugation system, the proteins named TraA through to TraG and

TraL through to TraO (VirB1-11) are thought to comprise the T4SS, including an extracellular pilus that is formed by TraM/VirB2 and TraC/VirB5 and two ATPases (TraB/VirB4 and TraG/VirB11) to fuel the transport (Fronzes et al., 2009a). The T4SS of the pR388 plasmid is thought to be comprised of the proteins TrwD through to TrwN (VirB11-1) and its organization is similar to that of the pKM101 and Ti-systems (Alvarez-Martinez & Christie, 2009).

1.5.1 Two cytoplasmatic ATPases fuel the system

Apart from the T4CP, two further ATPases are associated to the T4SS to fuel the DNA transport across the membrane: the VirB4- and VirB11-like proteins. Both proteins contain Walker A and Walker B motifs, and have been shown to exhibit ATPase activity (Krause et al., 2000b; Durand et al., 2010). Purification from the membrane and the cytoplasm has been reported for both proteins, indicating that they localise to the cytoplasmic side of the inner membrane in Gram-negative bacteria (Dang & Christie, 1997; Rashkova et al., 1997).

VirB4-like proteins are present in conjugative T4SSs from Gram-positive and Gram-negative bacteria (Fronzes et al., 2009a). From secondary structure predictions, the protein is organized into two distinct N- and C-terminal domains. Homology modelling results for TraB/VirB4 and VirB4 from *A. tumefaciens* predict that the C-terminal domain of VirB4-like proteins fold in a highly similar way as the T4CP TraJ/VirD4 and VirD4, and is also the most conserved domain among all VirB4-like proteins (Middleton et al., 2005). These findings were confirmed by the determination of the crystal structure of

the C-terminal domain of a VirB4-homologue from the organism *Thermoanaerobacter pseudoethanolicus*, and led to the expectation that VirB4-like proteins form hexameric structures comparable to T4CPs (Walldén et al., 2012).

Earlier results from the size exclusion chromatography of TraB/VirB4 have shown that it forms homodimers when purified from the membrane; however, these dimeric assemblies do not possess ATPase activity. When TraB/VirB4 is purified from the cytoplasm, it adopts a hexameric quaternary structure and is then able to hydrolyze ATP (Durand et al., 2010). The Walker A and B motifs and a consensus NTP-binding site are located in the C-terminal domain of the protein. Upon separate expression and purification, the N- and C-terminal domains were both able to bind ATP, thereby showing that both domains retain NTP-binding properties and the N-terminal domain possesses a degenerate NTP-binding motif (Durand et al., 2010). The N-terminal domain possesses a single predicted transmembrane domain, but purification results showed that equal amounts of protein could be purified from the cytoplasm and the membrane. The C-terminal domain alone could not be purified from the membrane, thereby determining that the N-terminal domain is responsible for VirB4 membrane association (Durand et al., 2010).

The homologous protein from plasmid pR388 TrwK/VirB4 was the first VirB4-like protein to be shown to exhibit ATPase activity *in vitro* (Arechaga et al., 2008). Biochemical analysis of this protein showed contrasting results to the properties defined for TraB/VirB4. The protein was located solely in the cytoplasm in a mainly monomeric state. Investigation of the oligomeric state of

TrwK/VirB4 showed, however, that under conditions where ATPase activity can be detected, higher oligomeric states, such as homo-dimers, -trimers and -hexamers, are favoured. The authors therefore concluded that the biochemically active form of TrwK/VirB4 is the hexamer, much like the T4CPs and VirB11-like proteins (Arechaga et al., 2008). These assumptions have been validated by the recent electron microscopy (EM) reconstruction of the TrwK/VirB4 hexamer from the pR388 T4SS (Peña et al., 2012).

VirB11-like proteins are structurally and biochemically well characterized. They belong to the family of "traffic" ATPases, and are associated to various secretion systems from Gram-negative bacteria, such as types II, III, IV and VI (Fronzes et al., 2009a). As previously mentioned, VirB11 from *A. tumefaciens* localises mainly to the inner membrane of Gram-negative bacteria, although it lacks continuous long stretches of hydrophobic amino acids (Rashkova et al., 1997). ATPase activity is stimulated upon interactions with phospholipids, which further underlines the biological relevance of VirB11's tight association with the bacterial membrane (Krause et al., 2000b). Upon EM visualization, VirB11-like proteins show a hexameric quaternary assembly, forming a ring-like structure with a diameter of approximately 120 Å (Krause et al., 2000a). The x-ray crystal structure of the adenosine diphosphate (ADP)-bound VirB11 homolog from the *cag* pathogenicity island of *H. pylori* revealed an organization into distinct N- and C-terminal domains, with the nucleotide-binding site built at the interface of the two domains (Yeo et al., 2000; Savvides et al., 2003). Arrangements in the hexameric assembly show that each domain forms an individual ring, resulting in a chamber of approximately 50 Å in

diameter. The ring formed by the N-terminal domains is closed towards one side of the chamber, whereas the ring formed by the C-terminal domains is open. In the nucleotide-free state, the N-terminal domain is organized into separate rigid bodies, which are flexible towards each other and an asymmetric ring structure, whereas the C-terminal domain is more rigid and retains the hexameric assembly interfaces between the subunits. Three of the six subunits' N-terminal domains change their conformation upon binding three ATP molecules to a rigid conformation, and upon ATP hydrolysis and binding of another three ATPs, the N-terminal ring transitions to a completely rigid and symmetrical conformation. The ring returns to its apo form upon nucleotide release (Savvides et al., 2003).

In contrast to VirB4-like proteins, VirB11-like proteins are less well conserved and not part of all T4SSs (Alvarez-Martinez & Christie, 2009). The crystal structure of the VirB11 homolog of *B. suis* differs substantially to that of *H. pylori* due to a domain swap caused by a linker sequence that is inserted between the N- and C-terminal domains (Hare et al., 2006). This modifies the nucleotide binding site, as well as the domain interface; however, the overall ring-like structure of the hexameric assembly is retained. Sequence comparisons predict that most VirB11-like proteins adopt a fold similar to that of *B. suis* VirB11 homolog (Alvarez-Martinez & Christie, 2009).

Yeast two-hybrid studies of peptides derived from the proteins of the Ti-plasmid-encoded T4SS suggest protein–protein interactions between all three ATPases involved in type IV secretion (Ward et al., 2002). Further, VirB4 is thought to interact with VirB8 and VirB10, which are part of the pore forming

protein complex across both Gram-negative bacterial membranes (Ward et al., 2002; Chandran et al., 2009). Co-purification experiments and a negative stain EM reconstruction of a TraB/VirB4 monomer have further identified the interaction of TraB/VirB4 with the core complex of the pKM101 system (Walldén et al., 2012). Additionally, recent pull-down experiments also suggest an interaction between TrwK/VirB4 and TrwD/VirB11 proteins from pR388 (Ripoll-Rozada et al., 2013). VirB11 exhibited further interactions with the core complex forming protein VirB9, as well as with the pilus-forming protein VirB2.

1.5.2 The T4SS core complex forms the secretion pore

A major advance in our understanding of the structure of T4SSs is the identification and structure of the so called "core complex, formed of the proteins TraN/VirB7, TraO/VirB9 and TraF/VirB10 from the pKM101 T4SS. This macromolecular assembly spans the periplasm and inserts in both the inner and outer membranes of *E. coli*. The 15 Ångström (Å) resolution cryo-EM structure of this 1.1 megadalton (MDa) complex revealed a cylindrical shape in which each protein is present in 14 copies, forming a two-chambered channel (Fronzes et al., 2009b). The two chambers, termed as O- and I-layer, are thought to insert into the outer and inner membrane, respectively. The O-layer consists of a main body and cap formed by the C-terminal domains of the proteins TraO/VirB9 and TraF/VirB10, as well as full length TraN/VirB7, with the cap forming a 20 Å wide opening towards the extracellular milieu. The I-

layer, formed of the N- termini of TraO/VirB9 and TraF/VirB10, resembles a cup with a 30 Å high and 55 Å diameter base structure. The whole complex is 185 Å in diameter and length. Further insight into the structure of the complex could be gained by the recently solved crystal structure of the O-layer, as shown in Figure 4 (Chandran et al., 2009). Surprisingly, it identified TraF/VirB10 as the protein forming the outer membrane channel, thereby determining TraF/VirB10 as the only known protein spanning both the inner and outer membrane of Gram-negative bacteria.

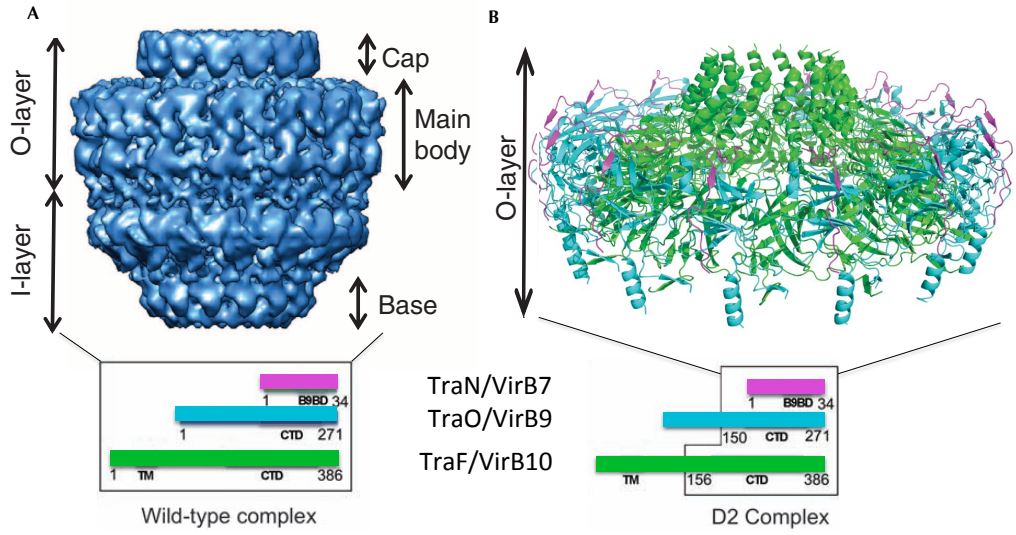

Figure 4. Advances in the imaging of the pKM101 Type IV Secretion System (T4SS). A) Side-view of the three- dimensional cryo-electron microscopy structure of the T4SS core complex, formed by TraF/VirB10 (green), TraN/VirB7 (magenta) and TraO/VirB9 (cyan) as shown in diagram below (Figure modified from Rivera-Calzada et al. (2013)). B) Ribbon diagram of the pKM101 T4SS outer membrane complex, formed by TraN/VirB7 (magenta), and the C-terminal domains of TraF/VirB10 (green) and TraO/VirB (cyan) (Figure modified from Chandran et al. (2009)).

Furthermore, it showed that the O-layer is composed of three proteins inserting into the outer membrane, a feature that is as well unprecedented. A unique

ring structure composed of 14 copies of a two α-helix bundle in each TraF/VirB10 subunit forms a 32 Å outer membrane pore. Higher resolution cryo-EM structures further elucidated the I-layer of the pKM101 core complex; these findings showed that the N-terminus of TraO/VirB9 is most likely located on the periphery of the I-layer, while the N-terminus of TraF/VirB10 forms the inner channel of the I-layer (Rivera-Calzada et al., 2013).

1.5.3 The inner membrane channel remains elusive

The structural studies of The T4SS core complex revealed that the inner membrane channel is partly formed by the N-terminal domains of the proteins VirB9 and VirB10 (Rivera-Calzada et al., 2013). However, two additional proteins are thought to be involved into forming this pore; the proteins VirB6 and VirB8.

The polytopic membrane protein VirB6 is essential for substrate transfer in *A. tumefaciens*. Experimental topology models and computational analysis of the structural features of VirB6 from *A. tumefaciens* suggest that it possess five transmembrane helices and a C-terminal cytoplasmic domain (Jakubowski et al. 2004). Similar structural predictions exist for the *H. pylori* VirB6-like protein (Karnholz et al. 2006). A large periplasmic loop is also present on both VirB6 and VirB8, which is essential for substrate contact (Jakubowski et al., 2004).

The structures of the periplasmic domain of the *B. suis* VirB8 homolog and VirB8 from *A. tumefaciens* have been determined by x-ray crystallography (Terradot et al., 2005; Bailey et al., 2006). They show similar folds and are

bitopic inner membrane proteins, whose N-terminal domains are embedded in the inner membrane. The C-terminal domain was shown to localise to the periplasm and direct interactions with the DNA substrate in *A. tumefaciens* have been reported (Cascales & Christie, 2004).

Complex formation of these proteins with the core complex has been difficult to prove experimentally and the stoichiometry of these proteins to the core complex is also not known to date. However, indications exist that VirB6 is important for substrate transfer from itself to VirB8 and additionally to VirB9 at the outer membrane (Jakubowski et al., 2004). Furthermore, both proteins are in direct contact with the substrate (Cascales & Christie, 2004). Their association with the inner membrane and these functional assessments underline the proposition that VirB6- and VirB8-like proteins form the inner membrane channel.

1.5.4 The pilus is essential for conjugation

In Gram-negative bacteria, the T4SS operon encodes a small protein structurally similar to the pilus-forming subunit TraM of the F-plasmid and VirB2 of The Ti-plasmid. An additional component of the pilus is the ViB5-like proteins; however, these proteins are present in lower quantities. It has been proposed that the pilus could serve as a hollow tube for DNA transfer from the donor to the recipient cell, but this assumption remains controversial. Further, the pilus is important for cell–cell contact. However, it has been demonstrated that DNA can be transferred between cells without apparent direct physical

contact during conjugation but impossible in mutants lacking the pilin subunit (Babic et al., 2008). In T4SSs not involved in conjugation, the pilus is not always essential for substrate transfer (Fronzes et al., 2009a).

The VirB2 protein from *A. tumefaciens* and TrbC/VirB2 from the RP4 conjugative plasmid (IncP) exhibit post-translational modification, resulting in a cyclic peptide (Eisenbrandt et al., 1999). After translation, a signal peptide of approximately 30-50 amino acids in length is cleaved off by a specific protease and the N- and C-termini are covalently joined (Haase & Lanka, 1997). F-like pilins have not been shown to undergo cyclisation, but are acetylated prior to insertion into the inner membrane (Moore et al., 1993; Majdalani & Ippen-Ihler, 1996).

VirB5 has been structurally characterized (Yeo et al., 2003). In *A. tumefaciens*, VirB5 localises to the tip of the pilus (Aly & Baron, 2007). In connection with mutational analyses performed on the TraL protein from pKM101, VirB5 is expected to serve as an adhesin (Yeo et al., 2003).

The morphology of the conjugative pilus is distinct for different types of conjugative systems. Classifications describe that pili can be grouped into F-like and P-like pili, where F-like pili are long and flexible and P-like pili short and rigid. Cryo-EM analysis of the F-plasmid pilus have shown the presence of a lumen, which is approximately 30 Å in diameter (Wang et al., 2009). This lumen could accommodate single stranded DNA but would be too small to allow passage of the relaxase–DNA substrate, if the protein remains in its folded state. Live cell imaging of fluorescently labelled F-pili further showed

their ability to polymerise and retract in response to an unknown signal (Clarke et al., 2008). This function may serve to enable the physical cell-to-cell contact required.

1.5.5 VirB1 and VirB3 proteins

VirB1 is thought to play an accessory rather than essential role within the secretion process. It shows a lysozyme-like fold and belongs to a large subfamily of proteins involved in the assembly of macromolecular complexes on the bacterial surface, such as flagella and other DNA uptake systems (Koraimann, 2003). It is proposed that they assist macromolecular assembly in the membrane by loosening the peptidoglycan-meshwork. In *A. tumefaciens*, VirB1-dysfunction diminishes Ti-DNA transfer, but does not abolish it (Berger & Christie, 1994).

The role and localization of VirB3-like proteins remains controversial. It was first postulated to be located in the both, but dominantly in the outer membrane (Jones et al., 1994). Hydropathy analysis point towards its association with the inner membrane, and its stabilizing effect on VirB4 proteins further underline this postulation (Alvarez-Martinez & Christie, 2009). Further, some T4SSs harbour chimeric VirB3/VirB4 proteins, suggesting a strong link between these two proteins (Batchelor et al., 2004).

1.6 The DNA pathway through the T4SS

A breakthrough in our understanding of substrate transfer through a T4SS was the work published by Cascales & Christie (2004). This work demonstrated the interaction of the Ti DNA substrate of the *A. tumefaciens* T4SS with various subunits of the T4SS by co-immunoprecipitation of the proteins cross-linked to the Ti DNA. In combination with deletion mutants of these subunits, a pathway of the DNA substrate through the T4SS channel was delineated.

The relaxase homologue VirD2 processes the DNA and remains covalently bound to the DNA throughout transfer. In the above-mentioned work, the DNA—Relaxase complex was co-precipitated from cells even if none of the other T4SS components were present, indicating that the initial step for secretion is the relaxase processing the Ti DNA.

Complexes of T4CP VirD4 and the Ti DNA could be observed only when the relaxase VirD2 was present, but their formation was independent from the presence of any other T4SS components. The T4CP VirD4 was thereby identified as the second protein to interact with the substrate.

The traffic ATPase VirB11 was determined to mediate contact between the substrate—T4CP complex and the secretion channel, since VirB11—Ti DNA complexes were only observed if VirD4 was present, but unaffected by the deletion of any other T4SS component.

The inner membrane proteins VirB6 and VirB8 were also shown to directly form complexes with the Ti DNA; it was, however, impossible to determine a sequence in which the Ti DNA is passed on between these two proteins. This

complex formation was dependent on VirB11 and VirB4 ATPases, but unaffected by VirB9 or VirB2 absence.

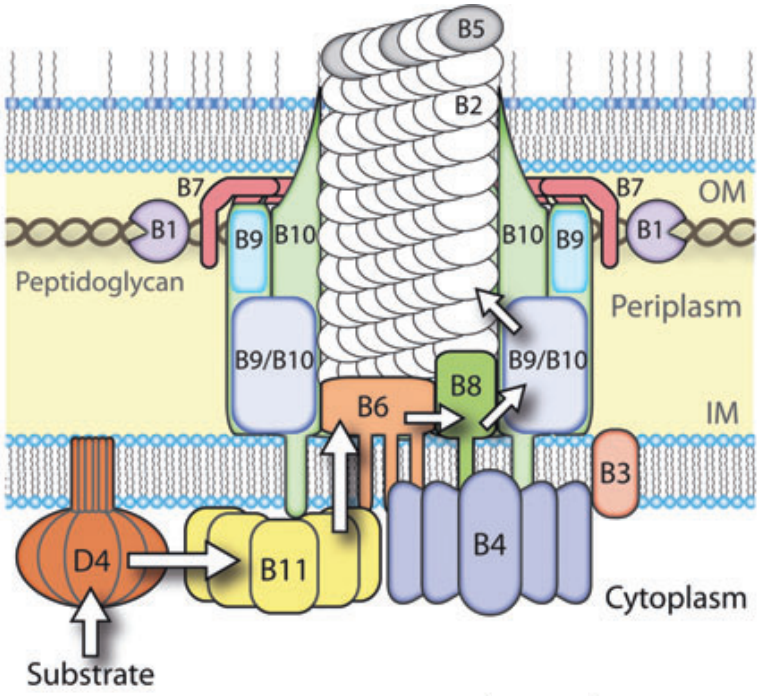

Figure 5. Complete working model of the Type IV Secretion System. Schematic summary of experimentally derived localisation studies of T4SS components. Arrows indicate the postulated substrate pathway from data published in Cascales & Christie (2004). The substrate is passed on from the coupling protein VirD4 to the traffic ATPase VirB11. It is then passed through the inner membrane channel via the Proteins VirB6 and VirB8, and the VirB4 ATPase aids this process. The proteins VirB9 and VirB10 then form the channel through which the substrate is passed through the outer membrane. The pilus subunits VirB2 and VirB5 also interact with the substrate and presumably pass it on to the recipient. Figure taken from Wallden et al. (2010).

Some components of the T4SS did not interact directly with the Ti DNA substrate; however, they could still co-precipitate small amounts of Ti DNA through their interaction with components that directly interact with the Ti DNA. The proteins VirB4, VirB5, VirB7 and VirB10 comprised this category. In mutants lacking the VirB4 protein, no VirB6/VirB8—Ti DNA complexes can be

detected. Therefore, it is likely that VirB4 assists in the substrate transfer from VirB11 to the inner membrane proteins VirB6 and VirB8.Similarly to VirB6 and VirB8, direct contact between the Ti DNA and the proteins VirB2 and VirB9 was detected but it was impossible to distinguish a sequence between these two. As both these proteins localise to the outer membrane, it is likely that the substrate is passed on to VirB2/VirB9 from VirB6/VirB8. This assumption was confirmed, since no VirB2/VirBB9—Ti DNA complexes could be observed upon deletion of VirB6 or VirB8.

VirB10 and VirB7 proteins were determined to not directly interact with the DNA substrate. Upon deletion of VirB7, however, no VirB11—Ti DNA complexes were observed. Combined with more recent findings that VirB7/VirB9/VirB10-homologues form the tightly associated core complex, it is possible that the VirB11—Ti DNA complex requires the association to the core complex to efficiently receive the DNA—relaxase substrate from the T4CP.

Figure 5 summarises the above-described findings and puts them into context with more recent findings from structural data.

1.7 Project Aim

The aims of this thesis are to (i) determine the minimal genetic requirements for conjugation; (ii) to generate a genetically tractable T4SS, which can (iii) be produced for imaging purposes and (iv) to provide a simple assay with which structure–function relationships derived from structure can be assessed by site-

directed mutagenesis of various T4SS components.

1.7.1 Determining the minimal genetic requirement for conjugation

As reviewed above, 14 proteins have been postulated to be involved in conjugative transfer of plasmid DNA. However, there are many other genes in plasmids, and their involvement in conjugation has never been clarified.

A study by Bolland et al. (1990) identified a 14.9 kbp region on the pR388 plasmid that mediates conjugation. However, this study precedes sequencing of the pR388 and the identification of all the *trw/vir* operon genes.

For the plasmid pKM101, a study by Winans & Walker (1985a) identified 11 complementation groups involved in conjugation, and located them to three distinct regions on the pKM101. Here again, the effort preceded the sequencing of pKM101 plasmid and the localisation of the *tra/vir* genes.

We propose here to take the 14 genes believed to be involved in conjugative transfer out of their genetic context and investigate whether conjugation is still possible. If conjugation still occurs, then this will establish for the first time that no other genes are required to mobilise an *oriT*-containing vector and transfer it into recipient cells. More specifically, the approach I have chosen is to clone the T4SS-encoding genes and the Relaxosome-encoding genes separately in different, well-established laboratory vectors and reconstitute the entire machinery by expressing these genes (under inducible promoters) in *E. coli* in the presence of a third vector containing the cognate *oriT*. The transfer of this *oriT*-containing plasmid will be monitored using a conjugation assay.

1.7.2 Generate a genetically tractable T4SS

Once the minimal conjugative transfer machinery is obtained, we aim to use it for several purposes: firstly, to overproduce the functional T4SSs in order to obtain their structure by either electron microscopy and by x-ray crystallography; secondly, to tag the system with fluorescent proteins so that it can be imaged *in vivo* by fluorescence microscopy, and thirdly, to introduce single site mutations at will anywhere in the genes to study the structure-function relationship in detail.

Overproduction of a functional T4SSs for structural study

The ultimate aim of the work on T4SSs is to determine the structure of entire T4SSs complexes arrested at various stages of the transfer process. The studies by Cascales & Christie (2004) described in section 1.6 provides the conceptual framework onto which approaches can be designed to block substrate at various stages of transport. However structural biological techniques rely on the production of functional complexes that can be purified in large quantities. Thus, to achieve our ultimate aim, we need to obtain a genetically tractable over-expression system where all components can be mutated/deleted/modified at will, and where the resulting system variants be overproduced and purified. A minimal conjugative transfer system as described above in the above section will satisfy all requirements to successfully achieve our long-term goals of imaging T4SSs at various stages of conjugative transfer.

Tag the system with fluorescent proteins so that it can be imaged in vivo by fluorescence microscopy

Another goal of T4SS research is to understand how T4SS assemble, i.e. in which order the various components of the system come together to form the entire machinery. As demonstrated in various published studies, this can be achieved by tagging the various component of the system with fluorescent proteins. Cornelis and co-workers used such an approach to decipher the assembly of the *Yersinia* Type III Secretion System (T3SS) *in vivo* (Diepold et al., 2010). In this study, fluorescent protein fusion constructs of T3SS components were used to localise the T3SS in the *Yersinia* membrane. Upon deletion of certain other components, the localisation of the fluorescently tagged component was re-assessed. If the localisation pattern remained unchanged, the deleted component has no influence on the correct assembly of the fluorescently tagged protein and the tagged component will, therefore, assemble before the deleted component. If, however, the fluorescently tagged component's localisation within the cell changes upon deletion of another component, it is clear that the deleted component has to assemble prior to the fluorescently tagged component so that this component can assemble correctly. In combination with functionality (substrate secretion) and needle assembly assessment (EM studies), the assembly of the T3SS was successfully dissected.

However, introducing sequences encoding tagging proteins within gene clusters is not easily achieved. The most intensely studied conjugative T4SSs are found on large, naturally occurring plasmids. The most convenient way to

genetically modify specific genes are DNA-polymerase chain reaction (PCR)-based methods, which allow the easy introduction of protein tags for affinity purification steps or localisation studies. These methods are, however, limited by the size of the fragment that is to be amplified, with fragment length of approximately 15,000 bp being the upper limit for efficient and error-free amplification. Although techniques have been developed to manipulate larger DNAs such as large plasmids, for example the λ Red manipulation system developed by Doubet et al. (2008), these methods are cumbersome and rather difficult to achieve. In contrast, a minimal conjugative transfer system such as the one described in previously has the distinct advantage of being easily manipulated.

Introduce single site mutations at will anywhere in the T4SS genes

Following the same rationale, a minimal conjugative transfer system as described above would be also be ideal to introduce mutations and dissect the meaning of protein—protein interactions observed in the various structures of the complexes obtained by x-ray crystallography or high-resolution cryo-EM. This will not only constitute an important validation tool for structural studies, but will also provide the platform on which a host of experiments can be conducted aiming to elucidate the mechanism of transport by T4SSs.

In this thesis, I present a body of work that establishes, for the first time, the minimal requirements for conjugative transfer, and use this system to explore

the possibility of fluorescently tagging T4SS components in view of monitoring their assembly *in vivo*.

2 Methods

In this chapter, an introduction to the methods used will be given, and will be brought into context with the literature. Further, the considerations taken into account whist determining the methods of choice will be presented.

2.1 Standard buffers and solutions

Table 1 lists all standard buffers and solution used if not stated otherwise.

Table 1. List of standard buffers and solutions

Solution	**Composition**
Luria Bertani (LB) media	0.5 g NaCl, 20 g tryptone, 5 g yeast extract in 1 l H_2O
LB Agar	1% Agar (w/v), 0.5 g NaCl, 20 g tryptone, 5 g yeast extract in 1 l H_2O
Water	MilliQ (Millipore) -filtered water was used for all applications
SDS PAGE loading dye	NuPAGE® LDS Sample Buffer (4X)
TBE running buffer (10x) for agarose gel electrophoresis	890 mM Tris, 890 mM boric acid, 20 mM EDTA, pH 8.0
Agarose gel for electrophoresis	1% (w/v) agarose in 0.5x TBE running buffer
DNA loading dye (10x)	40% (w/v) sucrose, 0.5% bromphenol blue in H_2O
MES SDS PAGE running buffer (20x)	50 mM MES, 50 mM Tris, 0.1% SDS, 1 mM EDTA, pH 7.3
Phosphate buffered saline (PBS)	4.3 mM Na_2HPO_4, 137 mM NaCl, 2.7 mM KCl, 1.4 mM KH_2PO_4, pH 7.4
PBS-Tween (PBST)	0.1% Tween-20 in PBS pH 7.4
PBS-Glucose-Tween (PBSGT)	50 mM glucose, 0.1% Tween-20 in PBS pH 7.4
16% Paraformaldehyde (PFA)	16% (w/v) PFA in PBS pH 7.4

Table 1. Continued

4-88 mounting media (4-88)	20% MOWIOL 4-88 (Sigma Aldrich), 30% (v/v) glycerol in PBS
NuPAGE® transfer buffer	500 mM Bicine, 500mM Bis-Tris, 20.5mM EDTA, pH 7.2

2.2 *Escherichia coli* strains and plasmids used in this study

Table 2 lists all *E. coli* strains used in this study.

Table 2. *Escherichia coli* strains used in this study.

Strain	**Genotype**	**Source**
DH5α	F^- *endA*1 *glnV44 thi-1 recA1 relA1 gyrA*96 *deoR nupG* Φ80d*lacZ*ΔM15 Δ(*lacZYA-argF*)U169, *hsdR17*(r_K^- m_K^-), λ^-	Grant et al. (1990)
Top10	F^- *mcrA* Δ(*mrr-hsdRMS-mcrBC*) Φ80d*lacZ*ΔM15 Δ*lacX74 nupG recA1 araD*139 Δ(*ara-leu*)7697 *galE15 galK16 rpsL*(Str^R) *endA1* λ^-	Invitrogen
HB101	F^- *mcrB mrr hsdS20*(r_B^- m_B^-) *recA13 leuB6 ara-14 proA2 lacY1 galK2 xyl-5 mtl-1 rpsL20*(Sm^R) *glnV44* λ^-	Mann et al. (1978)
BL21Star™	F^- *ompT hsdSB* (r_B^- m_B^-) *gal dcm rne131* (DE3)	Invitrogen
OverExpress™ C41(DE3)	F^- *ompT hsdSB* (r_B^- m_B^-) *gal dcm* (DE3)	Lucigen

All plasmids produced in this study were analysed by Sanger DNA sequencing (Sanger et al., 1977). The company GATC Biotech performed all reactions. Table 3 lists all plasmids used in this study.

Table 3. List of all plasmids used in this study (nt = nucleotide; *RoriT* = pR388 *oriT*; *KoriT* = pKM101 *oriT*)

Plasmid	**Description**	**Source**
pKM101	Wild-type conjugative plasmid, a deletion variant of plasmid R46	McCann et al. (1975) Langer & Walker (1981)
pKM101-XmaI	Deletion variant of pKM101 promoted by restriction digest with XmaI and intra-molecular re-ligation	This study
pKT4SS_B10cS	pASK_IBA-3C vector containing the genes *traL/virB1, traM/virB2, traA/virB3, traB/virB4, traC/virB5, traD/virB6, traN/virB7, traE/virB8, traO/virB9, traF/virB10* and *traG/virB11* with a *Strep* tag on the C-terminus of *traF//virB10*. The plasmid further contains the pKM101 *oriT* (*KoriT*) nic site following the gene *traG/virB11* from pKM101.	Dr Harry Low
pKT4SS_B10cS_oriT-rm	Identical to pKT4SS_B10cS but *KoriT* was removed	This study
pWT_KT4SS	pETDuet-1 vector containing the *Asc*I/*Pac*I fragment of pKM101-XmaI (nt positions 325-13047)	This study
pKRelax	pCDFDuet-1 vector containing the relaxosome genes *traIH, traJ* and *traK*.	This study
pKoriT	pRSFDuet-1 vector containing *KoriT*	This study
pMAK3	Wild-type conjugative plasmid, a variant of pR388 with the T4SS DNA sequences being 97.3% identical	Bradley & Cohen (1976) Revilla et al. (2008)
pRT4SS	pAsk-IBA3C vector containing the genes *trwN/virB1*, *trwL/virB2*, *trwM/virB3*, *trwK/virB4*, *trwJ/virB5*, *trwI/virB6*, *trwH/virB7*, *trwG/virB8*, *trwF/virB9*, *trwE/virB10* and *trwD/virB11* from pMAK3.	This study
pRT4SS_TrwK/VirB4-eGFP	Identical to pRT4SS but with a C-terminal eGFP fusion to TrwK/VirB4	This study

Table 3. continued

pRT4SS_TrwJ/VirB5-eGFP	Identical to pRT4SS but with a C-terminal eGFP fusion to TrwJ/VirB5	This study
pRT4SS_TrwI/VirB6-eGFP	Identical to pRT4SS but with a C-terminal eGFP fusion to TrwI/VirB6	This study
pRT4SS_eGFP-TrwG/VirB8	Identical to pRT4SS but with an N-terminal eGFP fusion to TrwG/VirB8	This study
pRT4SS_TrwE/VirB10-mCherry	Identical to pRT4SS but with a C-terminal mCherry fusion to TrwE/VirB10	This study
pRT4SS_TrwI/VirB6-FLAG	Identical to pRT4SS but with a C-terminal FLAG tag fusion to TrwI/VirB6	This study
pRT4SS_FLAG-TrwG/VirB8	Identical to pRT4SS but with an N-terminal FLAG tag fusion to TrwG/VirB8	This study
pRRelax	pCDFDuet-1 vector containing the genes *trwA, trwB* and *trwC*	This study
pRRelax_TrwC-mCherry	Identical to pRRelax but with a C-terminal mCherry fusion to TrwC	This study
pRoriT	pRSFDuet-1 vector containing the pR388 *oriT* sequence (*RoriT*)	This study
pAsk-IBA3C	Cloning vector providing Cam resistance. Protein production is under control of the *tet* promoter	IBA Lifesciences
pCDFDuet-1	Cloning vector providing Spec resistance. Protein production is under control of the T7 promoter	Novagen
pRSFDuet-1	Cloning vector providing Kan resistance. Protein production is under control of the T7 promoter	Novagen
pETDuet-1	Cloning vector providing Amp resistance. Protein production is under control of the T7 promoter	Novagen
pEGFP-C1	Vector containing the *egfp* gene	Clontech
pRVCHC-5	Vector containing the *mCherry* gene	Shaner et al. (2004)
pKD3	Template plasmid for deletions using PCR products with the λ Red recombinase	Datsenko & Wanner (2000)
pKD46-Gm	Helper plasmid expressing the λ Red recombinase	Doublet et al. (2008)

2.3 Oligonucleotide primers used in this study

Oligonucleotide primers were ordered from MWG Eurofins, dissolved in water to a concentration of 100 pmol/µl and stored at -20° C. Table 4 lists all oligonucleotide primers used in this study, including their sequence.

Table 4. List of all DNA oligonucleotides used in this study (bp = base pair)

Name	Nucleotide sequence (5′ → 3′ direction)
oFs_oriT-rm	taagcttgacctgtgaagtgaaaaatg
oFt_oriT-rm (tail region in capital letters)	GTGAACGGGAGCCTGTAAtaagcttgacctgtgaagtgaaaaatg
oRs_oriT-rm	acactgcattttatattcagggtc
oRt_oriT-rm (tail region in capital letters)	TTACAGGCTCCCGTTCACacactgcattttatattcagggtc
otraIJK_*Asc*I_1F (*Asc*I restriction site in capital letters)	ctaGGCGCGCCatgccaataataac
otraIJK_*Xho*I_2B (*Xho*I restriction site in capital letters)	gatCTCGAGTCATCAgatttcatggc
opKoriT_*Asc*I_1F (*Asc*I restriction site in capital letters)	tataGGCGCGCCaccggcaacatcaactg
opAsk-lin_ATG_1F	GGAGACCGCGGTCCCGAATTC
opAsk-lin_ATG_2B	CATTTTTTGCCCTCGTTATC
otrwop_pAsk_IF_1F (15 bp pAsk-IBA3c overhang in capital letters)	CGAGGGCAAAAAATGgcactggcagagttcgcggtgatcg
otrwop_pAsk_IF_2B (15 bp pAsk-IBA3c overhang in capital letters)	GGGACCGCGGTCTCCctaagccatcttggacttgg
ocat_lin_1F	CTCTGGAGTGAATACCAC
ocat_lin_2B	GTATTCACTCCAGAGCG
oeGFP_trwG_1F (15 bp *trwG/virB8* overhang in capital letters)	AGGGGCACTATGAGCgtgagcaagggcgaggag
oeGFP_trwG_2B (15 bp *trwG/virB8* overhang in capital letters)	TTTTGGTTGCTTCTTcttgtacagctcgtccat
otrwG_RT4SS_lin_1F	aagaagcaaccaaaaccggtcaag
otrwG_RT4SS_lin_2B	gctcatagtgcccctcgctg

Table 4. Continued

oIF_trwE-mCh_1F (15 bp *trwE/virB10* overhang in capital letters)	GATCTGGATTTCAGCgtgagcaagggcgaggag
oIF_trwE-mCh_2B (15 bp *trwE/virB10* overhang in capital letters)	GAGACTGTAGACATCcttgtacagctcgtccatg
olin_c-trwE_1F	gatgtctacagtctcgaaag
olin_c-trwE_2B	gctgaaatccagatcacgg
oIF_trwI-eGFP_1F (15 bp *trwI/virB6* overhang in capital letters)	GGACGCAAAGCAGGGgtgagcaagggcgaggag
oIF_trwI-eGFP_2B (15 bp *trwI/virB6* overhang in capital letters)	ACACCCTGACAACTActtgtacagctcgtccatgc
olin_trwI-cT_1F	tagttgtcagggtgtaaagcgg
olin_trwI-cT_2B	ccctgctttgcgtccccg
oIF_trwK-eGFP_1F (15 bp *trwK/virB4* overhang in capital letters)	GCCGAAAGGAGCGACgtgagcaagggcgaggagctg
oIF_trwK-eGFP_2B (15 bp *trwK/virB4* overhang in capital letters)	CCAGCTTCTTCATACcttgtacagctcgtccatg
oIF_trwJ-eGFP_1F (15 bp *trwJ/virB5* overhang in capital letters)	GGAATGCCGACTATCgtgagcaagggcgaggagc
oIF_trwJ-eGFP_2B (15 bp *trwJ/virB5* overhang in capital letters)	GTATCTTTTTCATTGcttgtacagctcgtccatg
oIF_trwG-FLAG_1F (FLAG tag sequence in capital letters)	GACTACAAAGACGATGACGACAAGtgaggggggcaccatgaag
oIF_trwG-FLAG_2B (15 bp overhang to FLAG tag sequence in capital letters)	ATCGTCTTTGTAGTCgttattgagtatttccgggtcagcgc
oIF_trwI-FLAG_1F (FLAG tag sequence in capital letters)	GACTACAAAGACGATGACGACAAGtagttgtcagggtgtaaag
oIF_trwI-FLAG_2B (15 bp overhang to FLAG tag sequence in capital letters)	ATCGTCTTTGTAGTCccctgctttgcgtccccggaag
otrwABC_*Asc*I_1F (*Asc*I restriction site in capital letters)	ctaGGCGCGCCatgctaggattgaac
otrwABC_*Xho*I_2B (*Xho*I restriction site in capital letters)	gatCTCGAGTCAttaccttccggcctc
oIF_trwC-mCh_F (15 bp *trwC* overhang in capital letters)	ATGGAGGCCGGAAGGgtgagcaagggcgaggag
oIF_trwC-mCh_B (15 bp *trwC* overhang in capital letters)	ACCAGACTCGAGTTActtgtacagctcgtccatg

Table 4. Continued

olin_c-trwC_F	Taactcgagtctggtaaagaaac
olin_c-trwC_B	ccttccggcctccatgcc
opRoriT_*Asc*I_1F (*Asc*I restriction site in capital letters)	tataGGCGCGCCactcattttctgcatcattg
opRoriT_*Asc*I_2B (*Asc*I restriction site in capital letters)	aattGGCGCGCCaccgcctcgtcctc
virB6/traD_RT_1F	gattacgtcaatggtgagcgc
virB6/traD_RT_2B	gaggccacccagcacaac
traI_RT_1F	ctactttccgccacgaaacg
traI_RT_2B	cagcttctggcgttcaaagc
traJ_RT_1F	gcaattactttgcctccagtg
traJ_RT_2B	caatatttttgccgcctctaatg
pAsk3C_SQ_2B	GACGCAGTAGCGGTAAACG
pASK-3C_1F_9100	ccgcccactctgtataaaaaccaaggc
odel-pKM101_1F (homologous region to pKM101 in capital letters)	CGTCTAAGGTGGGCCAATTCCCATAACAAGGTGGGCTA ATTCCCATAGTAAGGgtgtaggctggagctgcttc
odel-pKM101_2B (homologous region to pKM101 in capital letters)	CGCGGCAAATCCGGAAAAATGGAATGCACAATACACATG GAAGGATGCCatgggaattagccatggtcc

2.4 Standard methods in microbiology

2.4.1 Cultivation of *Escherichia coli*

Escherichia coli was cultivated in liquid and solid culture using Luria Bertani (LB) broth at 37° Celsius (C), if not indicated otherwise. Liquid cultures were shaken at 170 revolutions per minute (rmp). All culture media were autoclaved and sterile technique was used for inoculation and handling of cultures.

The optical density (OD) of cell cultures was measured photometrically at 600 nm (OD_{600}).

Antibiotics were sterile filtered and added to the medium. The following concentrations were used in solid and liquid medium: Ampicillin (Amp) 100 µg/ml; Chloramphenicol (Cam) 30 µg/ml, Spectinomycin (Spec) 100 µg/ml; Nalidixic acid (Nal) 10 µg/ml, Kanamycin (Kan) 50 µg/ml.

Expression of recombinant proteins was induced using 1 mM isopropyl-β-thiogalactoside (IPTG), 200 µg/l anhydrotetracycline (AHT) or 200 µg/l 4-epitetracycline if not stated otherwise.

2.4.2 Transformation of *Escherichia coli*

Electroporation after Fiedler & Wirth (1988) was performed to transform *E. coli* cells with plasmid DNA, PCR reactions or ligations. Electroporation cuvettes with 1 mm gap width (Flowgen) were used in a Biorad Gene Pulser Xcell electroporator (Voltage: 1800 V, Capacitance: 25 μF, Resistance: 200 Ω). Typically, a total of 40 ng of plasmid DNA was used for transformation. Ligation reactions were transformed using no more than 1.5 µl of a 10 µl reaction, and PCR reactions were transformed using up to 4.5 µl of a 50 µl reaction for restriction-free cloning.

Chemically competent cells were either purchased from Invitrogen (One Shot® BL21 Star™ (DE3) Chemically Competent *E. coli*) or generated using a modified protocol after Mandel & Higa (1970), which is described here. Cells were grown to an OD_{600} of approx. 0.3-0.5. Cells were then harvested at 4000 rmp at

4° C and resuspended in ½ the culture volume of ice-cold 100 mM $CaCl_2$. The cells were then incubated for 20 minutes (min) on ice, and harvested at 4000 rmp 4° C. Subsequently, they were resuspended $^1/_{10}$ the culture volume of ice-cold 100 mM $CaCl_2$ and incubated for 1 hour (h) prior to adding sterile glycerol to a final concentration of 15% (v/v). Cell aliquots were prepared and frozen at -80° C. For standard transformations, approx. 80 ng plasmid DNA was used. Up to 10 µl ligation reaction was used to transform competent cells. InFusion™ reactions were transformed using 2.5 µl (as per manufacturer's recommendation), as well as the residual 7.5 µl of the 10 µl reaction.

2.4.3 Conjugation assay

The conjugation assay is the method of choice for assessing the functionality of the reconstituted T4SS. It assesses the transport of an *oriT* containing plasmid from a donor cell to a recipient cell. Choosing a recipient strain that carries an antibiotic resistance not present in the genomic background of the donor strain facilitates the selection for the amount of donor and recipient cells. The conjugation (or transfer) efficiency of a plasmid and strain is determined by counting the colony formation on agar plates selective for donors or recipients.

Reconstitution experiments with the conjugation machinery will be pursued by dividing the needed machinery on two plasmids; one carrying the T4SS and one carrying the Relaxosome components. A third plasmid carrying the *oriT* will be used to analyse mobility. Donor strains will therefore be resistant to three antibiotics. The recipient strain DH5α carries the Nal resistance on its

genome.

Over-night cultures of donor and recipient *E. coli* strains were used to inoculate 5 ml LB cultures with or without antibiotics. Different donor strains were used and *E. coli* DH5α was used as recipient strain.

The cultures were grown to an OD_{600} of approximately 0.4 and protein production was induced for 1 h at 37° C, if not indicated otherwise. A total of 1.5 ml of donor culture, and the equivalent amount of recipient culture according to OD_{600} measurements were filtered on a hydrophilic MF-Millipore Membrane (Merck Millipore), made of mixed cellulose esters with a pore size of 0.45 µm. The filters were then incubated for 1 h lying on a LB agar plate, cells facing upwards. The cells were subsequently washed off the filter paper using 750 µl LB and 100 µl of different dilutions were plated LB agar plates containing Nal (selecting for *E. coli* DH5α recipient strains) and a second antibiotic, whose resistance is encoded on the transported plasmid (Kan in this study). Appropriate dilutions of the conjugation culture were also plated on antibiotics selecting for donors or total DH5α recipients.

The transfer efficiency was calculated by dividing transconjugant colony count by either donor or recipient colony count (Cellini et al., 1997).

2.4.4 Phage assay and phage purification

The phage or plaque assay tests the susceptibility of a bacterial strain to bacteriophage infection. A bacterial culture is infected with bacteriophage, and grown in a soft agar over night. If the bacteria are susceptible to infection,

small plaques will appear in a lawn of bacteria formed in the soft agar.

The bacterial strain is grown over night, and 200 µl of culture are mixed with 100 µl of phage-containing, sterile bacterial lysate. A total of 3 ml 0.7% LB agar, which was previously melted and cooled down to approx. 40° C, was poured into of the phage-bacteria mixture, and gently mixed. The soft agar was then immediately poured on top of a previously set 1% LB agar plate, and spread evenly without creating any air bubbles. The plates were then incubated at 37 °C over night until a lawn of bacteria appears in the soft agar.

Phage purification was performed by cutting the plaque from the soft agar using a sterile scalpel and placing the agar in a sterile Eppendorf tube. The agar was then topped with 500 µl sterile LB media supplemented with 1 mM $CaCl_2$ and incubated for 1 h at RT, vortexing occasionally. The LB media was then sterile filtered into a clean tube, and used to infect BL21Star® cells and cells transformed with plasmids pRT4SS + pRRelax + pRoriT.

2.4.5 Assessing pilus visibility by negative stain EM

Cells were grown under inducing conditions, and applied to copper grids. The negative stain agent phosphotungstic acid, titrated to pH 7 using potassium hydroxide (K-PTA), was applied for 30 s. After a wash step in water, the grids were air-dried and images were acquired on the Tecnai T10 microscope.

2.5 Standard methods in molecular biology

2.5.1 DNA purification, electrophoresis & imaging methods

All DNA was stored dissolved in water at -20° C.

Plasmids were prepared using the Wizard® Plus SV Miniprep DNA Purification System (Promega) and stored dissolved in water at -20° C.

DNA fragments were purified from agarose gels or after polymerase chain reactions (PCRs) using the QIAquick gel extraction or PCR purification kit (Qiagen), respectively, according to the manufacturer's protocol.

DNA concentrations were measured using a Nano Drop® ND-1000 spectrophotometer. The software ND-1000 V3.5.2 performed the calculation of the DNA concentration.

DNA gel electrophoresis was performed using 1% agarose gels containing SYBR® Safe DNA stain (Invitrogen). The DNA was then visualized under ultra violet (UV)-light (254 nm) and photographed.

The restriction endonuclease DpnI (New England Biolabs) was used to digest methylated DNA. For this purpose, 9 µl PCR product were incubated with 1 µl DpnI for 1 h at 37°C.

2.5.2 Polymerase chain reaction

The amplification of DNA fragments was performed using PCR after Mullis et al. (1986) using an MJ Research PTC-200 Reltier Thermal Cycler. The standard PCR cycle shown in Table 5 was adapted for each reaction according to the

primers (annealing temperature), the amplified gene (elongation time) and the type of polymerase used (elongation time and temperature). A total of 2.5 units of PfuUltra™ high-fidelity DNA polymerase (Stratagene) were used to amplify whole plasmids for restriction-free cloning after Van den Ent & Löwe (2006). The KOD hot start polymerase (Novagen) or the Phusion polymerase (New England Biolabs) were used for standard DNA amplifications, both at 1 unit per reaction. Only the Phusion polymerase was used for SLIM and InFusion™ cloning procedures, using 1 unit per reaction using the high fidelity buffer according to the manufacturers protocol.

Table 5. Standard PCR reaction used if not stated otherwise.

PCR		
Step	**Temperature [° C]**	**Time**
1. Denaturation	98	1 min
2. Denaturation	95	30 s
3. Primer annealing	60	10 s
4. Elongation	68 (PfuUltra™) or 72 (Kod or Phusion)	Kod (10 s/kbp), PfuUltra (2 min/kbp) Phusion (15-30 s/kbp)
25 cycles (step 2-4)		
5. Elongation	72	10 min
6. Store	4	∞

2.5.3 Restriction digest, dephosphorylation and ligation of DNA

Restriction enzymes were purchased from New England Biolabs, and buffer conditions were adjusted according to the manufacturer's protocol and incubated at 37° C for 1-3 h. Preparative restriction digests were conducted in a 50 µl volume, using 10 units of enzyme. Analytical digestion was conducted in a 10 µl volume, using 2 units of enzyme. Dephosphorylation of the digested vector was performed by adding 5 units of antarctic phosphatase (New England Biolabs) to the restriction digest and incubation at 37° C for 1 h.

DNA fragments created by restriction digest were gel purified prior to any ligation. Both vector and insert were added in a 1:1 molar ratio, if not indicated otherwise. A total of 400 units of T4 DNA ligase (New England Biolabs) was added to a 10 µl reaction, which was incubated at 4° C over night or 1.5 h at room temperature.

2.5.4 Western blot to detect a Strep or FLAG tag

Cells were grown under inducing conditions. Varying amounts of cells at different stages of growth were harvested by centrifugation and resuspended in varying amounts of water according to the cell density. Sodium dodecyl sulphate containing loading dye (Invitrogen) was added, and cells were boiled for 10 min. Varying amounts of sample were separated using denaturing sodiumdodecylsulfate polyacrylamide gel electrophoresis (SDS-PAGE) after Laemmli (1970). For this purpose, NuPAGE® 4-12% polyacrylamide bis-tris gels were used. A total of 7 µl pre-stained protein marker (Invitrogen) was used.

The protocol was performed according to the NuPAGE® western blot protocol (Invitrogen), using PVDF membrane (Invitrogen). The transfer was performed at 30 V for 1.

For Strep tag detection, a total of 2 µl monoclonal StrepMAB-Immo anti-strep antibody produced in mouse (IBA Lifesciences) was used in 10 ml 3% (w/v) milk in PBS for Strep tag detection.

FLAG-tag detection was performed using 2 µl anti-FLAG® M2 antibody produced in mouse (Sigma Aldrich) in 10 ml 3% (w/v) milk in PBS.

The PVDF membrane was incubated with the primary antibody for 1 h at RT, or over-night at 4° C, and subsequently washed twice with PBST buffer.

The secondary antibody in both cases was Anti-Mouse IgG (whole molecule) Alkaline Phosphatase antibody produced in goat (Sigma Aldrich). A total of 4 μl was added to 10 ml 3% milk in PBS to detect the primary anti-FLAG or anti-Strep antibodies, and the membranes were then incubated at RT for 1 h at RT prior to detection.

After 2 further wash steps in PBS, the detection of the alkaline phosphatase coupled to the anti mouse IgG was performed using the alkaline phosphatase precipitating substrate SIGMA *FAST*™ BCIP/NBT. One tablet was dissolved in 10 ml water, then added to the PVDF membrane and incubated for a maximum of 5 min.

2.6 Cloning T4SS and Relaxosome plasmids

Traditional cloning of DNA sequences relies on digesting the relevant insert and vector with restriction endonucleases. Thereby, complementary, single stranded DNA ends at the 5′ and 3′ ends of the fragment are generated. A ligase enzyme will then join the phosphodiester bond between the 3′ hydroxyl and the 5′ phosphate moieties of the complementary ends contained in the vector insert. The *in vitro* generated circular DNA can be transformed into genetically competent *E. coli* for replication (Cohen et al., 1973).

Restriction enzymes recognise specific target sequences and cut DNA at specific points within the recognised sequence. Cloning using this method therefore requires the presence of a restriction site at a specific point within the vector, as well as the gene of interest. Introducing specific restriction sites into the insert is easily achieved by introducing the restriction site into the primer used for amplification of the insert by PCR. The restriction site of choice must however not be present in the insert itself.

In the case of cloning large inserts into a replication and antibiotic resistance background, the chance of a restriction site being present in the insert rises. Further, introducing additional bp for a restriction site to the 3′-end of an operon structure may influence its expression by altering the distance between the promoter and the start codon. It is particularly difficult to create fusion proteins using restriction enzyme based methods, since the protein fusion has to be in frame. Achieving this using a restriction enzyme based method may result in several sub-cloning steps, as well as the introduction of additional

residues to keep the reading frame intact.

PCR-based, restriction-free cloning methods, as well as assembly-cloning methods using homologous stretches of DNA sequence, allow for seamless addition of sequence to any existing vector at any specific point (van den Ent & Löwe, 2006; Zhu et al., 2007; Gibson et al., 2009). This is of advantage, especially when creating fusion proteins.

2.6.1 InFusion™ cloning method

The InFusion™ method relies on an assembly cloning methods, where overlapping ss DNA cohesive ends are created between insert and linearized vector. The principle is termed Gibson assembly (Gibson et al., 2009).

Two DNA fragments (green and magenta in Figure 6) with overlapping ends are created, either both by PCR or restriction digest, and incubated with T5 exonuclease, Phusion polymerase and Taq ligase. The exonuclease creates single-stranded cohesive ends. Subsequent annealing of the cohesive ends allows the DNA polymerase to fill potential gaps and nicks are ligated by the Taq ligase. Figure 6 was taken from Gibson et al. (2009) and shows a schematic depiction of the Gibson assembly process. The enzyme T5 exonuclease removes nucleotides from the 5′ end of the end of the PCR products and thereby creates cohesive ends, which then spontaneously anneal. The DNA polymerase will then fill gaps that might occur due to the exonuclease treatment and the reaction can be transformed into chemically competent *E. coli* immediately. The InFusion™ cloning kit supplied by

Clontech, a similar method to the above described, was used in this project. The company supplies a 5x concentrated InFusion™ Enzyme and buffer mix, which is then added to the generated PCR products. The exact contents are not disclosed.

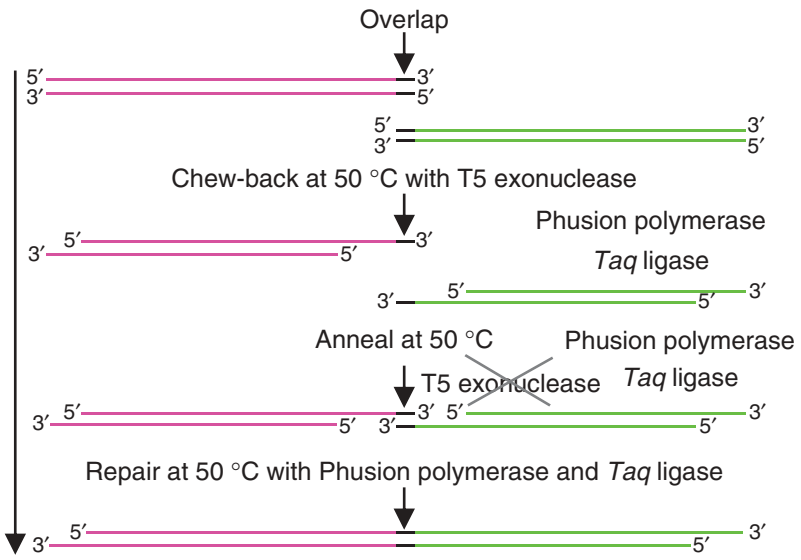

Figure 6. Schematic depicting the Gibson assembly. Figure taken from Gibson et al. (2009).

The following procedure was used for generating all InFusion™ clones produced in this study.

The overlapping ends were added to the 5′ ends of gene-specific or vector specific PCR primers. In the case of fusing tags to a protein, the tag DNA sequence was added to the forward or backward primer, depending on the location of the tag. The tag sequence was then also added to the correspondingly appropriate primer for vector amplification o create the overlapping 15 bp sequence.

The sequence to be cloned is amplified by standard PCR techniques (PCR 1), as

is the vector (PCR VEC) into which the sequence is to be cloned. The PCR products were always gel purified prior to performing InFusion™ reactions, as template DNA can contaminate the InFusion™ reaction. Equal concentrations (approx. 60 ng each) of the PCR products were mixed and the volume was adjusted to 8 µl. If the PCR products were not concentrated enough after gel purification, water was evaporated from the PCR product using a vacuum centrifuge until the desired concentration was achieved. A total of 2 µl 5x enzyme and buffer mix was added and the reaction was incubated at 50°C for 15 minutes.

2.6.2 Site-directed, ligase-independent mutagenesis (SLIM)

The SLIM method is designed for deleting sequences from existing plasmids (Chiu et al., 2004). The whole plasmid, apart from the deletion, is amplified in two separate PCRs.

For the first PCR, a forward primer is designed that contains hybrid sequence from approximately 18 nt upstream of the deletion (tail region), and approximately 20 nt downstream of the deletion (primer F_T). The reverse primer for the first PCR is complementary to approximately 20 nt immediately upstream of the tail region (primer R_S). The resulting PCR product will therefore contain a hybrid 5′ end containing a sequence fusion of the up- and downstream regions of the deletion (see Figure 7A and B).

The second PCR uses a forward primer F_S that comprises the sequence of the 20 nt downstream of the deletion (identical to the 3′ moiety of primer F_T), and a

reverse primer R_T that is complementary to the tail region (5′ end 18 nt of F_T), as well as the region immediately upstream of the tail region (identical to R_S). The resulting PCR product will contain all the sequence of the plasmid, apart from the sequence that is to be deleted (See Figure 7A and B).

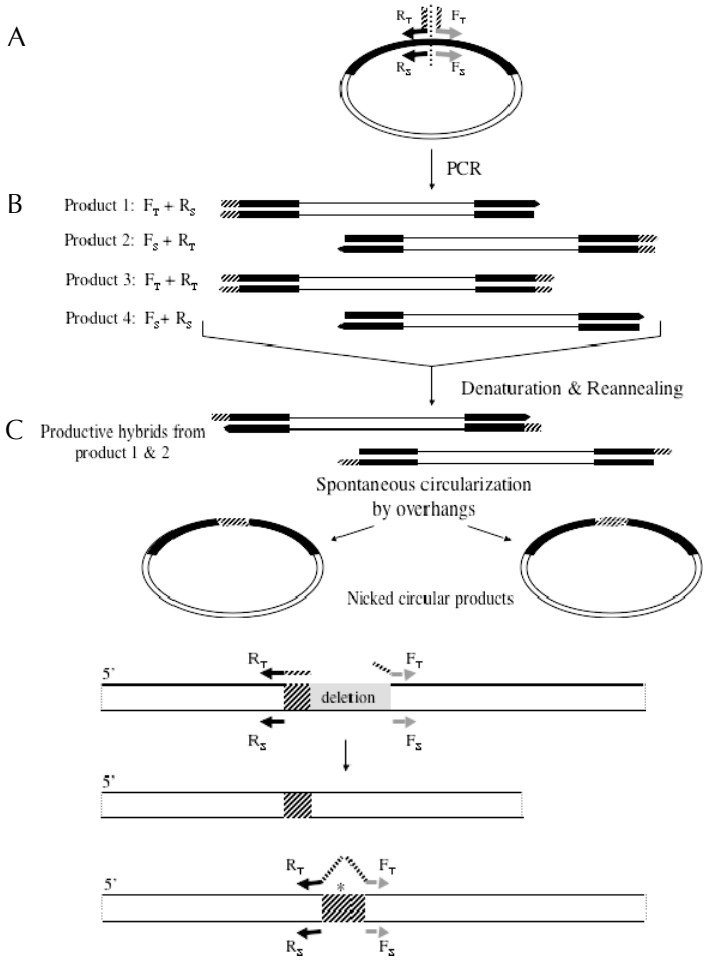

Figure 7. Schematic of the SLIM cloning method. **A)** Primer design for PCRs 1 and 2. **B)** Amplification of the plasmid in PCRs 1 and 2 **C)** Hybridisation of PCD products 1 and 2.

DpnI digest eliminates any template plasmid. The two PCR products are hybridized in cycles of denaturating and hybridizing conditions. The tail regions of the 5′ end of PCR product 1 and the 3′ end of PCR product 2 will be complementary and ss when hybridized together, and therefore anneal to form

a circular, nicked DNA molecule (see Figure 7). The nic will be repaired in *E. coli* after transformation.

2.6.3 Mutation by homologous recombination using PCR products

Datsenko & Wanner (2000) developed a method to delete large fragments from a genome or other genetic entities in bacteria using a λ Red recombinase-assisted approach. The method uses a PCR product with two 36 bp regions at its 5′ and 3′ ends (H1 and H2 in Figure 8) that are homologous to the flanking regions of the deletion site (Gene B in Figure 8), and an antibiotic resistance cassette, which then replaces the deletion site. The template plasmid for this PCR product is pKD3, containing the Kan resistance cassette flanked by recognition sites (FRT in Figure 8) for the site-specific recombinase FLT (the FLT recombinase can later be used to remove the Kan resistance cassette). The 36 bp homologous regions are added to the PCR primers, as well as the priming regions for pKD3 (P1 and P2 in Figure 8). The resulting PCR product is then transformed into an *E. coli* strain expressing the λ Red recombinase system on a helper plasmid under the control of an arabinose-inducible promoter. The λ Red recombinase then assists in the homologous recombination of the 36 bp homologous regions and the deletion site.

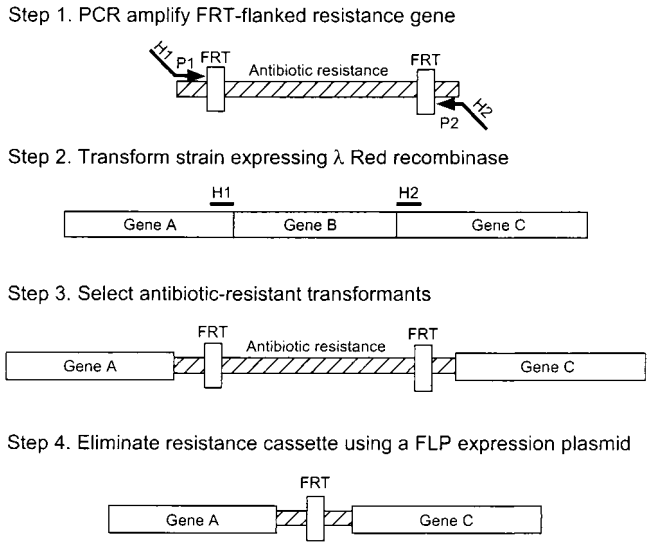

Figure 8. One-step inactivation of chromosomal genes using PCR products. H1 and H2 refer to homologous regions of the deletion target; P1 and P2 are the priming sites on the template plasmid. Figure taken from Datsenko & Wanner (2000).

2.6.4 Reconstituting the pR388 conjugation machinery

The below section describes the cloning of the Relaxosome plasmid pRRelax and the oriT plasmid pRoriT. Please see the chapter "Results II – The IncW conjugation machinery" for a detailed description of the T4SS expressing plasmid pRT4SS.

Cloning of pR388 oriT into pRSFDuet-1 – pRoriT

The *oriT* sequence was amplified from pR388 (*RoriT*, 420 bp) by PCR using the oligonucleotide primers OpRoriT_*Asc*I_1F and OpRoriT_*Asc*I_2B. Both primers contain a restriction site for the enzyme *Asc*I at their 5'-ends. The PCR product

was purified by elution from a 1% agarose gel and subsequently digested with 5 units of the enzyme *Asc*I in 1x Buffer 4 (New England Biolabs) for 3 h at 37°C. The enzyme was then heat- inactivated by incubating the reaction at 65° C for 20 min. The DNA was subsequently purified using the PCR Purification Kit (Qiagen). The vector pRSFDuet-1 was digested the enzyme *Asc*I in 1x Buffer 4 (New England Biolabs). The enzyme was heat-inactivated by incubating the reaction at 65° C for 20 min and DNA was purified subsequently using the PCR Purification Kit. A molar vector:insert ratio of 1:2 was used in a ligation reaction, which was incubated for 2 h at room temperature. The resulting plasmid was named pRoriT.

The operon containing the genes *trwA*, *trwB* and *trwC* (4850 bp) was amplified from pR388 using the oligonucleotide primers *trwABC_Asc*I_1F and *trwABC_Xho*I_2B. The primer trwABC_*Asc*I_1F contains a AscI restriction site at it's 5′-end, while the trwABC_*Xho*I_2B contains a *Xho*I restriction site at it's 5′-end to guarantee the appropriate orientation of the insert into pCDFDuet-1. All procedures were performed as described for the pKoriT cloning, using the enzymes *Asc*I and *Xho*I.

Cloning of the trwABC operon into pCDFDuet-1 – pRRelax

The operon containing the genes *trwA*, *trwB* and *trwC* (4850 bp) were cloned into pCDFDuet-1 using the restriction sites *Asc*I and *Xho*I according to standard methods described for pRoriT. The oligonucleotides otrwABC_*Asc*I_1F and otrwABC_*Xho*I_2B were used to amplify the *trwABC* operon.

2.6.5 Reconstituting the pKM101 conjugation machinery

This section describes the cloning methods used for all pKM101-derived plasmids produced in this study.

Cloning of pKRelax and pKoriT

The *oriT* sequence was amplified from pKM101 (*KoriT*, 667 bp) by PCR using the oligonucleotide primers OpKoriT_*Asc*I_1F and OpKoriT_*Asc*I_2B for pKM101. Both primers contain a restriction site for the enzyme *AscI* at their 5'-ends. Subsequent procedures were performed as described for pRoriT.

The operon containing the genes *traI*, *traK* and *traJ* (5198 bp) was amplified from pKM101 using the oligonucleotide primers traIJK_*Asc*I_1F and traIJK_*Xho*I_2B. A similar strategy was used as described for pRRelax.

The deletion derivative pKM101-XmaI

A total of 400 ng pKM101 DNA was digested with 0.5 u *Xma*I over-night at 37° C. DNA was subsequently precipitated by adding 0.7-times the reaction-volume of isopropanol and vortexing. The precipitate was then pelleted at 16.000 xg at 4° C for 30 minutes. Then, the supernatant was discarded and the pellet washed with room-tempered 70% ethanol, centrifuged another 10 m at 16000 xg and resuspended in 10 µl H_2O.

The ligation reactions were set up according to the manufacturer's instructions at 4° C over night, using 1:10, 1:100 and 1:1000 dilutions of the *Xma*I-digested

pKM101 DNA, as well as undiluted XmaI-digested pKM101 DNA. The reaction was then transformed into *E. coli* DH5α cells. The transformation culture was plated on Amp-containing LB agar.

The T4SS overexpression construct pKT4SS_B10cS_oriT-rm

The SLIM cloning method as described above was used to delete a 25 bp oriT sequence present on the plasmid pASK-IBA3c_virB1-11_TB10cStrep (provided by Dr Harry Low). Oligonucleotides oFt_oriT-rm and oRs_oriT-rm were used to amplify PCR product 1, while oligonucleotides oRt_oriT-rm and oFs_oriT-rm were used to amplify PCR product 2. Table 6 lists the PCR program used.

PCR products were gel-purified and DpnI digested, adding 5 µl of D-Buffer (20 mM MgCl2, 20 mM Tris, pH 8.0 and 5 mM DTT) and 5 units of DpnI, then incubating for 1 h at 37 ° C. A total of 20 µl PCR products 1 and 2 each were mixed, adding 10 µl H-Buffer (300 mM NaCl, 50 mM Tris, pH 9.0, 20 mM EDTA, pH 8.0) and hybridized as listed in table 6. The hybridisation reaction was transformed into chemically competent *E. coli* DH5α cells and plated on LB agar containing Cam.

Table 6. PCR and hybridisation programme for SLIM cloning of pKT4SS_B10cS_oriT-rm.

PCR		
Step	**Temperature [° C]**	**Time**
1. Denaturation	97	2 m
2. Denaturation	97	30 s
3. Primer annealing	65	10 s
4. Elongation	72	2 m 20 s
25 cycles (step 2-4)		
5. Elongation	72	10 m
6. Store	4	∞
Hybridisation		
Denaturation	97	3 m
1. Hybridisation	65	5 m
2. Hybridisation	30	15 m

Deletion of pKM101 parts using the λ Red recombinase system

The oligonucleotide primers odel-pKM101_1F and odel-pKM101_2B (see Table 4) were used to generate the deletion construct by PCR. The PCR was performed using the template plasmid pKD3. Subsequently, the PCR product was subjected to digestion with DpnI for 1 h at 37° C and gel-purified. The PCR product was then transformed into electrocompetent *E. coli* HB101 cells containing pKM101 and the λ Red recombinase system on the helper plasmid pKD46-Gm (Doublet et al., 2008). These cells were previously grown in the presence of 1 mM arabinose and made electrocompetent. After transformation, the cells were incubated 1 h at 30° C in LB, half of the culture was plated on kanamycin-containing LB agar plates and incubated over night at 37° C. The

other half of the culture was left at RT over night and plated on kanamycin-containing LB agar plates the next morning and then incubated over night at 37˚ C.

The wild-type promoter T4SS reconstitution pWT_KT4SS

The plasmid pKM101-XmaI was digested with the restriction enzymes *Asc*I and *Pac*I, generating two fragments of 12,722 and 7714 bp. The fragments were separated by agarose gel electrophoresis and the larger fragment, encoding the T4SS and an additional 1000 bp upstream of *traL/virB1*, was eluted from the gel. The vector pETDuet-1 was also digested with the restriction enzymes *Asc*I and *Pac*I, and subsequently gel purified. A ligation was set up as described above, using a molar ratio of 1:1 and incubated over night at 4° C. The ligation was transformed into *E. coli* DH5α cells and plated on Amp-containing LB agar.

2.7 Fluorescence Microscopy and Immunolabelling

Fluorescence is a natural phenomenon where a molecule absorbs light and subsequently emits light at a different, usually lower frequency. In microscopy, this phenomenon can be used for the subcellular localisation of a protein tagged with a fluorescent protein or an antibody conjugated to a fluorophore.

The green fluorescent protein (GFP) from a bioluminescent jellyfish was discovered in the 1950ies by Shimomura et al. (1962), and has since

revolutionised *in situ* protein detection by fluorescence microscopy. Countless mutations of the original GFP, as well as the discovery of fluorescent proteins from other species, have since resulted in proteins emitting light in a great variety of wavelengths, which are reviewed in Stepanenko et al. (2011). The chromophores are protein-derived and no co-factors are required for their function. In case of GFP, it is formed of a three amino acid sequence, which undergoes a cycle of cyclisation, oxidation and dehydration. An intermediate during these processes is able to emit green light of 508 nm wavelength upon excitation at wavelengths 396 and 475 nm. The surrounding rigid β barrel structure contributes to this ability. The chromophore formation is similar in all fluorescent proteins (see Stepanenko et al. (2011).

The fluorescent proteins used during this study were enhanced GFP (eGFP, Clontech) and mCherry (Shaner et al., 2004). The eGFP protein is an optimised version of wild-type GFP, where the amino acids Ser65 and Phe64 were mutated to Thr and Leu, respectively (Zhang et al., 1996). The mCherry protein is a variant of the red fluorescent protein DsRed from the coral *Discosoma* spec, which has been improved regarding DsRed's tendency for oligomerisation, quicker maturation and photo stability (Shaner et al., 2004).

Antibody labelling can also be used to detect proteins within the cell. A specific (primary) antibody is then used to specifically bind the protein of interest. The antibody is then detected by a second antibody (secondary) conjugated to a fluorescent dye, whose epitope is directed against the IgG of the organism the primary antibody was raised in. In this study, the primary antibody was a monoclonal antibody raised in mouse directed against the

FLAG-tag, while the secondary antibody was directed against the IgG of mouse and conjugated to Alexa Fluor594.

2.7.1 Microscopy

In brightfield microscopy, the image is formed by light passing through the specimen. Fluorescence microscopy images are created by the emitted light of a fluorophore in the specimen.

The excitation light is provided by a light source, which is then passed through the excitation filter to provide light of a specifically adjustable wavelength. This light is then reflected by a dichroic mirror and passes through the objective onto the specimen, which is then excited. The light emitted upon excitation passes back through the objective to the dichroic mirror. The dichroic mirror reflects all light up to a certain wavelength, while light of longer wavelength will pass through the mirror. Since the emitted light of a fluorophore is always of lower wavelength than the excitation light, the emitted light can pass through the mirror and create the image. Prior to reaching the eyepiece or camera, the light is passed through the emission filter so that only the emitted light of a selected fluorophore will create the image.

2.7.2 Deconvolution

Plasticity is difficult to achieve when acquiring images in one focal plane. Optical slicing, or Z-slices, through a specimen creates several 2D images,

which can later be assembled to a stack and create a 3D impression. Each image contains, however, information of the above and below focal planes, termed out-of-focus or scattered light. The result is a slightly distorted or blurry image, where the illuminated object appears to be of different shape. This effect occurs due to numerous physical properties of the microscope and the specimen, such as the objective or the refractive index of the specimen media, which reduce the ability of the microscope to depict a point-shaped light source. These parameters can be mathematically combined and described as the point-spread-function.

An experimental approach to reduce the effect of out-of-focus light is to use confocal microscopy, where the excitation and emission light is restricted to a pinhole, only illuminating a very specific point within the specimen. This method requires very high light dosage, and may not be beneficial for specimen integrity.

Deconvolution is a mathematical approach to cut out the information of scattered light in an image whereby the point-spread-function of a microscope is used to mathematically reverse to the actual shape of the object from the image where the scattered light information is still included. The point-spread-function of the microscope can be obtained experimentally; however, it is also possible to estimate it using computed algorithms. In this study, the deconvolution algorithm developed by Zeiss and included in the ZEN software package was applied to acquired Z-stacks. Z-stack images were acquired every 2 µm.

2.7.3 Experimental procedures

Cell fixation and application to microscopy slides

A volume of 2 ml cell culture was harvested at 1500 xg for 2 min, washed twice in PBS and resuspended in 150 µl PBS. To gain a final concentration of 4% paraformaldehyde (PFA), 50 µl 16% PFA was added to the cell suspension. The suspension was then incubated at RT for 20 min. Cells were then harvested again and resuspended in an appropriate volume of water (depending on cell density) to create a dense cell suspension. A volume of 20µl was applied to Multispot microscope slides PTFE with specialised coating (C. A. Hendley (ESSEX) LTD) and incubated at RT for 30 min. The cells are now attached to the specialised coating on the slide's spots and ready for antibody labelling. All following procedures were conducted by applying a 20 µl volume of all solutions onto the cells attached to the microscopy slide well.

Cell permeabilisation and blocking

Cells were treated with lysozyme to facilitate antibody penetration through the bacterial cell wall. Further, the detergent tween-20 is used to permeabilise the bacterial membranes. Prior to lysozyme treatment, the wells were washed with PBSGT buffer to adjust the osmotic pressure and prevent shock. Excess liquid was carefully blotted off each well using Whatman paper wedges. The cells were then incubated with 2 mg/ml lysozyme in PBSGT for 2 min. The lysozyme was washed off the slide with PBSGT, and excess liquid was again

blotted off. Blocking conditions were optimised to 3% goat serum + 3% bovine serum albumin (BSA) in PBSGT, and cells were incubated at these conditions for 30 min at RT. After several wash steps with PBSGT and blotting off excess liquid from the wells, the cells were ready for antibody labelling.

Antibody labelling

Conditions for antibody labelling were optimised for each antibody.

FLAG-tag recognition was most efficient with a 1:400 dilution of Monoclonal ANTI-FLAG® M2 antibody produced in mouse (Sigma Aldrich) and 1% BSA in PBSGT. The cells were incubated with the above-described solution for 1 h at RT, washed with PBSGT and excess liquid was blotted off.

The detection of the anti-FLAG antibody was facilitated using the Alexa Fluor® 594 Goat Anti-Mouse IgG antibody (Invitrogen). This anti-mouse antibody was diluted 1:300 in 1% BSA-PBSGT, and the cells were incubated in this condition for 30 min at RT. After rinsing each well with plenty of PBSGT and blotting, the samples were ready for mounting.

Mounting

A volume of 10 µl 4-88 mounting medium was applied to each well, and a clean cover slip covering all well was applied to the slide. The mounting medium was allowed to polymerise at 4° C over night prior to imaging.

eGFP and mCherry detection

Cells expressing eGFP- or mCherry-fusion proteins were fixed and applied to microscope slides as described above. Cells that did not attach to the slide after 30 min were washed off with PBS and excess liquid was blotted off prior to mounting, which was performed as described above.

Imaging fluorescent samples

All images were acquired using the Zeiss Axio Observer.Z1 fluorescence microscope at 100x magnification (ECPlam-Neofluar 100x/1.30 Oil M27 objective) using an AxioCam Mrm3 S/N 3884 camera. The exposure time was adjusted for each image. Images with the purpose of intensity comparison were acquired using the same exposure time.

eGFP was imaged in the green channel (Emission wavelength: 500-550 nm, Excitation wavelength 450-490 nm), while mCherry and Alexa Fluor594 labelled proteins were imaged in the red channel (Emission wavelength: 570-640 nm, Excitation wavelength 433-558 nm).

3 Results I – The IncN Conjugation System pKM101

The plasmid pKM101 is a deletion variant of the self-transmissible plasmid R46, promoted by the insertion sequence element IS46 (Hall, 1987). The plasmid pKM101 contains the two *tra* regions (see Figure 9) encoding the T4SS and the Relaxosome, and is therefore self-transmissible. While pKM101 encodes resistance to ß-lactam antibiotics only, R46 further confers resistance to sulphonamides and streptomycin/spectinomycin (Langer & Walker, 1981).

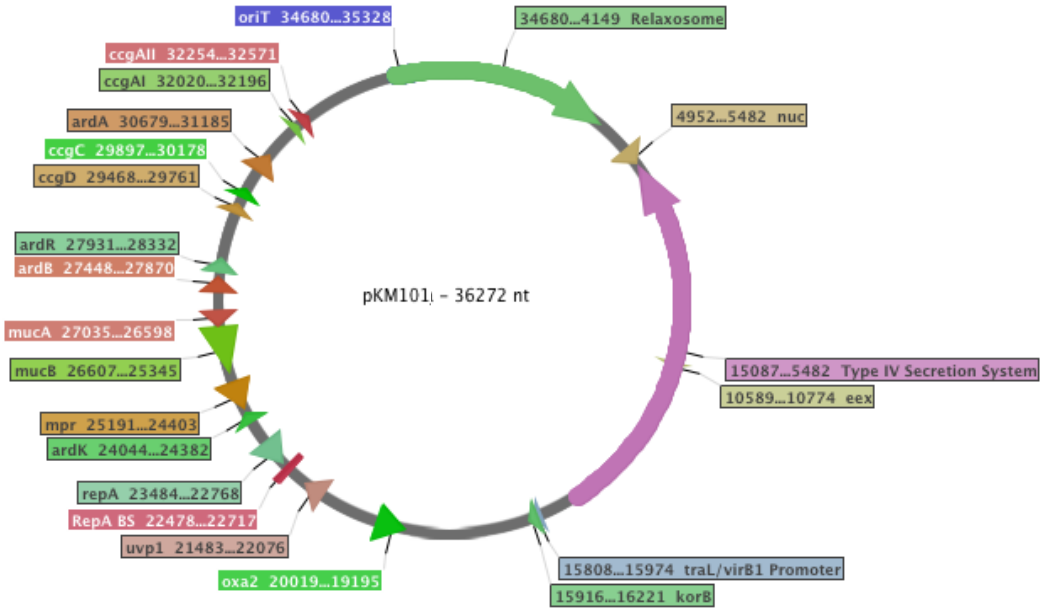

Figure 9. Plasmid map of pKM101. The T4SS region is displayed in pink and the relaxosome region in green.

Self-transmissible plasmids tend to grant genetic traits that may be advantageous to survival of the bacteria replicating it, as is often exemplified by multiple antibiotic resistance genes present on these extra-genomic entities. The plasmid pKM101 further contains the genes *mucA*, *mucB* (nt postions 24403-26607 in Figure 9) and *uvp1* (see Figure 9, nt position 21483-22076),

which have been shown to enhance bacterial survival following UV radiation due to their activation upon DNA damage as part of the SOS response system (Elledge & Walker, 1983; Gigliani et al., 1989). The activity of these genes further results in higher survival rates and enhanced mutagenesis in response to chemical mutagens; therefore, pKM101 has been introduced in the Ames *Salmonella* tester strains to asses the carcinogenic properties of chemical agents (McCann et al., 1975).

The two *tra* regions are important for conjugal transfer of pKM101, located between base pairs 35238-4149 transcribed in clock-wise orientation, and base pairs 6477-15807 transcribed in counter clock-wise orientation (see Figure 9, Winans & Walker 1985).

The larger region contains the genes encoding for a T4SS and its pilus, which is essential for conjugation. A total of 11 genes is postulated to be necessary to form the double-membrane spanning protein complex. The proteins named TraA through to TraG and TraL through to TraO (VirB1-11) are thought to form the T4SS, including an extracellular pilus that is composed TraM/VirB2 and TraC/VirB5, and two ATPases (TraB/VirB4 and TraG/VirB11) to fuel the DNA—protein substrate transport (reviewed in Alvarez-Martinez & Christie (2009), see Figure 10).

The proteins TraN/VirB7, TraO/VirB9 and TraF/VirB10 have been shown to form the core complex of the pKM101 T4SS, spanning the periplasm and inserting in both the inner and outer membrane of *E. coli* (Fronzes et al., 2009b).

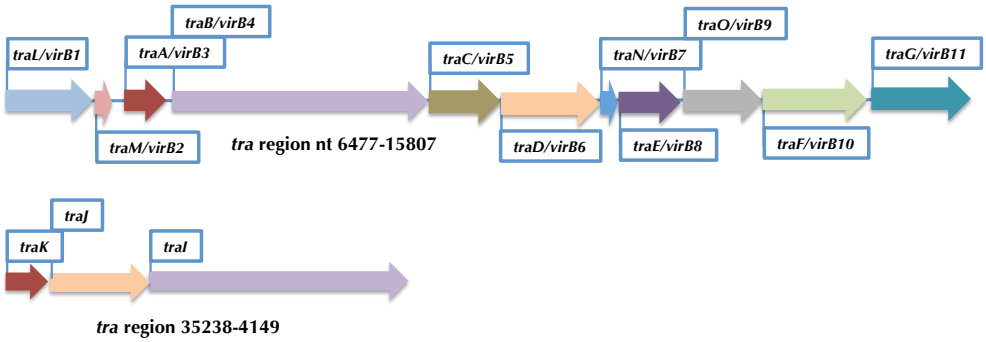

Figure 10. Schematic depicting the organisation of *tra* genes in pKM101.

The shorter region encodes the genes *traK, traJ* and *traI* (see Figure 10), which are thought to form the relaxosome of this conjugation system. TraI is homologous to the relaxase TrwC of the pR388 conjugation system (see Introduction chapter), while TraK is thought to correspond to the relaxase enhancer activity of TrwA in pR388. In the pKM101 conjugation system, the protein TraJ contains Walker A and B motifs, and is thought to play the role of the T4CP (homologous to the ATPase TrwB in pR388), being responsible for the recruitment of the DNA—relaxase substrate to the T4SS for secretion. The pKM101 *oriT* region (*KoriT*) is located 3′ adjacent to the relaxosome operon and partly overlaps with the coding sequence of *traK*.

The plasmid pKM101 encodes for many genes that are unrelated to the conjugation process, as has been described above. Only approx. 30% of the plasmid actually encodes for what is thought to be the T4SS and Relaxosome moieties. However, it is still unknown whether some of the genes outside the T4SS and Relaxosome regions are required for conjugation or whether the T4SS

and Relaxosome regions are sufficient to drive conjugative transfer. The aim of this project is to (i) determine the minimal genetic requirements for conjugation; (ii) generate a genetically tractable T4SS, which can be (iii) produced for imaging purposes using electron microscopy or fluorescence microscopy and (iv) provide a simple assay in which structure-function relationships derived from structure can be assessed by site-directed mutagenesis of various T4SS components.

3.1 The overexpression construct pKT4SS_B10cS

The genes to build the conjugation machinery were divided according to their natural operon organization on pKM101, i.e. the T4SS components and the relaxosome components were cloned on two separate vectors compatible for co-expression. The pKM101 *oriT* sequence (*KoriT*) was cloned onto a third compatible vector, whose transfer can be monitored by antibiotic resistance. If the VirB1-11 homologues, the coupling protein TraJ/VirD4, the relaxase TraI and the enhancer TraK are sufficient for conjugation, the expression of these proteins should mobilise a *KoriT*-containing plasmid and mediate its conjugation into a recipient cell.

3.1.1 The expression vectors

The most important consideration when choosing the expression vectors was that they have compatible origins of replication, meaning that the origins of replication cannot be similar or the same on the three vectors.

The vector pAsk-IBA3C (IBA Lifesciences) was chosen to harbour the T4SS operon, as it has been used to successfully overexpress the T4SS core complex of pKM101 (Fronzes et al., 2009b). It provides Cam resistance and protein expression is under the control of the *tet* promoter, inducible using tetracycline derivatives such as AHT or 4-epitetracycline. It harbours the *f1* origin of replication.

The vector pCDFDuet-1 (Novagen) was chosen to harbour the Relaxosome operon, and contains the CloDF13 replicon. The vector provides Spec resistance and is inducible via the T7 promoter. In an *E. coli* BL21 background, the T7 polymerase can be induced using the allolactose analogue IPTG, which then facilitates transcription of the T7 promoter.

The pRSFDuet-1 vector is similar to the pCDFDuet-1, but harbours the RSF1030 origin of replication. This vector was used to clone the *KoriT* sequence, and provides Kan resistance. Protein production from this vector is also T7 promoter driven and IPTG inducible in an *E. coli* BL21 background; however, this was irrelevant here as no proteins were expressed from this vector.

3.1.2 The constructs pKoriT, pKRelax and pKT4SS_B10cS

pKoriT

The *KoriT* sequence (650 bp) was amplified from pKM101 by PCR as described in Methods and ligated into pRSFDuet-1. The resulting construct will provide Kan resistance and is depicted in Figure 10-1.

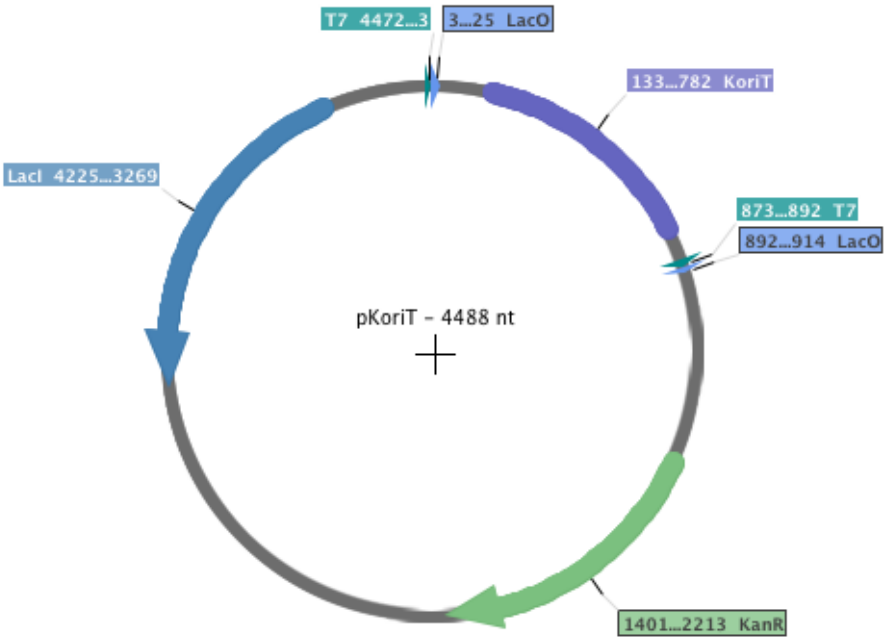

Figure 10-1. Plasmid map depicting the features of pKoriT. The plasmid contains the *oriT* region of the pKM101 plasmid (purple), and confers Kanamycin resistance (green). It further contains two T7 promoters and two *lac* operator sequences, as well as the coding sequence of the lac repressor *lacI* (blue).

The PCR products shown in Figure 11A correspond to the expected size for the *KoriT* sequence, which is 667 bp. The DNA was extracted from a 1% agarose gel, then *Asc*I treated and ligated into *Asc*I-digested pRSFDuet-1 as described in Methods, section 2.6.5. The ligation reaction was transformed into *E. coli* Top10 cells and analysis of Kan^R colonies by colony PCR showed *KoriT* presence in clone pKoriT #9 (data not shown). Subsequent analysis by Sanger sequencing showed the correct ligation of *KoriT* into pRSFDuet-1, resulting in the plasmid pKoriT.

pKRelax

The operon containing the genes *traK*, *traJ* and *traI* (5198 bp) was amplified from pKM101 and ligated into pCDFDuet-1. The resulting construct will position the *traKJI* operon under the control of the promoter P*lac*, which is inducible with the molecular mimic of allolactose IPTG, and provides Spec resistance (see Figure 10-2).

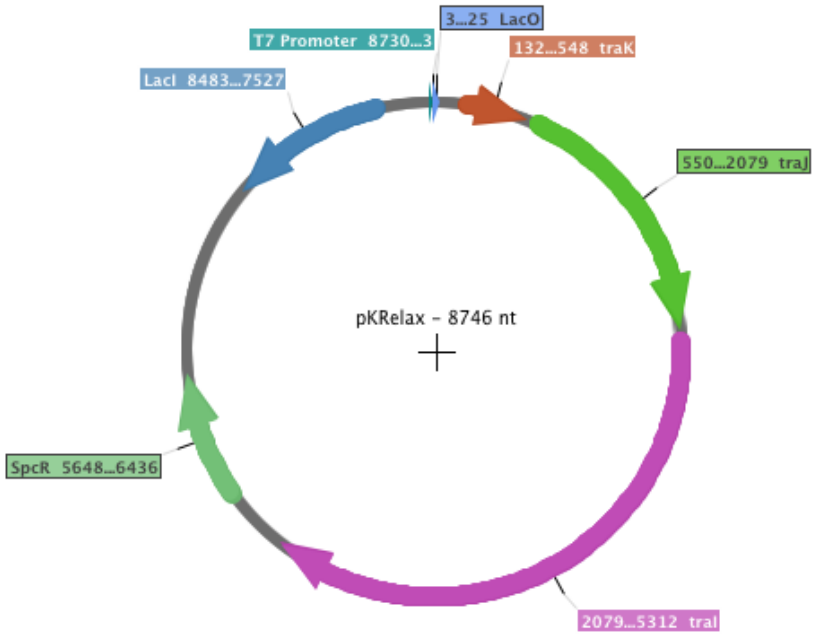

Figure 10-2. Plasmid map depicting the features of pKRelax. The plasmid contains the *traIJK* region, which is thought to form the relaxosome of the pKM101 plasmid under the control of T7 promoter, and confers spectinomycin resistance (green). It further contains the *lac* operator sequence, as well as the coding sequence of the lac repressor *lacI* (blue).

Figure 11B shows the PCR products amplified from the plasmid pKM101. The expected size for *traKJI* was 5198 bp. DNA fragments of several sizes were amplified during all PCR reactions; however, in both cases distinct fragments of the expected size were generated. Those fragments were subsequently purified from an agarose gel, *Asc*I/XhoI treated, ligated into *Asc*I/XhoI digested

pCDFDuet-1 and transformed into *E. coli* Top10 cells as described in Methods, section 2.4.2.

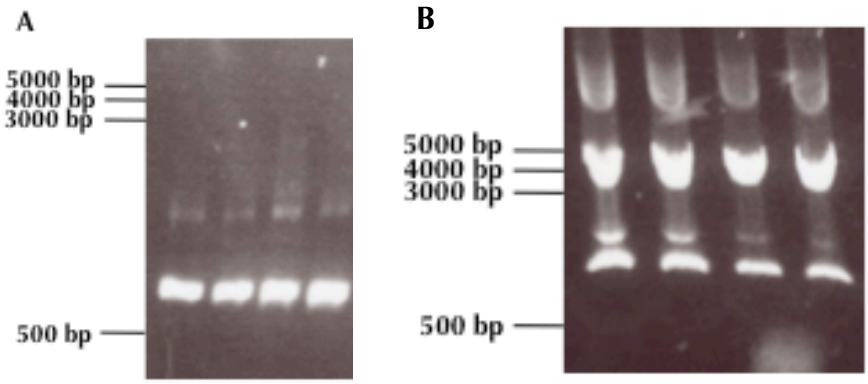

Figure 11. PCR products generated from pKM101 using (A) primers OpKoriT_*Asc*I_1F and OpKoriT_*Asc*I_2B and (B) traIJK_*Asc*I_1F and traIJK_*Xho*I_2B. The expected sizes of *KoriT* and the Relaxosome operon are 650 bp and 5198 bp, respectively.

Spec^R colonies were analysed by colony PCR using the primers otraJ_RT_1F and otraJ_RT_2B. The PCR reaction was expected to amplify a DNA fragment of 418 bp from the gene *traJ*. A fragment of this size could be amplified from clones #1-6, #9, #10, #12 and #13 (data not shown). The plasmids isolated from clones #3, #4, #9 and #12 were analysed by Sanger sequencing, which confirmed the correct ligation of the *traKJI* operon into pCDFDuet-1. Plasmid isolated from clone #4 was used for subsequent experiments.

pKT4SS_B10cS

Dr Harry Low kindly provided the construct pKT4SS_B10cS; it was generated using a restriction free cloning method after Van den Ent & Löwe (2006).

The construct contains the VirB1-VirB11 homologues from pKM101 from the ATG start codon of *traL/virB1* to the stop codon or *traG/virB11* under the control of the *tet* promoter cloned into pAsk-IBA3C, conferring Cam resistance. Protein production from this vector is induced via the *tet* promoter, using tetracycline derivatives such as AHT and 4-epitetracycline for induction. The plasmid further contains a Strep tag fused to the C-terminus of TraF/VirB10 (resulting in the protein TraF/VirB10cS), and the *KoriT* nick site cloned after *traG/virB11*.

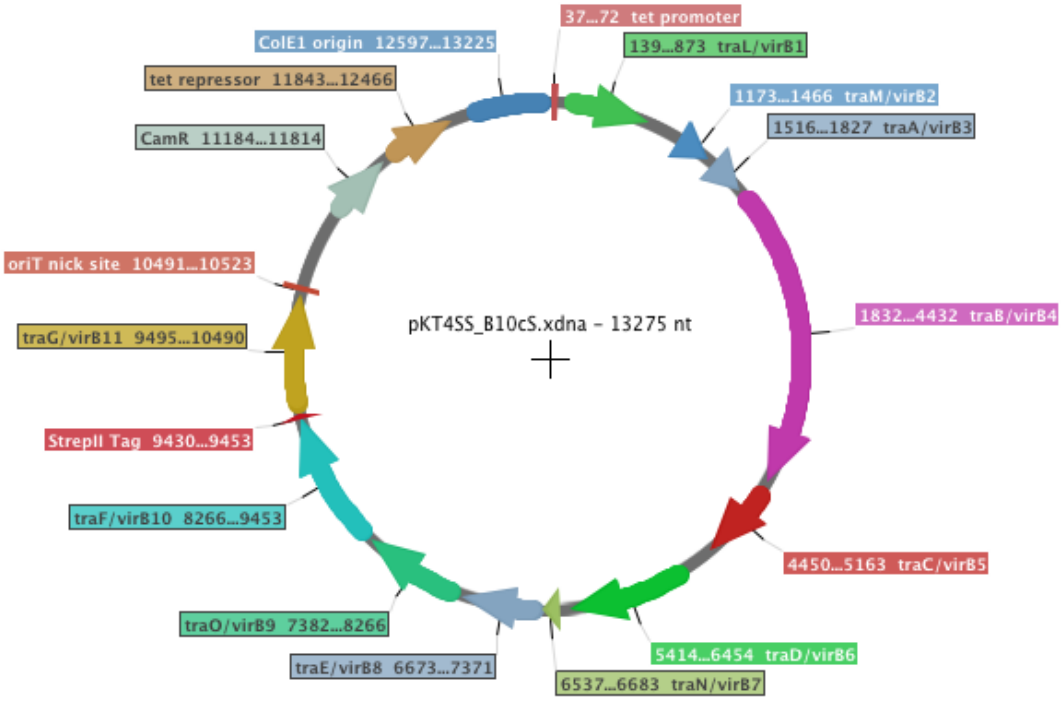

Figure 11-1. Plasmid map depicting the features of pKT4SS_B10cS. The plasmid contains the *tra* region, which is thought to form the Type IV Secretion System of the pKM101 plasmid under the control of the *tet* promoter, and confers chloramphenicol resistance. It further contains the tet repressor sequence, as well as the *oriT* nick site.

3.1.3 Conjugation assay pKT4SS_B10cS, pKRelax and pKoriT

The conjugation assay determines the transport of a plasmid from a donor cell to a recipient cell by assessing the antibiotic resistance of cells. It is paramount for this assay that donor and recipient strains are distinguishable by distinct antibiotic resistance genes. If a plasmid is transported during conjugation, this will result in a strain with a new combination of antibiotic resistance, forming the so-called transconjugant colonies. The *E. coli* strain DH5 α carries the Nal resistance on its genome, which makes this strain very convenient as a recipient strain because it is not a commonly used antibiotic in cloning vectors. *Escherichia coli* strain DH5 α was therefore used as a recipient strain throughout the work presented here.

Initially, it was important to determine whether the cognate pKM101 conjugation machinery will mobilise pKoriT for transport. Conjugation assays were performed to analyse whether the native pKM101 plasmid will suffice to transport the *KoriT*-containing pKoriT construct to a recipient cell.

For this purpose, the donor strain *E. coli* HB101 containing pKM101 was co-transformed with pKoriT or pRSFDuet-1 (serving as a negative control), leading to Amp^R/Kan^R donor strains. The conjugation assay was performed as described in Methods, using *E. coli* strain DH5 α (Nal^R) as the recipient strain. Nal^R/Kan^R transconjugant colonies could only be observed when conjugation was performed with pKM101- and pKoriT-containing cells, whereas no Nal^R/Kan^R colony growth was observed upon DH5 α conjugation with pKM101- and pRSFDuet-1-containing HB101 cells.

The conjugation culture of DH5α with pKM101 and pRSFDuet-1 was further plated on Nal/Amp containing media to test for functionality of pKM101 transfer, where ample transconjugant colony growth could be observed. This experiment served as a proof of principle that pKoriT is specifically recognised as substrate by the pKM101 T4SS.

To test whether the plasmid pKT4SS_B10cS is conjugation proficient, cells were co-transformed with the constructs pKT4SS_B10cS, pKRelax and pKoriT, resulting in a donor strain that is $Cam^R/Spec^R/Kan^R$. Over-night cultures of donors and DH5α were diluted into fresh LB medium without antibiotics, and grown shaking at 37° C. At an OD_{600} of approximately 0.3, 4-epitetracycline or AHT and IPTG were added to the culture to varying final concentrations. After 1 h conjugation time, the pKoriT transfer efficiency was determined by counting Nal^R/Kan^R colonies.

The plasmids pKT4SS_B10cS, pKRelax contain all the genes we hypothesised might be necessary for conjugation; however, initial experiments co-expressing the plasmids pKT4SS_B10cS, pKRelax and pKoriT and induction with 1 µg AHT and 1 mM IPTG did not lead to Nal^R/Kan^R transconjugant colonies.

The induction of protein expression may influence the correct assembly of the T4SS, as well as the timing of the experiment upon induction. An induction experiment using the inducers AHT, 4-epitetracycline and IPTG in varying concentrations was conducted to assess this possibility. AHT induces the *tet* promoter by irreversibly binding the Tet repressor protein, while 4-epitetracycline binds the tet repressor in a reversible fashion. An induction with 4-epitetracycline is therefore thought to be weaker than induction with AHT.

4-epitetracycline concentrations of 0.7 µg, 0.5 µg and 0.1 µg with a constant IPTG concentration of 0.5 mM were tested, as well as AHT concentrations of 0.7 µg, 0.5 µg and 0.1 µg with a constant IPTG concentration of 0.5 mM. Further, the experiment included varying IPTG concentrations of 0.7 mM, 0.5 mM and 0.1 mM IPTG with a constant AHT concentration of 0.5 µg. No Nal^R/Kan^R transconjugant colony growth could be observed under any of the above-mentioned conditions (data compiled in table 6-1).

Table 6-1. Induction experiments using the inducers IPTG, 4-epitetracycline and anhydrotetracycline in varying concentrations, conducted with cells transformed with pKT4SS_B10cS + pKRelax + pKoriT.

Inducer			**Transconjugants**
IPTG [mM]	4-epitetracycline [µg]	Anhydrotetracycline [µg]	
0.5	0.1	-	0
0.5	0.5	-	0
0.5	0.7	-	0
0.5	-	0.1	0
0.5	-	0.5	0
0.5	-	0.7	0
0.05	0.1	-	4
0.1	0.1	-	0
0.25	0.1	-	0
0.5	0.1	-	0

During the above-described experiment, whole cell samples were taken for Western Blot analysis using anti-Strep antibodies to analyse whether the TraF/VirB10cS protein is expressed (see Figure 12). The samples contained

similar amounts of whole cells according to OD_{600} measurements, and and samples were prepared as described in Methods. The TraF/VirB10cS protein is expected to be approx. 40 kDa in size.

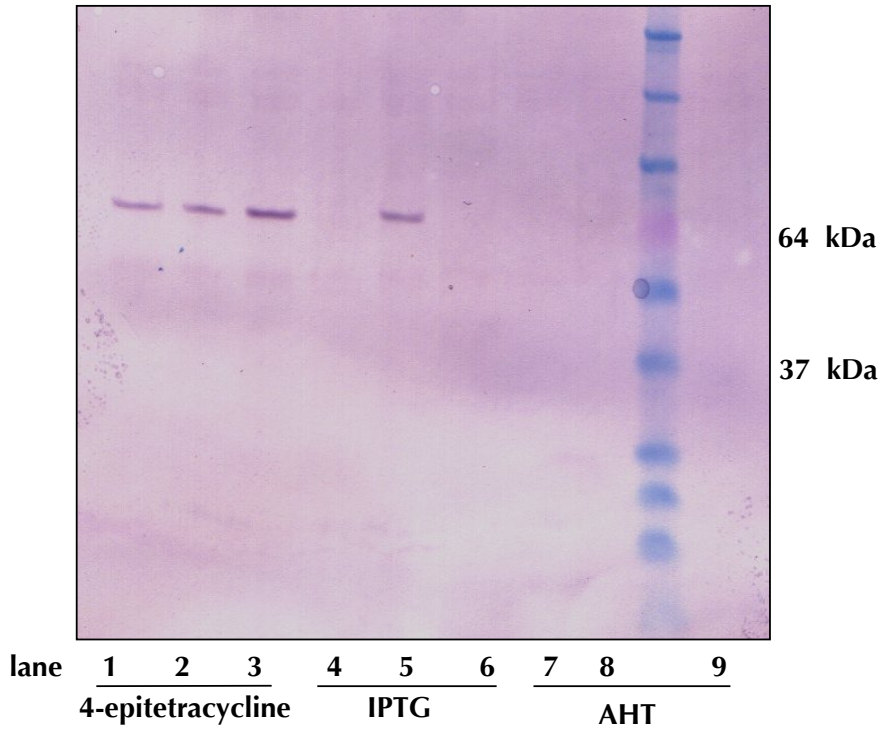

Figure 12. Western Blot using anti-Strep antibodies of samples taken during conjugation assay with varying concentrations of inducer. Lanes 1-3: 0.5 mM IPTG and 0.7 µg 4-epitetracycline (lane 1), 0.5 µg 4-epitetracycline (lane 2), 0.1 µg 4-epitetracycline (lane 3). Lanes 4-6: 0.5 µg AHT and 0.7 mM IPTG (lane 4), 0.5 mM IPTG (lane 5), 0.1 mM IPTG (lane 6). Lanes 7-9: 0.5 mM IPTG and 0.7 µg AHT (lane 7), 0.5 µg AHT (lane 8), 0.1 µg AHT (lane 9).

A specific signal for the Strep tag can be observed in cell samples in lanes 1, 2, 3 and 5 (Figure 12), running at a size of approximately 60 kDa. The pre-stained protein marker used in this experiment was calibrated using mass

spectrometry data and it was confirmed that in the gel system used TraF/VirB10cS indeed runs at approx. 60 kDa. The behaviour of the marker proteins may be influenced by the dye used. The specificity of the signal is high; therefore, it can be assumed that the Strep tag signal corresponds to the TraF/VirB10cS protein. The Strep tag signal present in lane 5 is inconsistent with the result presenting in lane 8, since identical induction conditions (0.5 mM IPTG and 0.5 µg AHT) were used in both cultures.

The most consistent results were observed in the 4-epitetracycline induction series, with the highest level of expression observed at low 4-epitetracycline and medium IPTG concentration (lane 3). Consequently, a conjugation experiment was undertaken using 0.1 µg 4-epitetracycline and varying concentrations of IPTG (0.05, 0.1, 0.25 and 0.5 mM) to induce the protein production. The conjugation assay resulted in four Nal^R/Kan^R transconjugant colonies on the 0.05 mM IPTG plate, and one on the 0.1 mM IPTG plate.

These colonies were analysed by colony PCR regarding the presence of *KoriT*, and the result is shown in Figure 13A. In lanes 1, 2 and 4, a PCR product corresponding to the expected size of 667 bp can be seen. These colonies were used to inoculate liquid Nal/Kan cultures, and plasmid was isolated from these cultures. The plasmids were digested with *Asc*I, and fragments of the expected sizes for pKoriT (3829 and 659 bp) were observed in all cases (Figure 13B). The additional smeared, large signal (exceeding 5000 bp) may be undigested pKoriT.

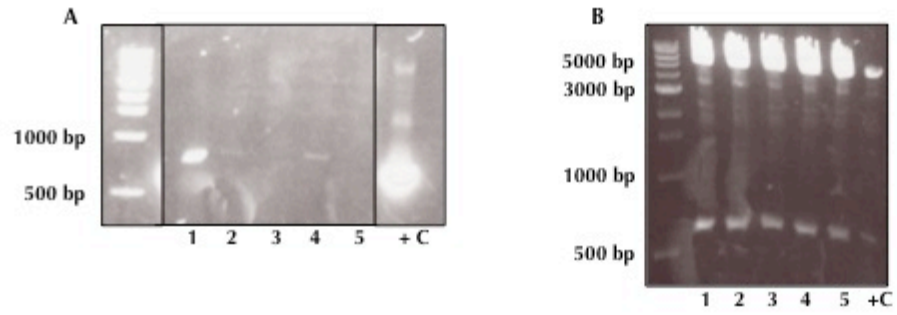

Figure 13. Analysis of transconjugant clones after conjugation assay with pKT4SS_B10cS, pKRelax and pKoriT. +C is the positive control where pKoriT was used as template DNA. **A)** Colony PCR with *KoriT* specific primers. Lanes 1-5 corresponds to clones 1-5. **B)** *Asc*I restriction digest of plasmid isolated from transconjugants clones 1-5 (lanes 1-5).

All subsequent conjugation assays were performed using 0.1 µg 4-epitetracycline and 0.05 mM IPTG. The assay was repeated in the same way 20 times without transconjugant colony growth on Nal/Kan-containing media.

All these assays were performed using the same strain co-transformed with the plasmids pKT4SS_B10cS, pKRelax and pKoriT. For the following conjugation assays, each culture was freshly transformed with the plasmids prior to performing the conjugation assay. One of the performed mating assays with fresh transformants resulted in many Nal^R/Kan^R, apparent transconjugant colonies; however, the presence of pKoriT in these transconjugants could not be determined by PCR or restriction digests. Furthermore, this result could not be reproduced in the following 46 mating assays with fresh transformants, or with the previously generated strain.

3.1.4 Generating pKT4SS_B10cS_oriT-rm

The putative *KoriT* nic site was included in the plasmid pKT4SS_B10cS following the 3′ end of *traG/virB11*. The possibility arises that the relaxosome would recognise and process pKT4SS_B10cS at this nic site, and thereby interfere with the expression of the T4SS proteins. Removing the *KoriT* nic site sequence from the plasmid should eliminate this possibility. The method of choice for this cloning step was the SLIM cloning method, designed for deletions (see Methods for a detailed description).

The plasmid was PCR amplified resulting in PCRs 1 (using oligonucleotides oFt_oriT-rm and oRs_oriT-rm) and 2 (using oligonucleotides oFs_oriT-rm and oRt_oriT-rm), each with an expected size of 13,246 bp. Figure 14A shows the PCR products after gel purification, which corresponded to the expected size.

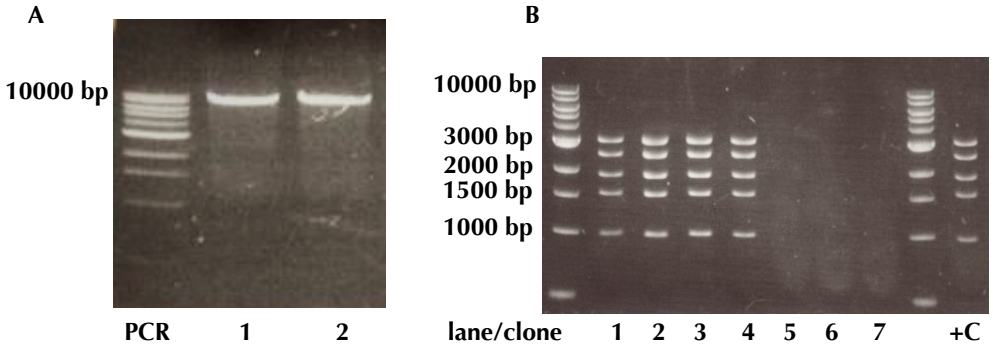

Figure 14. Cloning of pKT4SSB10cS_oriT-rm. **A)** PCR products obtained using primers oFt_oriT-rm and oRs_oriT-rm for PCR 1 (lane 1), and oFs_oriT-rm and oRt_oriT-rm for PCR 2 (lane 2) with template pKT4SS_B10cS, expected size is 13,246 bp. **B)** NdeI control digest of pKT4SS_B10cS_oriT-rm clones 1-7 (lanes 1-7, respectively) and positive control +C pKT4SS_B10cS. The expected pattern for pKT4SS_B10cS is 4212, 3319, 2493, 1975 and 1247 bp.

Both PCR products were then used for SLIM hybridization (see Methods chapter 2.6.2) and transformation.

Transformation of the SLIM hybridisation reaction into *E. coli* TOP10 resulted in the formation of only 7 colonies. Plasmid was isolated from each clone and digested with NdeI for analytical purposes, which is shown in Figure 14B. If the expected fragment pattern of 4212, 3319, 2493, 1975 and 1247 bp is observed, it is likely that the correct plasmid has been produced. Figure 14B shows the restriction pattern observed for the plasmids isolated from clones 1-7 corresponds to the expected pattern of pKT4SS_B10cS_oriT-rm.

In clones 1-4, the restriction digest shows the expected pattern for pKT4SS_B10cS_oriT-rm. However, it is impossible to distinguish the parent plasmid pKT4SS_B10cS from pKT4SS_B10cS_oriT-rm, since only 26 bp were removed. Additional Sanger sequencing of the plasmid isolated from clone 4 showed that the *KoriT* sequence had been removed successfully.

3.1.5 Conjugation assays with pKT4SS_B10cS_oriT-rm, pKRelax and pKoriT

The plasmid pKT4SS_B10cS_oriT-rm was transformed into electrocompetent *E. coli* BL21Star™ cells, since transformation of this clone into the BL21 strain did only result in very small colonies that did not grow in liquid media. *Escherichia coli* BL21Star™ cells are engineered for higher messenger ribonucleic acid (mRNA) stability due to a mutation in the *rne*131 gene encoding RNaseE. Transformation of pKT4SS_B10cS_oriT-rm into the BL21Star™ strain did result in the formation of colonies in some occasions;

however, often no growth in liquid cultures could be achieved with some of these colonies.

Over-night cultures were prepared for subsequent generation of electrocompetent cells and co-transformation with pKRelax and pKoriT. of pKT4SS_B10cS_oriT-rm, plasmid was isolated from some of the over-night cultures and analysed by NdeI restriction digest as to whether they contain the correct plasmid. Figure 15 shows the NdeI-digested plasmids from isolated from four colonies (clones 1-4). Only plasmid isolated from clone 4 displayed the expected fragment pattern of 4212, 3319, 2493, 1975 and 1247 bp. The remainder of this over-night culture was used to inoculate the culture used for generating electrocompetent cells for co-transformation with pKRelax and pKoriT.

Generally, transformation and cell growth of pKT4SS_B10cS_oriT-rm proved to be difficult. Cells harbouring the plasmid pKT4SS_B10cS_oriT-rm showed slow growth, and no growth upon induction. On many occasions, no growth occurred upon inoculation of single colonies into 5 ml over-night cultures. These characteristics increased when co-transformed with the plasmids pKRelax and pKoriT, and in many cases no growth occurred upon inoculation with single colonies for overnight cultures.

$Cam^R/Spec^R/Kan^R$ colonies were used to inoculate over-night cultures, and used to inoculate the donor conjugation culture 1:10. They were grown to an OD_{600} of approximately 0.3 and protein production from P*tet* and P*lac* was induced by the addition of 0.5 µg 4-epitetracycline and 0.5 mM IPTG. Thereafter, no

culture growth could be observed. The conjugation assay was performed 2 h thereafter.

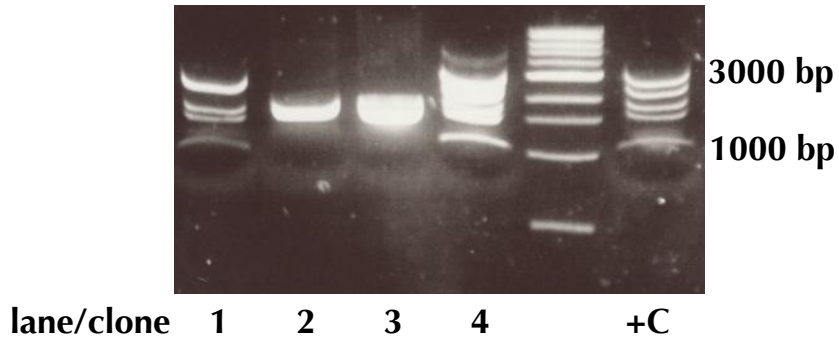

Figure 15. Control digest of pKT4SS_B10cS_oriT-rm isolated from BL21Star™ clones 1, 2, 3 and 4 with NdeI. The expected pattern for pKT4SS_B10cS_oriT-rm is 4212, 3319, 2493, 1975 and 1247 bp.

Cells were washed off the filter paper and diluted. Subsequently, they were plated on media selective for donors (Cam, Spec and Kan) and transconjugants (Nal and Kan).

NalR/KanR transconjugant colonies were obtained when *E. coli* BL21Star™ cells were co-transformed with the plasmids pKT4SS_B10cS_oriT-rm, pKRelax and pKoriT (see table 7). However, conjugation was still observed when no inducer was added to the cultures, although at lower rates.

Induction severely reduced the donor cell count on Cam-, Spec- and Kan-containing plates although similar amounts of donor cells were used in each repeat. The transconjugant cell count is similar in induced and not induced conjugation cultures.

Table 7. Conjugation efficiency pKT4SS_B10cS_oriT-rm + pKRelax + pKoriT induced and not induced. Conjugation efficiency equals the amount of transconjugants colonies divided by the number of donor colonies. Dilutions of each repeat were averaged to derive conjugation efficiency.

Induced	Repeat	Cell type	Approx. cell count/ml	Conjugation Efficiency
+	1	Transconjugants	361	0.06
		Donors	6123	
	2	Transconjugants	3123	0.4
		Donors	8484	
-	1	Transconjugants	$14*10^3$	0.007
		Donors	$2*10^6$	
	2	Transconjugants	707	0.0002
		Donors	$4*10^6$	

Plasmids isolated from transconjugant colonies were analysed by *Asc*I restriction digest, expecting fragments of 3829 and 659 bp for pKoriT. Although additional DNA fragments are visible after the digest, the plasmid pKoriT is present in the cells (see Figure 16). When conjugation cultures were plated on Spec and Nal, colony growth was also observed, pointing to the fact that pKRelax may also be transported during conjugation. This may be explained by the fact that the coding sequence for TraK overlaps with the a part of *oriT* sequence and is therefore present on pKRelax.

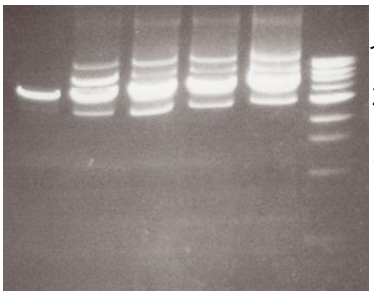

Figure 16. *Asc*I restriction digest of plasmid isolated from transconjugant colonies. Clones 1 and 2 were produced from induced cells, while clones 3 and 4 were produced from not induced cells. The positive control (+C) is pKoriT. Expected fragments for pKoriT: 3829 bp, 659 bp

3.2 The pKM101 deletion construct pKM101-*Xma*I

Since the conjugation assay with pKT4SS_B10cS did not result in reproducible mobilisation of pKoriT, and pKT4SS_B10cS-oriT-rm was notoriously difficult to propagate in *E. coli*, the possibility was to be examined whether other factors encoded on pKM101 may be of vital function during conjugation, or indeed maintain plasmid stability of T4SS containing plasmids. Therefore, we attempted to progressively remove some of the non-T4SS and non-Relaxosome regions in the native pKM101 plasmid while simultaneously testing for retaining its conjugation proficiency.

The *Xma*I restriction site is present twice on pKM101. *Xma*I cuts pKM101 at nucleotide position 4886 and 25322 (see Figure 17), resulting in two fragments of 20436 and 15836 bp in size. Genes that are thought to be important for replication (*repA* and its binding site), the Amp resistance gene (*oxa2*) and the *tra* region forming the T4SS will be located on the 20436 nt fragment. The

Relaxosome encoding genes and *KoriT* will be located on the 15836 nt fragment. In the event of an intramolecular re-ligation event of the 20436 nt fragment, a replication proficient plasmid conferring Amp^R should be formed, retaining the T4SS encoding genes.

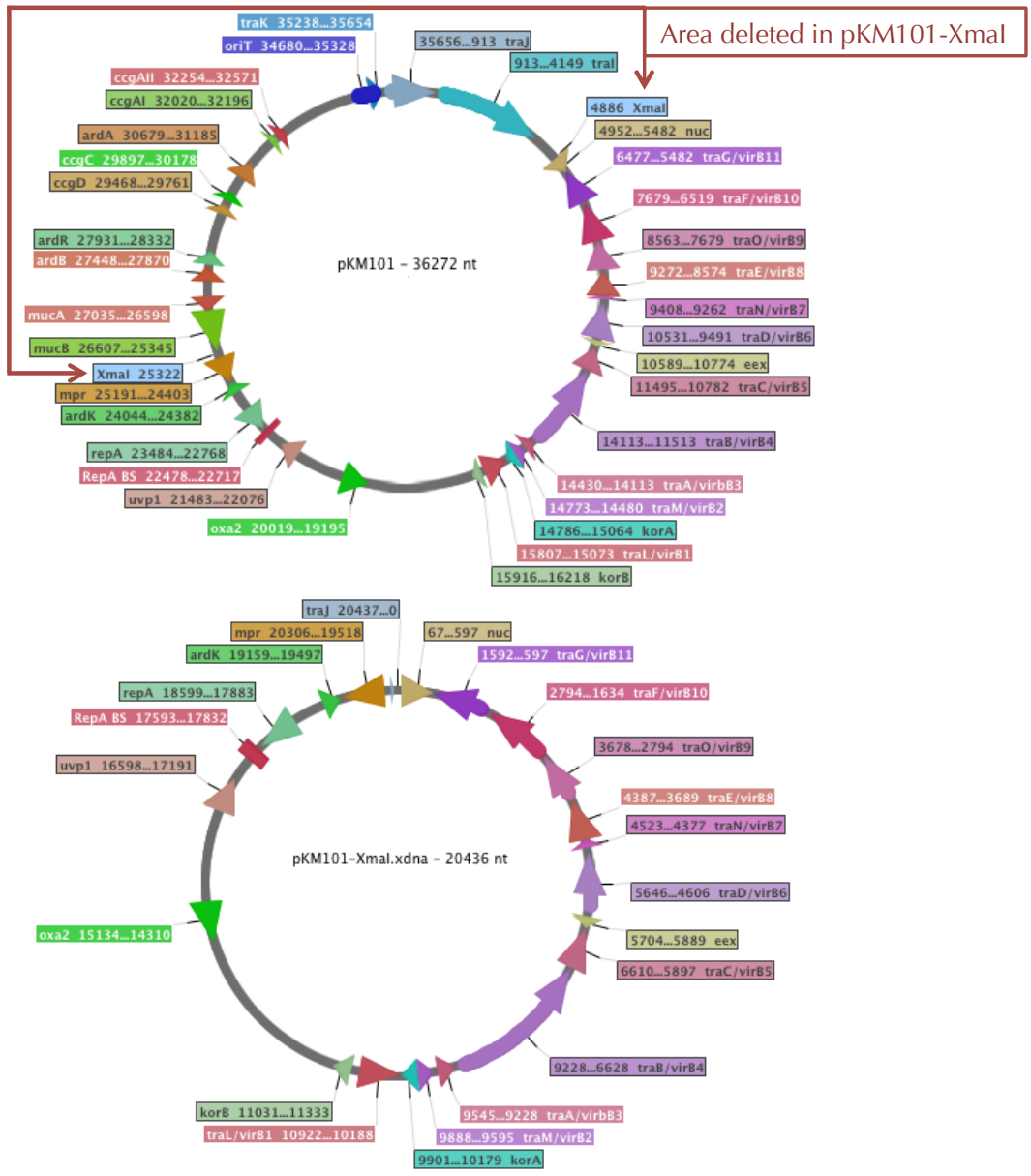

Figure 17. Plasmid map of pKM101 and the deletion variant pKM101-*Xma*I showing the differences of these two plasmids (T4SS *tra* region is displayed in pink/purple, and relaxosome *oriT* and *tra* regions are displayed in blue/cyan). Red arrow indicates the area in pKM101 which is not present in pKM101-*Xma*I.

Figure 17 shows the plasmid map of pKM101-*Xma*I in comparison to pKM101, where the deleted moiety if displayed by red arrows. The relaxosome components may then be complemented with pKRelax and pKoriT to form conjugation proficient *E. coli* strains, which allows for testing the functionality of pKRelax, as well as the modification relaxosome genes using PCR-based mutagenesis.

3.2.1 Generating pKM101-*Xma*I

The pKM101 deletion derivative pKM101-*Xma*I was generated as described in Methods. Figure 17A shows the *Xma*I digested pKM101 DNA before (lane 1) and after (lane 2) isopropanol precipitation. The expected sizes of fragments generated by *Xma*I digest were 20436 bp and 15836 bp, which approx. corresponds to the size of DNA fragments depicted in Figure 17A. It may be possible that the two fragments migrate as one band on the gel due to their large size, although the size difference between them is ca. 5000 bp. It is, however, unlikely that undigested plasmid is in this DNA sample, because such a species would migrate at a distinctly different size.

Transformation of the ligation reactions made with undiluted, 1:10, 1:100 and 1:1000 dilutions of *Xma*I-digested pKM101 DNA resulted in approx. 40 colonies on each plate. Liquid cultures for clones 1-4 (undiluted ligation), clones 5 and 6 (1:10 diluted), clones 7-10 (1:100 diluted) and clones 10-14 (1:1000) were inoculated; however, only clones 1-4 from the undiluted ligation plate grew in liquid, Amp-containing medium.

The total DNA was precipitated after from the restriction digest of pKM101 with *Xma*I, and used to set up the ligation reactions. Therefore, it is possible that either the complete pKM101 simply re-ligated from the two initial fragments, or pKM101-*Xma*I is formed upon intramolecular re-ligation of the 20436 bp fragment. PCR analysis was therefore performed to test for the presence of T4SS genes (present in pKM101-*Xma*I), and the absence of Relaxosome genes (not present in pKM101-*Xma*I).

PCR primers virB6/traD_RT_1F and virB6/traD_RT_2B specific for *traD/virB6* (see Table 4 and Figure 17, present in re-ligated pKM101-*Xma*I) and traI_RT_1F and traI_RT_2b specific for *traI* (see Table 4 and Figure 17, not present in re-ligated pKM101-*Xma*I) was performed to assess the resulting plasmids as to whether they are pKM101 or pKM101-*Xma*I. The plasmid pKM101 was used in comparison, and as positive control.

The results are shown in Figure 18B. All lanes containing a PCR reaction performed with *traD/virB6*-specific primers show a DNA fragment of the expected size (442 bp, Figure 18 lanes 1, 3, 5, 7 and 9) that is identical to the positive control (Figure 18B, lane 9). No PCR product was generated in any PCR reaction using *traI*-specific primers (Figure 18, lanes 2, 4, 6, 8 and 10).

Since the *traI*-specific PCR was also negative in the pKM101 positive control, the *traI*-specific PCR was repeated and additional relaxosome-specific PCR reactions were performed using *traJ*-specific primers (see Table 4 and Figure 16, traJ_RT_1F and traJ_RT_2B). The DNA isolated from the potential

pKM101-*Xma*I clones was used as template DNA, as well as pKM101 and pKRelax as positive control templates.

These results are shown in Figure 18C. In this case, a positive result for *traI* and *traJ* could be observed from the positive control plasmids pKM101 and pKRelax (expected sizes: *traI* – 605 bp; *traJ* – 439 bp, see Figure 18C, lanes 9-12), whereas no PCR products were generated when pKM101-*Xma*I was used as template (Figure 18C, lanes 1-8). The PCR results therefore show that a pKM101 variety was created that contains the *traD/virB6* gene, but neither the *traI*- nor the *traJ*- encoding regions.

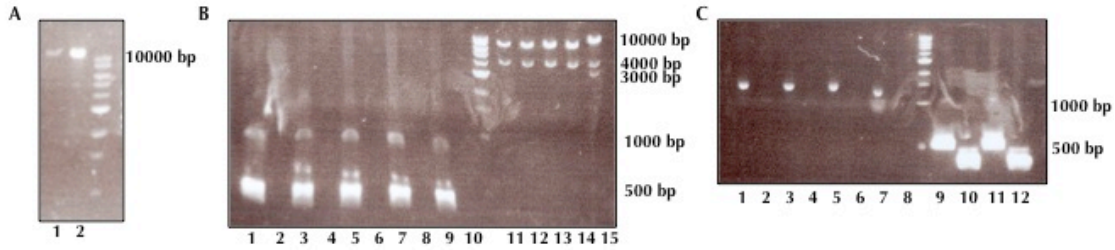

Figure 18. Generating pKM101-*Xma*I. **A)** pKM101 DNA after digestion with *Xma*I (lane 1: before isopropanol precipitation, lane 2: after isopropanol precipitation). **B)** *traD/virB6*- and *traI*-specific PCR reaction. Lanes 1 and 2: *traD/virB6* and *traI* PCR clone 1, lanes 3 and 4: *traD/virB6* and traI PCR clone 2, lanes 5 and 6: *traD/virB6* and traI PCR clone 3, lanes 7 and 8: *traD/virB6* and traI PCR clone 4, lanes 9 and 10: *traD/virB6* and *traI* PCR pKM101 (positive control). Lanes 11-14: *Kpn*I restriction digest of plasmid isolated from potential pKM101-*Xma*I clones 1, 2, 3 and 4 (expected fragment size: 14437 and 5999 bp). Lane 15: *Kpn*I restriction digest of pKM101 (expected fragment size: 25654, 5999 and 4619 bp). **C)** Repeated relaxosome specific PCR. *traI* and *traJ* specific PCR reactions for clone 1 (lanes 1 and 2), clone 2 (lanes 3 and 4), clone 3 (lanes 5 and 6) and clone 4 (lanes 7 and 8). Lanes 9 and 10: *traI* and *traJ* specific PCR reactions using pKRelax as template. Lanes 11 and 12: *traI* and *traJ* specific PCR reactions using pKM101 as template.

A restriction digest using the enzyme *Kpn*I was used to ascertain the PCR results that, indeed, pKM101-*Xma*I was generated. *Kpn*I was expected to generate two fragments of 14437 and 5999 bp when cutting pKM101-*Xma*I, while pKM101 digestion with *Kpn*I should generate three fragments of 25654, 5999 and 4619 bp in size. Figure 18B shows the result of the restriction digest. Three fragments were generated for pKM101 (Figure 18B, lane 15), while only two fragments are visible for the pKM101-*Xma*I clones 1-4 digestion (Figure 18B, lanes 11-14). The results show the expected fragment sizes for pKM101-*Xma*I, and we can assume that this deletion variant has been created successfully.

3.2.2 Conjugation assay with pKM101-*Xma*I, pKRelax and pKoriT

Initial experiments were undertaken to determine the conjugation efficiency of pKM101 for comparative purposes. *Escherichia coli* BL21(DE3) cells harbouring pKM101 were used as donor strains (Amp^R), and DH5 α cells were used as the recipient strain (Nal^R). Resulting transconjugant are expected to be Amp^R/Nal^R.

Conjugation assays were performed as previously described. The conjugation cultures were diluted 10^{-4}, 10^{-5} and 10^{-6}, and plated on LB agar containing Nal and Amp. The conjugation efficiency for pKM101 is approx. 0.5, as is shown in Table 8.

Table 8. Conjugation efficiency of the plasmid pKM101.

Cell type	Approx. cell count/ml	Conjugation efficiency
Transconjugants	$196*10^6$	0.5
Donors	$391*10^6$	

To analyse whether pKM101-*Xma*I will be able to facilitate transport of pKoriT when complemented with pKRelax, *E. coli* BL21(DE3) pKM101-*Xma*I cells were co-transformed with pKoriT, and either pRRelax or pCDFDuet-1, resulting in a donor strain that is Amp^R/$Spec^R$/Kan^R. Conjugation assays were performed as described previously and conjugation cultures were subsequently diluted, and plated on media containing NaI and Kan selecting for pKoriT transconjugants, and Amp/Spec/Kan for donors. Further, a BL21(DE3) donor strain harbouring pKM101 for pKoriT was used as a positive control.

The results are shown in Table 9. Cells containing pKM101 were able to transport pKoriT with wild-type efficiency (on average 0.9). Cells transformed with pKM101-*Xma*I and pKRelax still showed efficient transport of pKoriT, although the efficiency was slightly reduced (approx. 0.4). These results show that pKM101-*Xma*I is not conjugation proficient if no relaxosome components are present *in trans* (donor strain harbouring pKM101-*Xma*I, pCDFDuet-1 and pKoriT). Upon complementation with pKRelax, however, conjugation proficiency can be restored to almost wild-type level (donor strain harbouring pKM101-*Xma*I, pKRelax and pKoriT).

Table 9. Transport efficiency for pKoriT. Conjugation assay results from *E. coli* BL21(DE3) pKM101-*Xma*I + pKRelax + pKoriT, pKM101-*Xma*I + pCDFDuet-1 + pKoriT and pKM101 + pKoriT. Conjugation efficiency equals the amount of transconjugants colonies divided by the number of donor colonies. Dilutions of each repeat were averaged to derive conjugation efficiency.

Strain	Repeat	Cell Type	Approx. cell count/ml	Conjugation Efficiency
pKM101-XmaI + pKRelax + pKoriT	1	Transconjugants	$3.5*10^6$	0.3
		Donors	$11.4*10^6$	
	2	Transconjugants	$4*10^6$	0.4
		Donors	$10.7*10^6$	
	3	Transconjugants	$3.5*10^6$	0.4
		Donors	$8.3*10^6$	
pKM101-XmaI + pCDFDuet-1 + pKoriT	1	Transconjugants	0	0
		Donors	$0.7*10^6$	
	2	Transconjugants	0	0
		Donors	$0.7*10^6$	
	3	Transconjugants	0	0
		Donors	$0.7*10^6$	
pKM101 + pKoriT	1	Transconjugants	$2.5*10^6$	1.5
		Donors	$1.6*10^6$	
	2	Transconjugants	$0.9*10^6$	0.4
		Donors	$2.2*10^6$	
	3	Transconjugants	$3.6*10^6$	1
		Donors	$3.6*10^6$	

3.3 Further minimisation attempts of pKM101

The plasmid pKM101-*Xma*I is 20436 nt in size, and still contains many genes which are thought to be irrelevant for conjugation. Methods to accomplish large deletions from the chromosome usually use homologous recombination approaches. Such an approach could be used to further delete genes from pKM101, as well as pKM101-*Xma*I. One example is a study by Doublet et al. (2008), where such an approach was used to delete a pathogenicity island on the *Salmonella* genome.

In order to genetically access pKM101 and achieve a minimal conjugation system from the native pKM101 plasmid, attempts were made to modify pKM101 using such a homologous recombination-based method, the λ Red recombinase system (see Methods section 2.6.3). The method of choice was a one-step inactivation and deletion protocol based on PCR products published by Datsenko & Wanner (2000). The aim was to delete the region downstream of *repA* until the beginning of *KoriT* (nt positions 23484-34680 in Figure 9), which contains genes thought to be irrelevant for conjugation (see Figure 9). For this purpose, the PCR product del-pKM101 was generated, containing the 5′ and 3′ flanking regions of the deletion target at its 5′ and 3′ ends. Using the plasmid pKD3 as template and the oligonucleotides odel-pKM101_1F odel-pKM101_2B (see Table 4), a fragment of the expected size (1135 bp) could be generated (see Figure 19).

This PCR product was transformed into *E. coli* HB101 cells, which also contained pKM101 and pKD46-Gm. However, no Kan^R colonies could be generated if the cells were plated after 1 h of incubation. The culture that was

left at room temperature over night without antibiotics and subsequently plated on kanamycin-containing agar gave rise to four colonies. Liquid cultures were inoculated and plasmid DNA isolated; however, no DNA was visible on agarose gel electrophoresis.

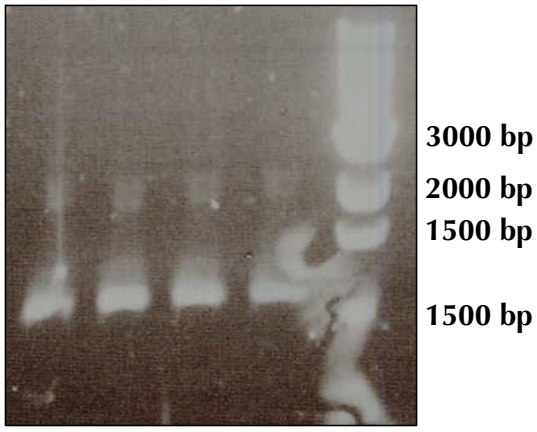

Figure 19. Four identical PCR products del-pKM101 to delete parts of pKM101 by homologous recombination (expected size 1135 bp).

Several attempts to generate Kan^R colonies using the λ Red recombinase system, such as varying donor strains from HB101 to Top10 (cannot metabolise arabinose) or changing induction conditions to higher arabinose concentrations did not result in Kan^R colonies.

3.4 The wild-type promoter construct pWT_KT4SS

Attempts at further trimming down the pKM101 using the λ Red recombinase system, and thereby establishing a method that could potentially be used for pKM101-*Xma*I, proved to be difficult. We therefore sought to investigate another way of identifying the minimal requirements for conjugative transfer.

We reasoned that one possibility for our failed attempts described in section 3.1 was that the proteins were over-expressed. Over-expression can be problematic, particularly because a number of T4SS and the T4CP are proteins inserting in the membranes and thus rely on specific machineries (the Sec or Tat complex for inner membrane proteins, and Bam complex for outer membrane proteins) to do so. By over-expressing the T4SS and relaxosome proteins, we might have incidentally clogged or jammed these machineries. Thus, we thought of revisiting the experiments described in section 3.1, but this time including the native promoters to drive protein expression.

The restriction enzymes *Asc*I and *Pac*I cut pKM101-*Xma*I once each at nt positions 325 and 13047 (see Figure 20). The *Pac*I restriction site is located approx. 2000 nt 5′ to the *virB1* start codon, and the *Asc*I restriction site is located approximately 250 nt 3′ to the *traG/virB11* stop codon. Digestion with those two enzymes will therefore result in two fragments of 12722 and 7714 bp in size, with the entire T4SS operon located on the 12722 nt fragment, including approx. 2000 bp upstream of the *traL/virB1* start codon. This additional region contains the coding region for *korB*, and should also contain the wild-type promoter region of the T4SS.

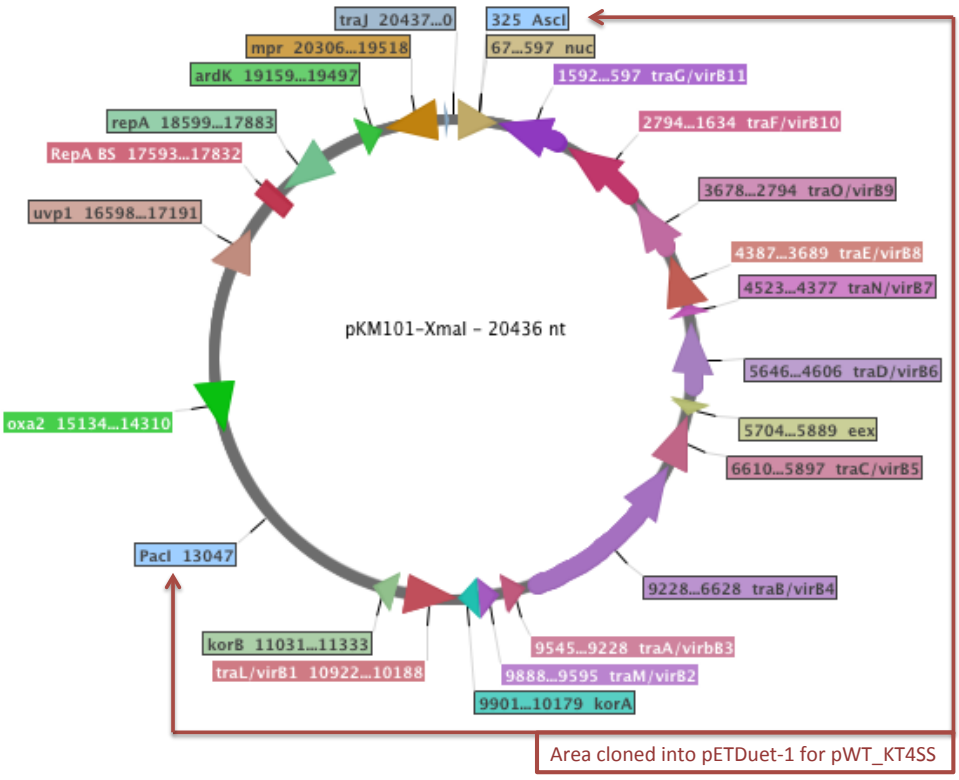

Figure 20. Plasmid map of pKM101-*Xma*I highlighting the *Pac*I/*Asc*I fragment (enclosed in red arrows) cloned into pETDuet-1 to form pWT_KT4SS.

This fragment could then be ligated into *Asc*I/*Pac*I cut replication and antibiotic resistance backgrounds, such as the vector pETDuet-1 (Novagen). The resulting plasmid would then be 17841 bp in size. If the plasmid were functional when complemented with pKRelax, it would mean a significant step towards making the pKM101 T4SS manageable. Although the size would not be much reduced, the T4SS would then reside in a well-defined vector background. From such a construct, the indigenous promoter would drive the T4SS production, while pETDuet-1 T7 promoter would not be used to drive the T4SS expression.

3.4.1 Generating pWT_KT4SS

The plasmid pKM101-*Xma*I was digested with the enzymes *Asc*I and *Pac*I, generating two fragments of 12722 and 7714 bp (see Figure 21). The larger fragment was gel extracted, ligated into *Pac*I/*Asc*I-digested pETDuet-1 and transformed into *E. coli* Top10 cells. Figure 21 shows an analytical *Pac*I/*Asc*I restriction digest of plasmids isolated from the resulting Amp^R colonies. Apart from plasmid isolated from clone 1, all plasmids show the expected fragment pattern of 12,722 and 5119 bp. PCR results specifically amplifying fragments from each of the *tra* genes thought to comprise the T4SS further confirmed that all genes from the *tra* operon are present on this plasmid (data not shown).

We can therefore assume that the plasmid pWT_KT4SS was created successfully.

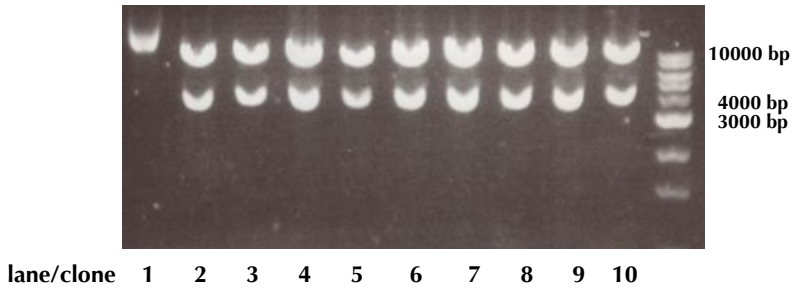

Figure 21. pWT_KT4SS restriction digest with *Asc*I and *Pac*I. Two fragments of 12,722 and 5119 bp are expected.

3.4.2 Conjugation assay with pWT_KT4SS, pKRelax and pKoriT

To test whether pWT_KT4SS contains all components necessary for conjugation, *E. coli* BL21Star™ cells harbouring pWT_KT4SS were co-transformed with the plasmids pKoriT, and either pKRelax or pCDFDuet-1. The resulting donor strain was $Amp^R/Spec^R/Kan^R$. Relaxosome production was induced with 1 mM IPTG at an OD_{600} of approximately 0.3. Culture growth was observed after induction, and the conjugation assay using DH5α as a recipient strain (Nal^R) was performed at a donor strain OD_{600} of approximately 0.6, at 1 h after induction.

Cells were washed off the filter paper and diluted. Subsequently, the conjugation cultures were plated on media selective for donors (Amp, Spec and Kan) and transconjugants (Nal and Kan). Table 10 shows the results of this experiment.

Complemented with pKRelax and pKoriT, pWT_KT4SS is conjugation proficient. Induction seems to affect the efficiency, as without induction it appears to be approx. 100 times lower (see Table 10). When conjugation cultures were plated on Spec and Nal, colony growth was also observed, indicating that pKRelax is also transported during conjugation (data not shown). The efficiency of pKoriT transport is similar to wild-type pKM101 and pKM101-*Xma*I complemented with pKRelax.

Table 10. Conjugation efficiency with pWT_KT4SS, pKRelax and pKoriT Conjugation efficiency equals the amount of transconjugants colonies divided by the number of donor colonies. Dilutions of each repeat were averaged to derive conjugation efficiency. N.d. = not determined

Strain	Repeat	Cell Type	Approx. cell count/ml	Conjugation Efficiency
Induced pWT_KT4SS + pKRelax + pKoriT	1	Transconjugants	$0.2*10^6$	0.01
		Donors	$28*10^6$	
	2	Transconjugants	$1*10^6$	0.4
		Donors	$2.5*10^6$	
Not induced pKM101-XmaI + pCDFDuet-1 + pKoriT	1	Transconjugants	$0.14*10^6$	0.0005
		Donors	$324*10^6$	
	2	Transconjugants	$0.07*10^6$	0.0003
		Donors	$202*10^6$	

3.5 Discussion

This project set out to determine the minimal requirements for conjugation with the pKM101 system, and to produce a T4SS expression platform, which is (i) fully functional in conjugation, (ii) genetically accessible and (iii) overproduced for structural studies.

The plasmid pKoriT was designed to monitor conjugation proficiency of a strain containing the further T4SS and relaxosome components by conferring Kan resistance. Initial conjugation experiments using *E. coli* strains co-transformed with pKM101 and pKoriT produced transconjugant colonies that were Nal^R/Kan^R, thereby confirming that pKoriT is indeed mobilisable by the pKM101 conjugation system.

The over-expression construct pKT4SS_B10cS did not reliably produce transconjugant colonies when co-transformed with pKRelax and pKoriT. Initial experiments using induction conditions of 1 µg AHT and 1 mM IPTG did not lead to Nal^R/Kan^R transconjugant colonies. An induction experiment using different inducer concentrations (4-epitetracycline and AHT for T4SS induction and IPTG for relaxosome induction) was conducted in combination with a Western blot testing for the expression of the *traF/virB10* gene. Although no transconjugant colonies were observed under any conditions in this experiment, the Western blot results showed that TraF/VirB10-expression was strongest in the 0.1µg 4-epitetracycline, 0.5 mM IPTG condition (see Figure 12). The Western blot experiment showed no signal for the varying AHT conditions using 0.5 mM IPTG (Figure 12, lanes 7, 8 and 9); however, a signal was obtained under the condition 0.5 µg AHT and 0.5 mM IPTG (Figure 12, lane 5). This condition is identical to the condition presented in Figure 12, lane 8. This inconsistency creates difficulties interpreting the results from these conditions; although, repeating the conjugation assay under conditions where the TraF/VirB10 Strep tag signal was strongest on the Western blot resulted in four transconjugant colonies. This result was, however, not reproducible.

Removing the *oriT* nic site from the plasmid facilitated the reproducibility of conjugation proficiency (see Table 7), but also drastically reduced cell viability. The conjugation efficiencies were approximately 0.06 and 0.4 for two repeats of induced pKT4SS_B10cS_oriT-rm, while the conjugation efficiency for not induced cultures was approx. 0.007 and 0.0002 for the two repeats. Notably, the donor cell counts for the induced cultures are 300-500 times lower than for

the not-induced culture, and the transconjugant cell count is also higher in the not-induced culture. The reason may be that more cells were used as input in the not-induced culture, although OD_{600} measurements were used to compare the culture's growth and similar mounts of cells were used according to these measurements. Further, no growth can be observed upon induction. It is therefore possible that the increased efficiency of induced cells may be attributed to the loss of donor cells upon induction. The induced donor cells might not be viable enough to divide after plating due to the stress of induction, but still be able to conjugate.

DNA restriction analysis of total plasmid isolated from transconjugant colonies showed multiple DNA fragments, compared to only two expected bands for pKoriT. This result indicates that pKRelax may also be transported during conjugation as the *oriT* sequence partially overlaps with the *traK* gene. The strongest band was, however, corresponding to the size expected for pKoriT (see Figure 13, +C pKoriT positive control). A further experiment where conjugation cultures were also plated on Nal/Spec containing media was conducted, and $Nal^R/Spec^R$ transconjugant colonies indicates that pKRelax was also transported to the recipient cells. The plasmid pKT4SS_B10cS_oriT-rm is genetically instable and difficult to transform, as was shown by restriction analysis of transformants (Figure 14) and transformant colonies often appeared small and did subsequently not grow in liquid media. The metabolic burden imposed on the bacteria by overexpressing the T4SS may be a contributing factor.

Further, a report by Winans & Walker (1985b) identified two lethal gene products on pKM101, previously named *kilA* and *kilB*. These gene products were later identified as being allelic to *traL/virB1* and *traE/virB8* (Pohlman et al., 1994; Moré et al., 1996). The authors further identified two promoter regions, one preceding *traL/virB1* and another immediately adjacent to *traN/virB7*, which are negatively regulated by the *korA* and *korB* gene products, thereby counteracting the lethality of *traL/virB1* and *traE/virB8*. The plasmid pKT4SS_B10cS_oriT-rm contains the *korA gene* (it lies between *traL/virB1* and *traM/virB2*), but not the *korB* gene (it lies between upstream of *traL/virB1*). The *korB* gene lays immediately antecedent to *traL/virB1* and was therefore not included in pKT4SS_B10cS. The absence of the negative regulator protein *korB* may cause further stress to the cells, as well as genetic instability of pKT4SS_B10cS_oriT-rm.

The above-discussed problems with the over-expression construct pKT4SS_B10cS suggests the possibility that other factors encoded on pKM101 are required for plasmid stability and efficient conjugation. Therefore, further plasmids were generated to achieve the reconstitution of the pKM101 T4SS, initially without overexpression. The aim was to minimise pKM101 in size to render it genetically accessible. Therefore, the deletion variant pKM101-*Xma*I was successfully created. Among other traits, the relaxosome and *oriT* moieties were deleted. The plasmid does therefore not retain self-transmissibility; however, it was shown that it is still conjugation proficient when complemented with pKRelax and pKoriT, but pKoriT was not transported when no relaxosome components were present (table 9). The plasmid is conjugation

proficient with comparable conjugation efficiencies to the wild-type pKM101 (table 8). While pKM101-*Xma*I is considerably smaller (20436 bp) than pKM101 (36272 bp), it is still too large for routine PCR-based modification and still contains many genes we believe to be irrelevant for conjugation. Attempts to establish a method to delete large regions from pKM101 using a λ Red recombinase approach having failed, we could not find a way to trim the pKM101-*Xma*I plasmid further. Thus, this approach was abandoned and another approach was selected to achieve a minimal T4SS.

Indeed, one of potential problems with our strategy of cloning out the *tra* genes and putting them in a different context, as described in section 3.1, is that all genes were under an artificial over-expressing promoter. What would happen if, instead, we clone out the *tra* genes and leave their expression control intact?

The deletion variant pKM101-*Xma*I opened the opportunity to sub-clone the *tra* operon encoding the T4SS into a pETDuet-1 vector using the restriction enzyme *Asc*I and *Pac*I. The resulting construct contained the entire T4SS, and an additional 2000 bp upstream of *traL/virB1,* putting the T4SS under wild-type promoter control. The construct is conjugation proficient when complemented with pKRelax and pKoriT (see table 10), and is also stably propagated in the cells. The reconstitution of a fully functional and genetically accessible T4SS was therefore successful, although no over-expression promoter has been included in the construct to date. The construct will be valuable for further analysis of the pKM101 conjugation system.

In the upcoming section, we investigate a conjugation system very similar to the pKM101, the pR388. Establishing a PCR-based assembly cloning method (InFusion™, see Methods, section 2.6.1) enabled the cloning of the entire *trw* operon of the pR388 T4SS, which was then used to further analyse the minimal T4SS. The minimal pKM101 T4SS will be followed up in the future using the InFusion™ method and sequential deletions of the 2000 bp upstream of *traL/virB1* will deliver further insights into the minimal T4SS.

4 Results II – The IncW Conjugation System pR388

Efforts to reconstitute a functional, overproduced T4SS using the pKM101 were hampered by plasmid instability and, possibly, the need for the gene *korB* located in the region upstream of *traL/virB1*.

Type IV Secretion Systems are highly versatile, and there are many homologous systems to be found, even among the conjugative T4SSs (Guglielmini et al., 2013). The T4SS of the self-transmissible plasmid pR388 is closely related to pKM101, and is comprised of the same amount of putative components (see Figure 22). This T4SS was chosen to further investigate the minimal requirements for conjugative transfer, and production of a reconstituted and overproduced T4SS, as it might not have the same regulatory necessities as the pKM101 T4SS.

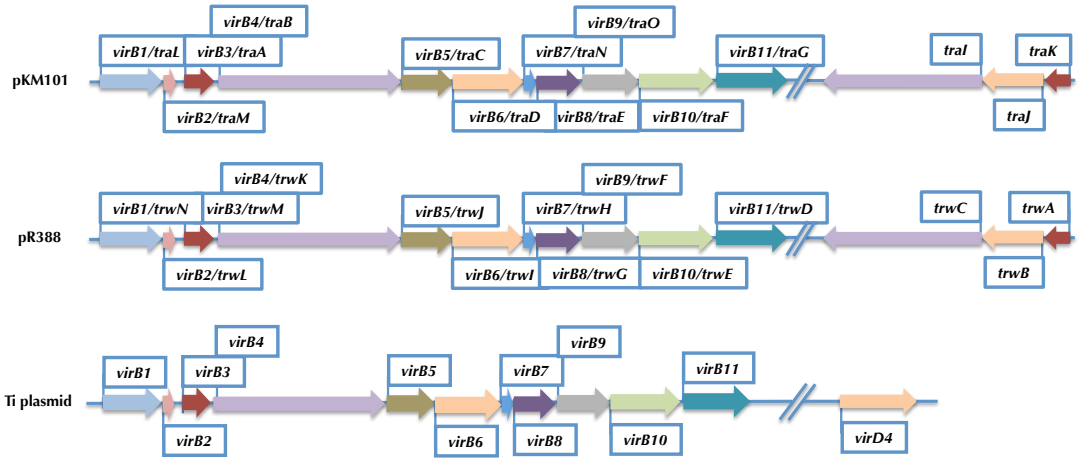

Figure 22. Relationship between conjugative plasmids pKM101 and pR388 with the Ti plasmid from *Agrobacterium tumefaciens*. Homologous genes are coloured similarly.

The plasmid pR388 belongs to the IncW group of self-transmissible plasmids (Couturier et al., 1988). Apart from the conjugation machinery, the plasmid pR388 encodes for antibiotic resistance to trimethoprim (*dfrB2*) and sulphonamides (*sul1*). Figure 23 shows the general organisation of pR388. The regions relevant for conjugal transfer on this plasmid have been mapped on two distinct regions, named Pil_W and Mob_W (Bolland et al., 1990). The region Pil_W has been identified to express the genes necessary for pilus formation, and is therefore likely to build the T4SS of the pR388 conjugation system.

The Mob_W region contains genes necessary for DNA mobilisation and comprises therefore the relaxosome components of the conjugation system. The Pil_W and Mob_W regions are transcriptional units, which are transcribed in opposite directions but located in close proximity (Figure 23).

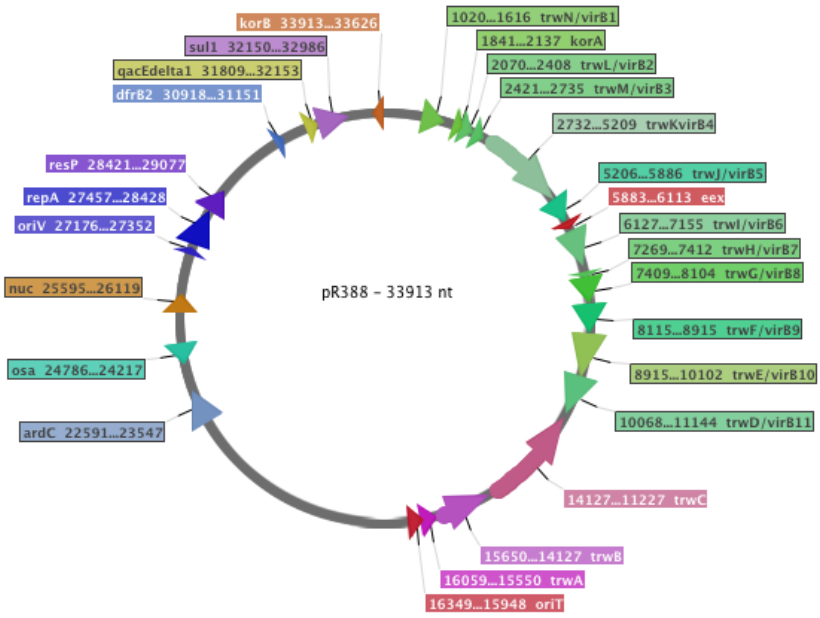

Figure 23. Plasmid map of pR388. The region previously termed PilW is pictured in green colours, the region previously termed MobW is depicted in pink.

As with pKM101 plasmid, a total of 14 genes organised in two operons are postulated to be involved in conjugation, and these are homologous to the T4SS and relaxosome components of pKM101. The two operons were termed *trw* and their genes named *trwA* through to *trwN* (see Figure 22). The operon *trwABC* encodes for the relaxosome genes, with TrwA expected to be the relaxase enhancer protein, TrwB the T4CP and TrwI the relaxase. The genes *trwD/virB11* to *trwN/virB1* are likely to encode the T4SS components. The organisation of the *trw* operons and the nomenclature relationship with the pKM101 conjugation system and the archetypal *A. tumefaciens vir* operon of the Ti plasmid is depicted in detail in Figure 22.

4.1 Examining the minimal requirements for conjugative transfer: generating the construct pRT4SS, pRRelax, and pRoriT

The approach to examining the minimal requirements for conjugative transfer was identical to the previously described efforts for pKM101, i.e. take the *virB* gene homologues and relaxosome-encoding genes out of the plasmid context and clone them into a laboratory plasmid. The two *trw* operons encoding the Relaxosome (Mob_W, *trwABC*) and the T4SS (Pil_W, *trwN/virB1-trwD/virB11*) were to be cloned on two separate, compatible vectors. As for pKM101, the vectors pAsk-IBA3C (confers Cam resistance) was chosen to express the T4SS, while the Relaxosome components were cloned into pCDFDuet-1 (confers Spec resistance). The pR388 *oriT* sequence (*RoriT*) was cloned into the pRSFDuet-1 vector, whose transport will be monitored by the transmission of

Kan resistance. Please see section 3.1.1 for a more detailed description of these expression vectors.

Previous efforts to clone the whole *trw* operon encoding for the T4SS of pR388 using a restriction-free cloning method have been unsuccessful (van den Ent & Löwe, 2006). Therefore, an entirely new approach was selected to carry out this challenging cloning exercise. The method of choice was the Gibson assembly, as described in Methods (Gibson et al., 2009). This powerful method allows the seamless joining of PCR products only requiring a 15 bp overlap at each end. Three enzymes catalyse the process (see Methods chapter, Figure 6).

For this purpose, the oligonucleotides otrwop_pAsk_IF_1F and otrwop_pAsk_IF_2B were used to amplify the entire Pil_W *trw* operon after the start codon of *trwN/virB1* until the stop codon of *trwD/virB11*, using pR388 as template DNA. A 15 bp overhang identical to the ATG region of the vector pAsk-IBA3C was added to the 5′ ends of each primer. The PCR product is expected to be 10125 bp in size and is shown in Figure 24A. The vector pAsk-IBA3C was PCR-amplified using the oligonucleotides opAsk-lin_ATG_1F and opAsk-lin_ATG_2B, and thereby linearized at the ATG start codon. The resulting PCR product is shown in Figure 24B and the InFusion™ reaction was performed as described in Methods.

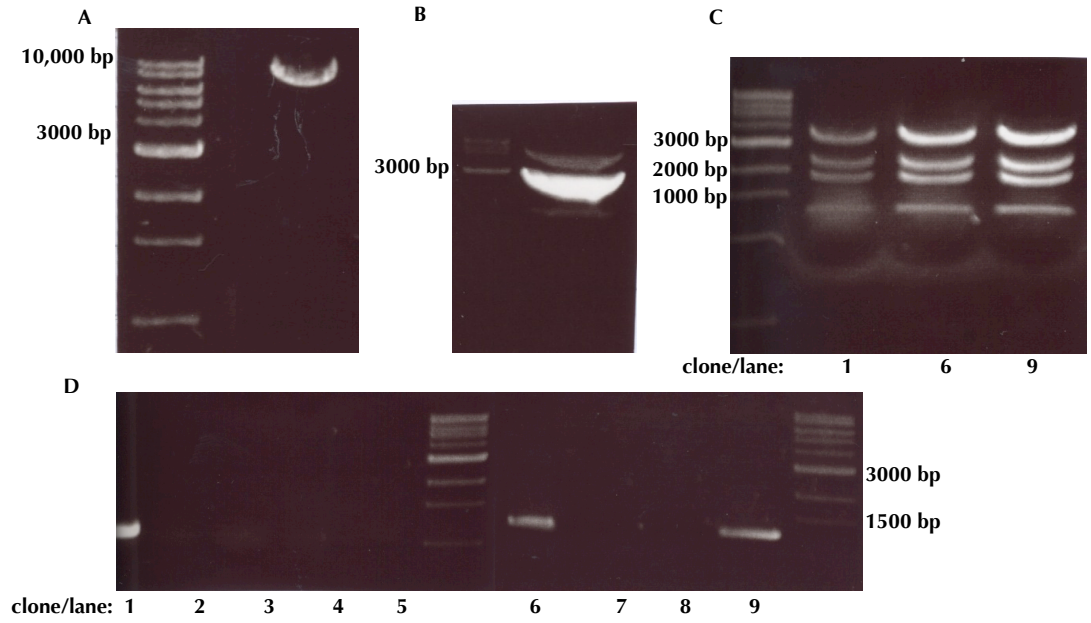

Figure 24. Cloning of pRT4SS. **A)** Gel purified PCR product amplified from pR388 using primers otrwop_pAsk_IF_1F and otrwop_pAsk_IF_2B. **B)** PCR product amplified from pAskIBA-3C using primers opAsk-lin_ATG_1F and opAsk-lin_ATG_2B. **C)** NotI/PvuII restriction digest of plasmid isolated from clones 1, 6 and 9. Expected size for pRT4SS: 5028, 3906, 2586 and 1603 bp. **D)** Colony PCR results for clones 1-9 using primers pASK-3C_1F_9100 and pAsk3C_SQ_2B. Expected size if pRT4SS is present: 1332 bp.

Colonies were screened by colony PCR using oligonucleotide primers pASK-3C_1F_9100 (gene specific primer for *trwD/virB11*) and pAsk3C_SQ_2B (binding on the vector after the *trw* operon if cloning was successful). Successful insertion of the trw operon should result in a PCR product of 1332 bp, while no PCR product should be obtained if the *trw* operon insertion was unsuccessful. Figure 24D shows the results for the colony PCR. A PCR product of approx. 1300 bp was generated from clones 1, 6 and 9. Plasmid from these clones was isolated and subjected to a restriction digest using the enzymes NotI and PvuII. A fragment pattern of 5028, 3906, 2586 and 160 bp

should be observed if pRT4SS was generated successfully. Figure 24C shows that the expected pattern was visible for DNA isolated from all three clones. Subsequent Sanger sequencing showed the correct assembly of all *trw* genes into the vector pAsk-IBA3C.

4.2 Conjugation assay with pRT4SS, pRRelax and pRoriT

As previously described for pKT4SS_B10cS, the conjugation assay determines the ability of a T4SS to transport an *oriT*-containing plasmid by assessing antibiotic resistances present in donor and recipient cells before and after conjugation. If a strain with the expected combination of antibiotic resistances occurs after conjugation, the T4SS under scrutiny can be assumed to function properly. In this work, the mobility of the *RoriT*-containing plasmid pRoriT, which confers Kan resistance, is monitored. The donor strain is resistant to Cam (from pRT4SS), Spec (from pRRelax) and Kan (from pRoriT), while the recipient strain DH5 α is Nal^R. If pRoriT is successfully transported by the T4SS, DH5 α transconjugant strains should appear which have newly acquired the pRoriT plasmid and are therefore Kan^R.

BL21Star™ DE3 was co-transformed with pRT4SS, pRoriT and pRRelax or pCDFDuet-1 (functioning as the negative control), thereby creating a $Cam^R/Spec^R/Kan^R$ donor strains. Overnight cultures for donors and DH5α recipient strains (Nal^R) were diluted and grown at 37° C with Cam, Spec and Kan to an OD_{600} of approx. 0.5. A total of 1 µg of 4-epitetracycline and 1 mM IPTG was added, and cells were incubated for another hour prior to performing

the conjugation assay. Cell cultures were washed in LB without antibiotics before mixing them for conjugation. Cells were then plated on LB agar containing Cam, Spec and Kan to select for donors (containing pRT4SS, pRRelax or pCDFDuet-1 and pRoriT), and on Nal and Kan to select for transconjugants.

Initial conjugation assays showed ample growth of Nal^R/Kan^R colonies when DH5α was conjugated with strains containing pRT4SS, pRRelax and pRoriT, and no Nal^R/Kan^R colony growth was observed when pRRelax was substituted with pCDFDuet-1; however, no donor colonies on plates containing Cam/Spec/Kan were observed on the equivalent dilutions. Analysis of plasmid DNA isolated from transconjugants by *RoriT*-specific PCR and *Asc*I restriction digest nevertheless showed presence of pRoriT in transconjugant colonies, as shown in Figure 25.

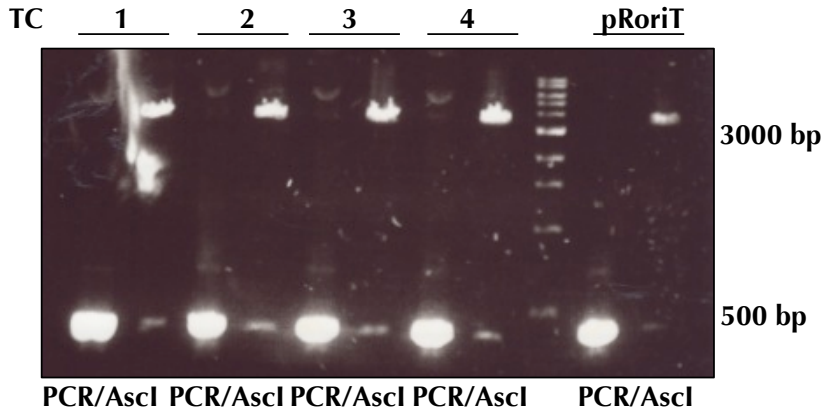

Figure 25. Analysis of DNA isolated from transconjugants 1-4 obtained from conjugation assay with pRT4SS, pRRelax and pRoriT by *Asc*I restriction digest and PCR specific for *oriT*. Expected pattern for *Asc*I digest: 3829 and 412 bp. Expected size of PCR fragment amplified with oligonucleotides opRoriT_*Asc*I_1F and opRoriT_*Asc*I_2B: 428 bp.

The DNA isolated from all transconjugants resulted the same pattern in PCR and *Asc*I restriction digest as the positive control of isolated pRoriT DNA. Since the strains carrying these plasmids were also resistant to Nal, it can be assumed that those are genuine transconjugants.

Further conjugation assays produced similar results. However, incubation of the donor plates for a longer time resulted in colony growth on the donor plates. They were, nevertheless, far fewer in numbers than transconjugant cells.

Experiments were conducted to assess whether the transport of pRoriT to the recipient cell results in loss of the plasmid in the donor strain due to a replication defect. Conjugation cultures were therefore plated on agar containing Cam only (selecting for donors harbouring pRT4SS), Cam and Spec (selecting for donors harbouring pRT4SS and pRRelax/pCDFDuet-1), and Cam, Spec and Kan (selecting for donors harbouring pRT4SS, pRRelax/pCDFDuet-1 and pRoriT). If pRoriT cannot be replicated after transport to recipient cells, donor colony growth should still be abundant on Cam and Spec containing plates. Further, the effect of adding inducer to the cell culture was investigated with the identical experiment, except that no 4-epitetracycline or IPTG was added to the donor culture prior to conjugation.

The results of this experiment are shown in Table 11. Plasmid loss after conjugation does not seem to occur, since the cell counts in donors and transconjugants do not reduce in the same proportion between the different antibiotics. Induction, however, seems to be majorly responsible for the reduction of donor cell counts, which is most likely due to the deleterious

effect of overproducing the T4SS and/or the relaxosome components. Growth however still occurs after induction in conjugation cultures.

Table 11. Conjugation assay cell counts to assess plasmid loss in donor cultures after conjugation, and influence of inducer added prior to conjugation assay on donor and transconjugant cell counts. Cam = chloramphenicol, Kan = kanamycin, Nal = nalidixic acid, TC = Transconjugants, D = Donors

Induction	Repeat	Cell type	Antibiotic on Plate	Cell count/ml	Conjugation Efficiency [TC/D]
+	1	Donors	Cam	$1.7*10^6$	82
			Cam + Spec	$1.1*10^6$	
			Cam + Spec + Kan	$0.9*10^6$	
		Transconjugants	Nal + Kan	$74*10^6$	
	2	Donors	Cam	$9.6*10^6$	29
			Cam + Spec	$6.3*10^6$	
			Cam + Spec + Kan	$2.8*10^6$	
		Transconjugants	Nal + Kan	$81*10^6$	
-	1	Donors	Cam	$64*10^6$	0.3
			Cam + Spec	$58*10^6$	
			Cam + Spec + Kan	$55*10^6$	
		Transconjugants	Nal + Kan	$16*10^6$	
	2	Donors	Cam	$72*10^6$	0.3
			Cam + Spec	$78*10^6$	
			Cam + Spec + Kan	$56*10^6$	
		Transconjugants	Nal + Kan	$17*10^6$	

The conjugation efficiency was determined as approx. 0.3 in not induced cultures, as opposed to approx. 50 on average in induced cultures. Conjugation efficiency was determined by donor colony count divided by transconjugant cell count. In this case, this efficiency calculation produced large numbers, as donor cells appear to die after conjugation. Ideally, transconjugant count would not exceed the donor count and therefore, the maximum efficiency should be 1. For future conjugation efficiency data, determining the total recipient count and using this number instead of donor cell counts to calculate the transport efficiency may result in more appropriate numbers, and better reflect the actual efficiency of conjugative transfer.

Conjugation assays were performed and cultures were subsequently also plated on LB agar containing NaI only. Colony count on those plates should correspond to the total DH5α recipient count added to the conjugation assay.

The results are presented in table 12 and show that using the recipient cell count for efficiency determination is more appropriate, as it shows how many times pRoriT is transported to a recipient cell.

Table 12. Conjugation experiment to compare efficiency numbers derived from division of transconjugant (TC) cell counts by either recipient (R) or donor (D) cell count, and to assess the influence of inducing agent 4-epitetracycline (EpiT) and IPTG.

EpiT + IPTG	Repeat	Efficiency TC/R	Efficiency TC/D
+	1	0.4	129
	2	0.35	108
-	1	0,03	0.5
	2	0.01	1.7

Further, recipient cells are not in contact with the inducing agent and are also not affected by it.

4.3 Additional functional studies: assessing pilus assembly

Another criterion for the establishment of a functional T4SS is the production of pili. The ability of the T4SS to form pili on the cell surface can be assessed by two methods. One would be electron microscopy, as pili have previously been visualised by such means (Bradley & Cohen, 1976). A simpler and more specific method would however be to employ bacteriophages for the task of assessing pilus assembly. Bacteriophages are bacterial viruses that infect a certain host, sometimes using a host-specific entry pathway. One such entry pathway can be a T4SS associated pilus, and some phages specifically infect cells harbouring a specific T4SS. Experiments using bacteriophage R17, which specifically infects host cells harbouring the F-like conjugative plasmids, have shown that a fully assembled relaxosome is required in the host cell to facilitate phage entry (Lang et al., 2011). A further criterion for phage adsorption and subsequent entry into the host is a fully assembled T4SS pilus (Valentine & Strand, 1965). Phage adsorption is further dependent on VirB5-like protein, and mutations can disrupt efficient phage infection even though conjugation is still functional (Yeo et al., 2003). Testing T4SS constructs for phage sensitivity may provide valuable insight into the assembly processes of the T4SS.

The pR388 conjugation system belongs to the IncW group of pili (Bradley & Cohen, 1976). The literature reports that bacteriophages PR3, PR4 and PRD1 use the pR388-associated pilus as their entry pathway into the host cell (Olsen et al., 1974; Bradley & Rutherford, 1975). The phages PR3 and PR4 were unavailable; therefore, the phage PRD1 was used in this study. Bacteriophage PRD1 is a broad host range icosahedral ds DNA phage that infects *Enterobacteriaceae* harbouring conjugative plasmids from the IncN, W and P incompatibility groups. The phage belongs to the Tectiviriidae family and contains a membrane below its capsid.

4.3.1 Assessing T4SS pilus visibility

The pR388 T4SS pilus is thought to be formed by the major subunit TrwL/VirB5 and TrwJ/VirB5, and pili had been observed in previous studies by Bradley & Cohen (1976) by staining whole cells with antibodies against pili. By overexpression of the T4SS with pRT4SS, pRRelax and pRoriT, the possibility arises that cells expressing the system could be multi-piliated. The appendages should be visible on the cell surface in the electron microscope. Whole cells from induced cultures were therefore loaded onto copper grids and the negative stain agent phosphotungstic acid titrated to pH 7 using potassium hydroxide (K-PTA) was applied. After a wash step in water, the grids were air-dried and images were acquired on the Tecnai T10 microscope. The images are shown in Figure 26A and B. Figure 26C shows an image of pR388 pili taken from Bradley & Cohen (1976) for comparative purposes. When taken

from liquid cultures, no pili could be observed on the cell surface (Figure 26A and B).

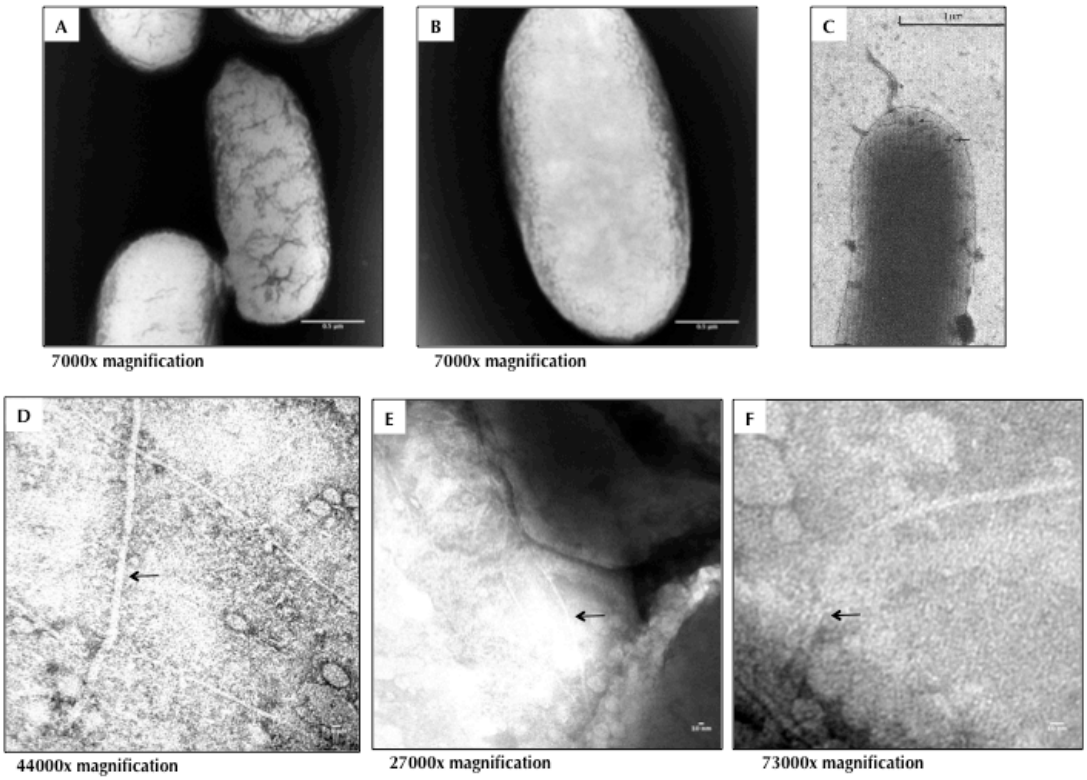

Figure 26. Negative-stain electron microscope images of whole *E. coli* cells. Arrows mark cell surface appendages. **A)** and **B)** Negative-stain electron microscope images of whole *E. coli* BL21Star™ DE3 cells expressing pRT4SS, pRRelax and pRoriT (scale bar 0.5 µm). **C)** Electron micrograph of *E. coli* CR34(R388) stained with antibodies against W-pili taken from Bradley & Cohen 1976. **D)**, **E)** and **F)** Negative-stain electron microscope images of whole *E. coli* BL21Star™ DE3 cells expressing pRT4SS, pRRelax and pRoriT during conjugation with *E. coli* DH5α (scale bar 10 nm).

W-pili belong to the group of rigid pili and conjugation is only efficient on solid surfaces (Bradley, 1980). A copper grid was therefore dropped face down onto a filter paper with conjugating bacteria and subsequently stained with K-PTA and air-dried immediately. Images were taken on the Tecnai T10 microscope and are shown in Figures 26D, E, and F. Appendages were visible

in all images shown, with Figure 26F showing an appendage protruding from the cell surface.

4.3.2 Phage susceptibility

The appendages visible between cells could be T4SS pili; however, they cannot be distinguished from other cell appendages such as flagella or other types of pili, e.g. Type I pili. Phage infection assays were carried out to further investigate whether these cells produce T4SS associated pili.

The phage assay was carried out as described in Methods. *Escherichia coli* BL21Star® cells were transformed with either pR388, pRT4SS + pRRelax + pRoriT, pRP4, or no plasmid and infected with PRD1 phage containing sterile-filtered lysate obtained from Professor Dennis Bamford, University of Helsinki. After over-night incubation, plaque formation was assessed.

In the initial experiment, plaques formed on all other plates where cells containing T4SS plasmids were, and no plaque formation was observed on the *E. coli* BL21Star® plate. Figure 26-1 shows the results of this experiment. Cells in Figure 26-1A are *E. coli* BL21Star cells and no plaques occurred on this plate, whereas on Figures 26-1B and C, where cells BL21Star were transformed with pR388 and pRT4SS + pRRelax + pRoriT, plaques in the cell lawn are clearly visible. Upon repetition, however, opaque plaques also appeared on the *E. coli* BL21Star® plates.

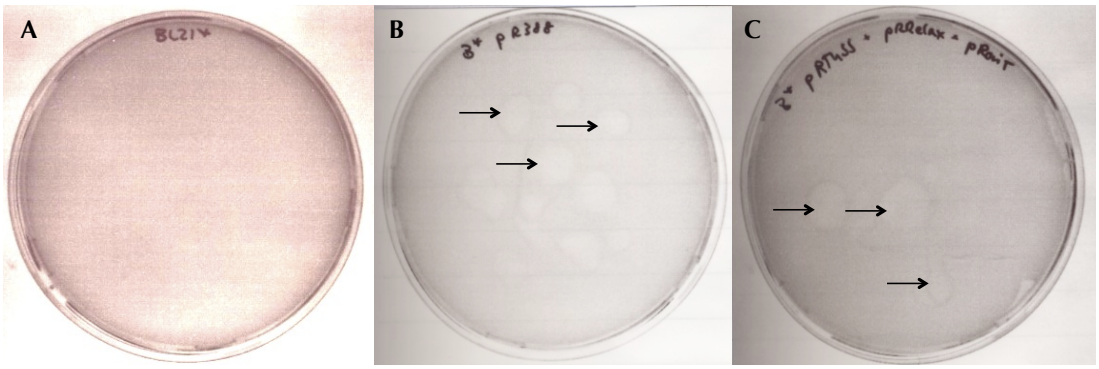

Figure 26-1. Phage PRD1 susceptibility assay. Black arrows indicate plaques formed by PRD1 infection. **A.** Plate containing a lawn of *Escherichia coli* BL21Star cells. **B.** Plate containing a lawn *Escherichia coli* BL21Star cells transformed with plasmid pR388. **C.** Plate containing a lawn *Escherichia coli* BL21Star cells transformed with plasmids pRT4SS + pRRelax + pRoriT.

A concentrically round plaque is formed by a single phage. PRD1 phage was therefore purified by re-isolation from clear plaques on plates using cells harbouring the plasmids pRT4SS + pRRelax + pRoriT. The procedure was performed for 10 individual plaques. The purified phage was then used to infect BL21Star cells with and without pRT4SS + pRRelax + pRoriT. Plaque formation on newly infected cell cultures were then assessed as to whether plaques were formed on cell cultures containing the plasmids pRT4SS + pRRelax + pRoriT, and not forming plaques on BL21Star® cells. Even though 3 further isolation steps were performed, no phage culture that only infected cells harbouring the T4SS could be isolated and opaque plaques were observed all BL21Star® plates.

4.4 Discussion

The above described results show that the pR388 T4SS was successfully reconstituted in an over-expression vector background. The minimal requirements for pR388 conjugation were delineated as being the genes *trwN/virB1-trwD/virB11*, as well as *trwABC*. Further, the plasmid pRT4SS is only 13123 bp in size, which is easily genetically tractable by standard PCR methods.

We showed that the plasmid pRT4SS is conjugation proficient when complemented with pRRelax and pRoriT. The conjugation efficiency of pRT4SS + pRRelax + pRoriT (approx. 0.4, see table 12) is comparable to that of wild-type pR388, which is published at approx. 0.4 when determined from transconjugant cell count per donor cell count (Guynet et al., 2011). Plasmid isolated from transconjugant colonies contained only pRoriT, which was shown by restriction digest (Figure 25). Presence of *RoriT* in transconjugants was further shown by specific a PCR amplifying *RoriT* (Figure 25). These experiments further outline the minimal requirements for conjugation as being the genes TrwN/VirB1 to TrwD/VirB11, as well as TrwA, TrwB and TrwC.

The donor cell-count after conjugation is consistently much lower than the recipient cell count (see Table 10), although equal amounts of cells were used according to OD_{600} measurements. This factor resulted in conjugation efficiencies largely exceeding 1, which could either be caused by donors transporting pRoriT to several recipients or impaired donor viability, with the latter being more likely.

The relaxase protein processes the plasmid pRoriT, and a single strand is transported to the recipient cell leaving single stranded pRoriT DNA in the donor cell that must be replicated. A replication defect of the *oriT* plasmid, or a partitioning defect may be the reason for poor donor cell survival. Donors are usually plated on Cam, Spec and Kan to select for pRT4SS, pRRelax and pRoriT. A plating experiment where conjugation cultures are plated on Cam only, Cam and Spec only, and Cam, Spec and Kan tested for possible plasmid loss. Donor numbers did, however, not significantly decrease with the different combinations of antibiotics (see Table 11).

The experiment further tested for the influence of induction on donor cell counts. The donor cell count was significantly higher in not-induced cells than in induced cell, and conjugation efficiencies reflect this tendency. While conjugation efficiency in not-induced cells was determined to be approx. 0.3, induced cells showed a conjugation efficiency exceeding 50. This is mainly due to lower donor cell counts compared to not-induced cells. When transconjugant cell counts are compared to recipient cell counts, the efficiency data suggests that induced cells conjugate approx. 10 times more efficiently than not-induced cultures (see Table 12), which makes the data more comparable to published results.

Identifying pili on pRT4SS expressing bacteria proved to be difficult. Although appendages were visible on negative stain EM images (see Figure 26), it was impossible to conclusively show that the appendages actually corresponded to T4SS associated pili. The bacteriophage PRD1 did not further elucidate the nature of these visible appendages, as PRD1's specificity for T4SS-carrying

E. coli was low and the phage consistently infected the strain BL21Star without any T4SS plasmids. An assumption was that the phage sample might have been contaminated. After several attempts of phage purification, however, the phage still infected BL21Star and could therefore not be used to conclusively show the presence of T4SS pili.

5 Results III – Localisation Studies with the IncW Conjugation System pR388

The localisation patterns of bacterial membrane proteins can be associated to their function, and give insight into their association with other functionalities in the cell. Localisation studies with the *A. tumefaciens* Vir T4SS have shown that it is localised in a distinct helical pattern around the cell periphery (Aguilar et al., 2010). This helical assembly pattern has been shown for the fusion proteins GFP-VirB8 and VirD4-GFP, and several substrate proteins fused to fluorescent proteins of this T4SS. All fusion proteins were further shown to be functional by tumorgenesis assays.

The protein GFP-VirB8 is responsible for the distinct localisation of the T4SS, as it assembles in the same helical pattern without any other T4SS components present in the cell. The study further assessed that the T4SS co-localises with the protein MinD, a cytoskeletal protein known to form helical arrays in *E. coli* (Aguilar et al., 2010). The pKM101 core complex does, however, not spontaneously assemble in a helical array around the cell perimeter. FLAG tags inserted in the TraF/VirB10 were visualised by immunofluorescence and did not display a helical pattern (Chandran et al., 2009).

The assembly of membrane protein complexes often requires a discrete sequence of proteins to be inserted into the bacterial membranes. The Type III Secretion System is one such example, where the rigid secretin ring is inserted into the outer membrane first, assisted only by its pilotin (Diepold et al., 2010). Similar observations were made with the secretin assembly from the Type II

Secretion System (Buddelmeijer et al., 2009). Other membrane components are then added stepwise towards the inner membrane. In the T3SS, two structural membrane ring components are added to the secretin ring progressing from the outer towards the inner membrane. These assembly processes are required before any of the cytoplasmic ring components containing ATPases and further structural components can assemble. The assembly process is however not dependant on ATPase activity. Some proteins are, however, not required for the basal structures to assemble, although they are essential for functionality. Some components appear to be beneficial for the assembly process, or have a stabilising effect on the fully assembled structure. Distinct proteins are thereby required to insert into the membrane first before others can be added to form the functional membrane protein complex (Diepold et al., 2010).

The assembly order was unravelled using fluorescently labelled proteins and observing their localisation in the bacterial membrane. The effects of deleting other components of the Type III Secretion System on the localisation of a fluorescently labelled component can then be observed by fluorescence microscopy. If no effect is observed, the deleted protein will be assembled after the fluorescently labelled protein and have no impact on the assembly of the fluorescently labelled protein (Diepold et al., 2010).

The assembly steps of the Gram-negative T4SSs remain elusive to date. Further, nothing is known about the arrangement of conjugative T4SSs on the cell surface. We have shown here that 14 proteins are sufficient to assemble a fully functional pR388-based conjugative system. Of the 11 VirB-homologues necessary for T4SS function, three proteins (TrwH/VirB7, TrwF/VirB9 and

TrwE/VirB10) are assumed to form the core complex, a central assembly spanning both the inner and outer membranes. This sub-assembly does not require any other components to be present to fold properly, and is comprised of 14 copies of each of the proteins (Fronzes et al., 2009b).

The reconstituted T4SS can further answer questions regarding the role of a T4SS component by creating non-polar deletions or mutations in specific components and determining the effects regarding localisation (fluorescence microscopy) of the T4SS, functionality (conjugation assay) and pilus assembly (phage assay/negative stain EM). These assays can also provide insight into the assembly of this T4SS and may even be useful to investigate protein—protein interactions and mutations in certain components of the T4SS.

In this study, we set out to determine the localisation of the T4SS in the cell to assess whether any distinct distribution occurs. If a specific pattern is visible within cells, the localisation output may be valuable for T4SS analysis. Further, we will investigate whether genetic modification of T4SS subunits, such as fluorescent protein tags and affinity tags, will affect the functionality of the reconstituted T4SS.

5.1 Finding functional fluorescence fusions of the T4SS

Efficient assessment of the T4SS's assembly requires several components to be tagged with fluorescent proteins without impairing the functionality of the T4SS. Therefore, several T4SS components were fused with eGFP or mCherry and their functionality was assessed.

5.1.1 eGFP-TrwG/VirB8

The initial candidate for a fluorescent fusion protein was TrwG/VirB8, as this protein is located in the membrane but the N-terminus protrudes into the cytoplasm, which is required for eGFP chromophore formation. Further, the VirB8 protein from *A. tumefaciens* has been shown to tolerate an N-terminal GFP fusion without causing functional impairment (Aguilar et al., 2010).

The construct pRT4SS_eGFP-TrwG/VirB8 was created using the InFusion™ cloning method after the Gibson assembly, and is shown in Figure 27A (Gibson et al., 2009). The eGFP gene was PCR amplified from pEGFP-E1 (Clontech) using the primers oeGFP_trwG_1F and oeGFP_trwG_2B, which create a 15 bp overlap with the 5′ region of *trwG/virB8* at both ends (see Figure 27A, eGFP PCR).

The plasmid pRT4SS was split into two parts by PCR due to its size. This was achieved by generating four primers that amplify the two parts in separate PCRs, both resulting in PCR products with 15 bp overlap to each other at one end. The primer pair otrwG_RT4SS_lin_1F and ocat_lin_2B resulted in a PCR product starting after the start codon of *trwG/virB8* and ending within the Cam resistance gene *cat* (see Figure 25A, PCR 1). The second primer pair otrwG_RT4SS_lin_2B and ocat_lin_1F generated a PCR product containing the start codon of *trwG/virB8* at its 3′end and reaching until the *cat* gene, overlapping with the *cat* gene in the first PCR product by 15 bp (see Figure 27A, PCR 2).

The InFusion™ reaction was performed as described in Methods. Plasmid isolated from Cam resistant colonies were subjected to analytical NotI/PvuII digests. The expected pattern for pRT4SS_eGFP-TrwG/VirB8 is 6265, 3906, 2586 and 1603 bp.

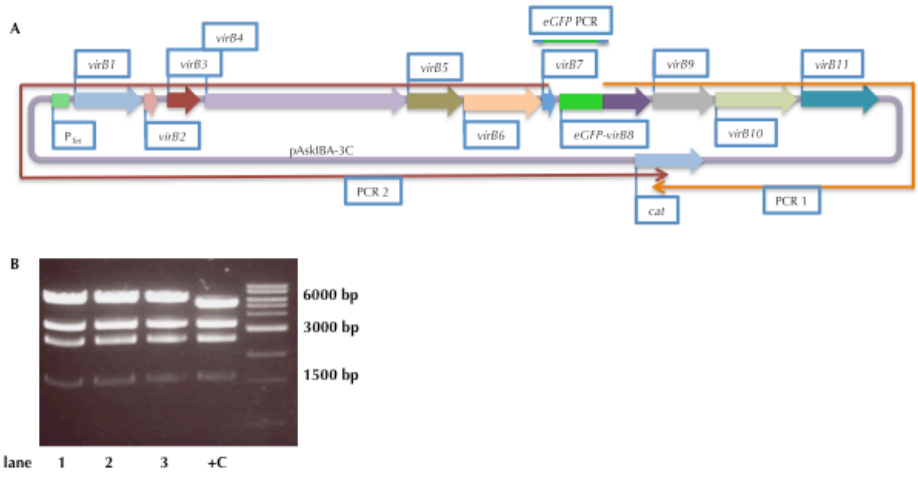

Figure 27. Generating pRT4SS_eGFP-trwG/virB8. **A)** Schematic depicting the organisation of pRT4SS_eGFP-trwG/virB8. eGFP PCR (thin line in green) was amplified from pEGFP-C1 using primers oeGFP_trwG_1F and oeGFP_trwG_2B. PCR 1 (orange) was amplified from pRT4SS using primers otrwG_RT4SS_lin_1F and ocat_lin_2B. PCR 2 (red) was generated from pRT4SS using primers otrwG_RT4SS_lin_2B and ocat_lin_1F. **B)** NotI/PvuII restriction digest of potential pRT4SS_eGFP-trwG/virB8 clone 1-4. +C is the positive control digesting pRT4SS with NotI/PvuII.

The result is shown in lanes 1, 2, 3 and 4 of Figure 25B, and all clones exhibit the expected pattern. A slight shift towards a larger size in the top band can be observed compared to pRT4SS, where fragment sizes of 5028, 3906, 2586 and 1603 bp are expected (lane +C), resulting from the insertion of the eGFP gene

before *trwG/virB8*. Subsequent analysis by Sanger sequencing confirmed the correct insertion of eGFP to create an N-terminal fusion protein with TrwG/VirB8.

Initial experiments assessed whether the eGFP fusion will inhibit conjugation. For this purpose, *E. coli* C43 cells were co-transformed with pRT4SS_eGFP-trwG/virB8, pRRelax and pRoriT, resulting in a $Cam^R/Spec^R/Kan^R$ donor strain. The conjugation efficiency was determined to be approx. 0.02. Conjugation is therefore inhibited by the GFP fusion, but not abolished.

Subsequently, *E. coli* C43 cells were co-transformed with pRT4SS_eGFP-trwG/virB8 + pRRelax + pRoriT or pRT4SS + pRRelax + pRoriT to test whether specific fluorescence is present resulting from the eGFP-TrwG/VirB8 fusion protein. For this purpose, cells of both cultures were grown to an OD_{600} of 0.4 and induced with 1 µg 4-epitetracycline for 1 h. A total of 2 ml cell culture was then transferred to an Eppendorf tube, where cells were harvested by centrifugation at 1500 xg. The media was discarded and cells were washed twice in 1 ml PBS. The cells were then fixed in 4% PFA in PBS for 20 min at RT and subsequently washed twice in TBS, before resuspending in 200 µl water. A total of 20 µl was then applied to Multispot microscope slides PTFE (Henley, Essex) and incubated for 30 min.

The eGFP protein has a single excitation peak at 488 nm and emits light at 507 nm as a response, which is visible in the green spectrum in a fluorescence microscope, where images were acquired in the DIC and green channels at 0.5 and 2.5 s exposure times, respectively.

Figure 28 shows *E. coli* cells expressing either pRT4SS + pRRelax + pRoriT (Figure 28A and B), or pRT4SS_eGFP-trwG/virB8 + pRRelax + pRoriT (Figure 28C, D and E).

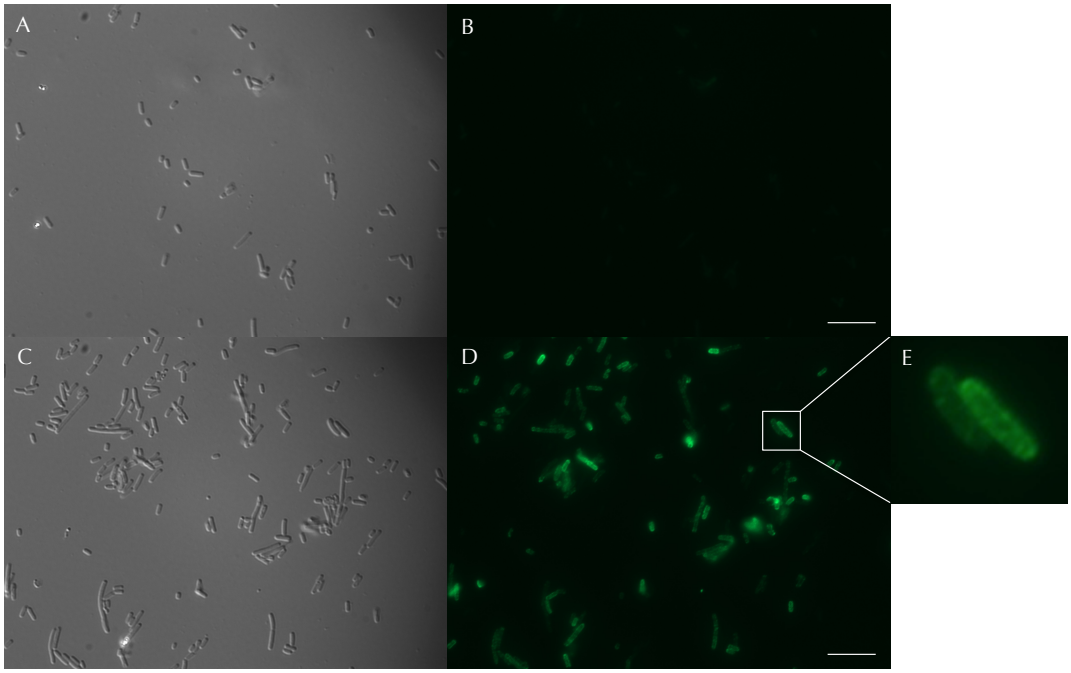

Figure 28. Differential interference contrast (DIC) and green channel images of *Escherichia coli* cells expressing pRoriT + pRRelax and pRT4SS (**A** and **B**) or pRT4SS_eGFP-TrwG/VirB8 (**C** and **D**). **E.** Zoomed in image of D. Scale bar = 10 μ m

Green fluorescence can only be detected in cells expressing the eGFP-TrwG/VirB8 fusion protein (Figure 28D), while no green fluorescence can be detected in cells expressing pRT4SS (Figure 28B). Further, the eGFP fusion protein is expressed in the majority of cells visible in this image. The eGFP protein further localises distinctly in the membrane of the cells due to its fusion to the TrwG/VirB8 protein (Figure 28E).

It can further be assumed that the localisation of eGFP-TrwG/VirB8 protein represents the localisation of the T4SS, since TrwG/VirB8 is essential for conjugation and the construct pRT4SS_eGFP-TrwG/VirB8 is functional. The zoomed-in image shown in Figure 28E localisation of eGFP-TrwG/VirB8 shows that the T4SS forms distinct spots in the membrane of *E. coli*.

Further analysis of Z-stacks acquired with pRT4SS_eGFP-TrwG/VirB8 using deconvolution revealed that the T4SS arranges in a helical pattern around the cell (Figure 29).

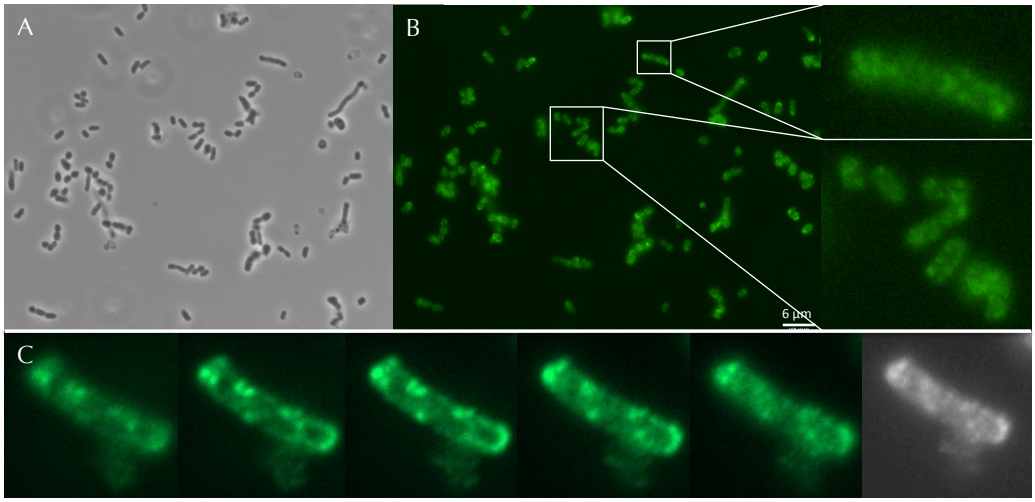

Figure 29. *Escherichia coli* ells expressing pRT4SS_eGFP-TrwG/VirB8 + pRRelax + pRoriT. **A)** Differential interference contrast (DIC) image, **B)** eGFP fluorescence image with zoomed in areas showing eGFP-TrwG/VirB8 spots in the bacterial membrane. **C)** Individual slices of a deconvolved Z-stack showing the helical arrangement of eGFP-TrwG/VirB8.

5.1.2 Further fluorescence fusion constructs

The aim is to establish a system to assess the T4SS's assembly using several fluorescent protein-fusion constructs requires the localisation assessment of various different components. These, however, must be tested for functionality in conjugation, as non-functional constructs may not reliably locate in the cell. Therefore, the constructs pRT4SS_TrwK/VirB4-eGFP, _TrwJ/VirB5-eGFP, _TrwI/VirB6-eGFP and _TrwE/VirB10-mCherry were generated as described above for pRT4SS_eGFP-TrwG/VirB8, as well as the double-labelled construct _eGFP-TrwG/VirB8_TrwE/VirB10-mCherry (oligonucleotides used for each construct are indicated in Table 13). The conjugation experiments showed, however, that none of these constructs were functional.

Since many of the integral T4SS components do not tolerate fluorescent protein fusions, the relaxase TrwC, the substrate of the R388 T4SS, may be a suitable candidate for labelling. A construct creating an N-terminal mCherry fusion, as well as a C-terminal m-Cherry fusion with TrwC was created. The constructs pRRelax_TrwC-mCherry was then co-transformed with the plasmids pRT4SS and pRoriT, or pRT4SS_eGFP-TrwG/VirB8 and pRoriT and conjugation assays were performed. The construct was functional in combination with both the pRT4SS and pRT4SS_eGFP-TrwG/VirB8 constructs, although to a significantly lesser degree compared to the untagged versions (approx. 0.02).

The imaging results with pRT4SS_eGFP-TrwG/VirB8 + pRRelax_TrwC-mCherry + pRoriT are shown in Figure 30.

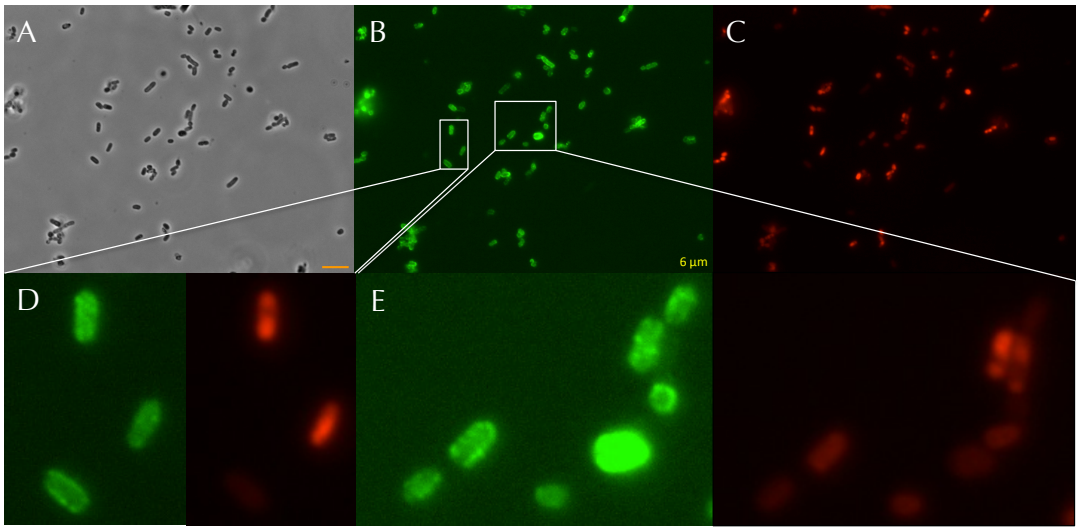

Figure 30. *Escherichia coli* cells expressing pRT4SS_eGFP-TrwG/VirB8 + pRRelax-TrwC-mCherry + pRoriT. **A)** Differential interference contrast image **B)** eGFP fluorescence image **C)** mCherry fluorescence **D)** and **E)** Enlarged areas as indicated showing eGFP-B8 and TrwC-mCherry fluorescence.

Figure 30 A, B and C show images of cells expressing pRT4SS_eGFP-TrwG/VirB8 + pRRelax_TrwC-mCherry + pRoriT in the DIC, green and red channels, respectively. The cells are expressing both the green fluorescent protein eGFP and the red fluorescent protein mCherry, as depicted in Figure 30B and C. The green fluorescence is located in membrane spots, as has been previously observed for the constructs pRT4SS_eGFP-TrwG/VirB8. The red fluorescent TrwC fusion protein is located diffusely in the cytoplasm (Figure 30E), and in some cells at the poles (Figure 30D). The plasmid pRRelax_TrwC-mCherry showed similar results when combined with pRT4SS (data not shown). The TrwC-mCherry protein therefore does not co-localise with the T4SS, likely because it is excessively expressed, and cannot be used as an indicator for an assembled T4SS. Table 13 summarises all generated constructs and indicates their functionality.

Table 13. Fluorescent protein fusion constructs generated with pRT4SS and pRRelax, indicating oligonucleotides used and their functionality on the conjugation assay.

Construct name	Oligonucleotides		Functionality
	Template linearisation	Fluorescence gene	
pRT4SS_TrwK/VirB4-eGFP	olin_trwK-cT_1F olin_trwK-cT_2B	oIF_trwK-eGFP_1F oIF_trwK-eGFP_2B	-
pRT4SS_TrwJ/VirB5-eGFP	olin_trwJ-cT_1F olin_trwJ-cT_2B	oIF_trwJ-eGFP_1F oIF_trwJ-eGFP_2B	-
pRT4SS_TrwI/VirB6-eGFP	olin_trwI-cT_1F olin_trwI-cT_2B	oIF_trwI-eGFP_1F oIF_trwI-eGFP_2B	-
pRT4SS_eGFP-TrwG/VirB8	otrwG_RT4SS_lin_1F otrwG_RT4SS_lin_2B	oeGFP_trwG_1F oeGFP_trwG_2B	+
pRT4SS_TrwE/VirB10-mCherry	olin_c-trwE_1F olin_c-trwE_2B	oIF_trwE-mCh_1F oIF_trwE-mCh_2B	-
pRT4SS_eGFP-TrwG/VirB8_TrwE/VirB10-mCherry	olin_c-trwE_1F olin_c-trwE_2B	oIF_trwE-mCh_1F oIF_trwE-mCh_2B	-
pRRelax_trwC-mCherry	oIF_trwC-mCh_F oIF_trwC-mCh_B	olin_c-trwC_F olin_c-trwC_B	+

5.2 Immunofluorescence with the pR388 T4SS

Tagging the R388 T4SS with fluorescent proteins abolished the function for most T4SS components. Immunofluorescence provides an alternative option to detect specific components of the T4SS within the cells. Specific antibodies to T4SS components were, however, not available. Therefore, the FLAG tag was genetically fused to components of the T4SS and the commercially available Monoclonal ANTI-FLAG® M2 antibody produced in mouse (Sigma-Aldrich) was used for detection of these tagged proteins. The FLAG-tag is a synthetic epitope tag with the sequence DYKDDDDK. This peptide tag was specifically created to facilitate the detection and purification of recombinant proteins using antibodies and is not a naturally occurring epitope (Hopp et al., 1988). It is hydrophilic and only 1012 Da in size, and therefore interferes only minimally with the protein it is attached to.

5.2.1 FLAG-TrwG/VirB8

The FLAG tag was positioned at the N-terminus of TrwG/VirB8 in an identical position as the eGFP tag, in order to whether the pattern of helical arrangement around the cell will be equally pronounced using the FLAG tag. The construct pRT4SS_FLAG-TrwG/VirB8 was generated with the InFusion™ cloning kit, using the oligonucleotides oIF_FLAG-trwG_1F and ocat_lin_2B for PCR1, and ocat_lin_1F and oIF_FLAG-trwG_2B for PCR2. The plasmid sequence was analysed by Sanger sequencing, which confirmed the insertion of the FLAG tag at the N-terminus of TrwG/VirB8. The construct was tested for functionality

using the conjugation assay by co-transforming pRT4SS_FLAG-TrwG/VirB8 cells with pRRelax and pRoriT, and it conjugated at an efficiency equal to the non-tagged pRT4SS (approx. 0.7).

Escherichia coli cells were grown to an OD_{600} of 0.4-0.5 and induced for 1 h at 37 C Initial experiments using an in-suspension labelling approach did not lead to efficient labelling of FLAG-TrwG/VirB8 in cells expressing pRT4SS_FLAG-TrwG/VirB8 + pRRelax + pRoriT. Therefore, conditions were optimised for an on-slide labelling approach, as described in Methods.

Images of antibody labelled *E. coli* C43 cells expressing either pRT4SS + pRRelax + pRoriT or pRT4SS_FLAG-TrwG/VirB8 + pRRelax + pRoriT were acquired in the DIC and red channels. Figures 31A and B show FLAG-TrwG/VirB8 expressing cells, while C and D show cells expressing pRT4SS.

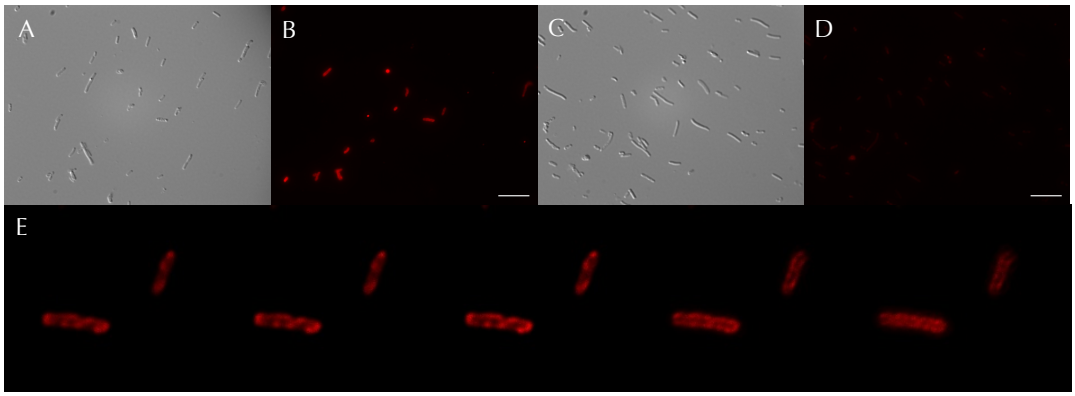

Figure 31. DIC and red channel images of immunofluorescence experiments using an anti_FLAG antibody produced in mouse and an anti-mouse antibody conjugated to Alexa Fluor 594 *Escherichia coli* cells expressing **A)** and **B)** pRT4SS + pRRelax + pRoriT **C)** and **D)** pRT4SS_FLAG-TrwG/VirB8 + pRRelax + pRoriT **E)** Individual slices of a deconvolved Z-stack of *Escherichia coli* cells expressing pRT4SS_FLAG-TrwG/VirB8 + pRRelax + pRoriT showing the helical arrangement of FLAG-TrwG/VirB8. Scale bar = 10 μm.

Red fluorescence, and therefore anti-FLAG AB binding, can only be observed in Figure 31B, while no red fluorescence is visible in Figure 31D. The AB staining is therefore specific for FLAG tag expression. Figure 31E shows deconvolved, individual slices of a Z stack acquired from cells expressing pRT4SS_FLAG-TrwG/VirB8 + pRRelax + pRoriT. The arrangement of the labelled spots is helical, similar to observations made with the construct pRT4SS_eGFP-TrwG/VirB8 (see Figure 29).

5.2.2 TrwI/VirB6-FLAG

FLAG and eGFP-tagged TrwG/VirB8 proteins arrange a helical manner around the cell periphery. Tagging a second component of the T4SS would ascertain the assumption that the assembled T4SS located in this specific way, and that the observation is not only caused by TrwG/VirB8 locating helically.

The protein TrwI/VirB6 is an integral membrane protein with four to five predicted transmembrane helices (Judd et al., 2005). It is thought to be the structural anchor for the T4SS in the inner membrane; however, no structural information on this protein is available to date (also see Introduction chapter).

The FLAG tag was positioned at the C-terminus of TrwI/VirB6, using the InFusion™ cloning method with the oligonucleotides oIF_trwI-FLAG_1F with ocat_lin_2B for PCR1, and ocat_lin_1F and oIF_trwI-FLAG_2B for PCR2. Sanger sequencing confirmed the correct insertion of the FLAG tag at the C-terminus of TrwI/VirB6. The construct pRT4SS_TrwI/VirB6-FLAG was transformed into *E. coli* C43 cells carrying the plasmids pRRelax and pRoriT,

and tested in the conjugation assay. The transfer efficiency of this construct was similar to the untagged construct pRT4SS (approx. 0.6).

Initial experiments using the TrwI/VirB6-FLAG construct were conducted using an identical protocol as for the pRT4SS_FLAG-TrwG/VirB8 construct. However, the labelling efficiency of TrwI/VirB6-FLAG was very poor and barely distinguishable from the negative control. Optimisation attempts, such as longer lysozyme treatment, different antibody concentrations and different detergents to permeabilise the membrane, did not lead to an improvement of labelling to date. Western blot experiments further showed that the antibody does not recognise TrwI/VirB6 as efficiently as TrwG/VirB8 (see Figure 32). Lane 1 (cell extract from cells expressing pRT4SS_TrwI/VirB6-FLAG) in Figure 32 shows a very weak signal around 35 kDa, while lane 2 shows a strong specific signal at 37 kDa (cell extract expressing pRT4SS_FLAG-TrwG/VirB8). No signal can be observed when cell extract from pRT4SS expressing clones is used (Figure 32, lane 3). Similar amounts of cells according to OD_{600} measurements were used for this experiment.

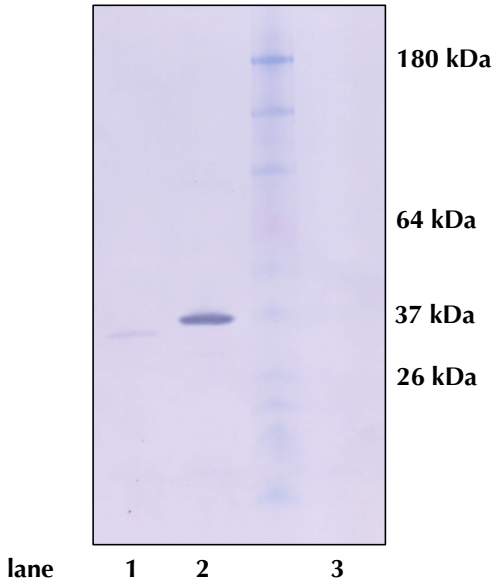

Figure 32. Western blot experiment using the monoclonal ANTI-FLAG® M2 antibody produced in mouse (Sigma) on whole, lysed cell extract expressing pRT4SS_trwI/virB6-FLAG (lane 1), pRT4SS_FLAG-trwG/virB8 (lane 2) or pRT4SS (lane 3).

5.3 Discussion

We could show here that the conjugative pR388 T4SS localises in a helical array around the cell perimeter, similarly to the T4SS of *A. tumefaciens* (Aguilar et al., 2010). Labelling TrwG/VirB8 with eGFP on the N-terminus showed that the T4SS is arranged around the cell envelope in a helical manner (see Figure 29). The conjugation efficiency of pRT4SS_eGFP-TrwG/VirB8 was impaired, but not abolished. Therefore, the T4SS is assumed to be assembled correctly and the helical arrangement biologically relevant. Results from immunofluorescence experiments using the FLAG-tag at the N-terminus of TrwG/VirB8 underlined the helical arrangement (see Figure 31) and suggest

that the arrangement is not an effect of tagging TrwG/VirB8 with eGFP (see Figure 29).

Assessing the localisation of further R388 T4SS components proved to be rather difficult, as most T4SS components did not tolerate eGFP or mCherry fusions, and were dysfunctional upon their addition (see Table 13). Similar effects were observed in the *A. tumefaciens* VirB T4SS (Aguilar et al., 2010).

The substrate relaxase TrwC was, however, not affected by a C-terminal mCherry fusion, as was shown by the conjugation assay. Localisation experiments did not show a distinct localisation of the protein to the membrane, but showed that TrwC localises diffuse in the cytoplasm (Figure 30). The result is not unexpected, as TrwC is a soluble protein and not all TrwC proteins expressed from pRRelax will localise to the T4SS. The over-expression of TrwC-mCherry may also contribute to the diffuse localisation.

The labelling with fluorescent proteins suffers from the significant drawback of impaired function of the T4SS. Therefore, the opportunity of using immunofluorescence to detect the FLAG-tag in *E. coli* cells was explored. FLAG-TrwG/VirB8 was readily detectable using the monoclonal M2 ANTI-FLAG antibody from Sigma Aldrich. Figure 31 shows the helical arrangement observed for FLAG-TrwG/VirB8, which confirms the helical arrangement observed for eGFP-TrwG/VirB8 (Figure 29) as being genuine rather than an artefact produced by the eGFP fusion.

FLAG-TrwI/VirB6 could however not be labelled efficiently to date. Western Blot experiments using equal amounts of cells for both FLAG-TrwG/VirB8- and

TrwI/VirB6-FLAG-expressing clones showed that the anti-FLAG M2 antibody recognition of FLAG TrwI/VirB6 is much weaker than for FLAG-TrwG/VirB8 (see Figure 32). The poor recognition may be due to the stoichiometry of TrwI/VirB6 and TrwG/VirB8, as TrwI/VirB6 may be present in smaller quantities than TrwG/VirB8. Since TrwI/VirB6 is an integral membrane protein, lipids may still be surrounding the protein and impair the antibody binding. In purified T4SS complexes, it was also impossible to determine the exact stoichiometry of TrwI/VirB6 compared to other T4SS components (Low et al., unpublished).

6 Conclusions & Outlook

Type IV Secretion Systems are versatile machineries that secrete a wide variety of substrates across the bacterial cell envelope. Their core structure and function, however, are highly related. Conjugative T4SSs are therefore very attractive for the study of T4SSs, since they are relatively simple in their substrate range and are found in *E. coli*, which is easy to handle in a standard laboratory.

Conjugative T4SSs are encoded on self-transmissible plasmids, alongside other genetic traits that may benefit bacteria in certain circumstances, such as multiple antibiotic resistance genes or increased UV tolerance (Winans & Walker, 1985a; Bolland et al., 1990). These plasmids are usually very large (exceeding 30 kbp), and therefore unsuitable for efficient, PCR-based genetic modification. Further, these plasmids encode a multitude of traits that are not required for conjugation, and thereby not required for the study of T4SSs.

It is therefore of paramount importance for structural and functional studies to (i) delineate the minimal requirements for functional Type IV secretion, (ii) to isolate the T4SS to assess only the process of Type IV secretion without the influence of additional factors present on the plasmids, and (iii) providing genetic accessibility of the T4SS in order to make straight forward mutations without the need of complementation of the mutated component on separate vectors, where issues such as differences in gene dosage and expression may hamper the analysis. Here, two fully functional T4SSs from the conjugative plasmids pKM101 and pR388 could be reconstituted in a well-defined vector backbone that is suitable for easy manipulation.

The pKM101 conjugation system was reconstituted in the construct pWT_KT4SS, using the well-documented vector pETDuet-1. The construct includes approx. 2000 bp upstream of the *traL/virB1* start codon, and the T4SS components are therefore expressed under wild-type promoter control. When complemented with the relaxosome components on pRRelax, the *KoriT*-containing plasmid pKoriT is efficiently transported. This construct will be valuable for the functional analysis of the pKM101 T4SS. Further, a deletion construct of the native pKM101 plasmid was produced by *Xma*I-digest, which was also functional when complemented with pKRelax and pKoriT. The construct pKT4SS_B10cS was, however, very unstable and did not reproducibly produce transconjugant colonies. Removing the *KoriT* nic site from the plasmid rendered the construct more reliable in terms of transconjugant production; however, at the expense of plasmid stability. The possibility that the negative regulators KorA and KorB are required for plasmid stability due to toxicity of TraL/VirB1 and TraG/VirB8, as was reported Moré et al. (1996), is likely to have caused these effects. The plasmid pWT_KT4SS includes *korA* and *korB*, and is very stably maintained in cells, while pKT4SS_B10cS_oriT-rm only includes *korA*. The toxicity of the highly driven TraL/VirB1 expression may cause the plasmid instability.

The reconstituted pKM101 T4SS encoded on the plasmid pWT_KT4SS bears much potential for the further analysis of this conjugation system, due to its manageable size and defined vector background. Systematic deletion of the 2000 bp upstream of *traL/virB1* can eventually lead to the determination of the

minimal requirements for this conjugation system. Further, the promoter region can be altered to an overproduction promoter for protein purification purposes. The pR388 T4SS (*trw* operon) was shown to conjugate to wild-type level (see Table 12), and the presence of *RoriT* was confirmed for resulting transconjugants. Here, we not only present the first fully reconstituted T4SS, but further delineate the minimal requirements for conjugation in the pR388 conjugation system. This plasmid can be used for structural studies, as the overexpression of the T4SS components should facilitate the purification on complexes from the cells. Further, the manageable size of the pRT4SS plasmid facilitates its easy modification to create fusion proteins and add affinity tags for purification. The influence of such tags on the functionality can further be assessed using the conjugation assay, as has been shown here using fluorescence fusions and tags for immunodetection. Future work in progress will include the purification of large protein complexes using affinity tags, which will include several, if not all components of the T4SS. The structural analysis of such large assemblies will provide the next breakthrough in the T4SS field.

We further report the helical arrangement around the cell perimeter of a conjugative T4SS, similar to the arrangement previously reported for the *A. tumefaciens* T4SS. In the *A. tumefaciens* T4SS, the protein TrwG/VirB8 is solely responsible for the helical arrangement (Aguilar et al., 2010). Further localisation studies regarding other T4SS components will be crucial to support these findings.

Aguilar et al. (2010) further report that the T4SS is associated to the helically arranged cytoskeletal component MinD, which is also present in *E. coli*. For the conjugative T4SS, such an association of the T4SS with cytoskeletal components provides many interesting options to consider, as many of them assemble around the cell perimeter in a helical fashion.

An example is the partitioning protein ParA, which falls into the same ATPase superfamily as MinD, containing a deviant Walker A motif (Shih & Rothfield, 2006). Par proteins are usually responsible for the segregation of low copy number plasmids during cell division, and are encoded on the plasmids themselves. As other cytoskeletal components, ParA has been shown to spontaneously polymerise *in vitro* and form helical arrays *in vivo* (reviewed in Shih & Rothfield (2006)). The protein ParA from *Neisseria gonorrhoeae* is also required for DNA secretion of its T4SS (Hamilton et al., 2005).

The protein VirC2 also belongs to the MinD/ParA superfamily of ATPases, and is encoded on the Ti plasmid of *A. tumefaciens* (Atmakuri et al., 2007). It was shown to bind a specific sequence on the Ti plasmid and, in complex with VirC1, positions the relaxosome—DNA substrate to the cell poles (Atmakuri et al., 2007). Although this study suggests a localisation of the VirC2 and the T4SS towards the cell poles, this may be due to a dynamic effect of oscillation of VirC2 between the cell poles and a helical arrangement, as has been previously demonstrated for MinD and ParA (Shih et al., 2003; Ebersbach & Gerdes, 2004).

If the T4SS is indeed associated to the bacterial cytoskeleton, the localisation of the T4SS may be dynamic and associated to the cell cycle or growth phase of

the bacteria. The pR388 plasmid does, however, not encode a VirC2 homologue and its segregation may be associated to other cellular processes. Future work to investigate the role of TrwG/VirB8 in localising the T4SS in helical arrays, as well as the identification of its association partner, will provide further valuable insight into conjugative Type IV secretion and their association with other cellular functions.

7 Bibliography

Aguilar, J., Zupan, J., Cameron, T.A. & Zambryski, P.C. (2010). Agrobacterium type IV secretion system and its substrates form helical arrays around the circumference of virulence-induced cells. *Proceedings of the National Academy of Sciences of the United States of America*. 107 (8). p.pp. 3758–3763.

Alvarez-Martinez, C.E. & Christie, P. (2009). Biological diversity of prokaryotic type IV secretion systems. *Microbiology and molecular biology reviews : MMBR*. 73 (4). p.pp. 775–808.

Aly, K.A. & Baron, C. (2007). The VirB5 protein localizes to the T-pilus tips in Agrobacterium tumefaciens. *Microbiology (Reading, England)*. 153 (Pt 11). p.pp. 3766–3775.

Arechaga, I., Peña, A., Zunzunegui, S., del Carmen Fernández-Alonso, M., Rivas, G. & De La Cruz, F. (2008). ATPase activity and oligomeric state of TrwK, the VirB4 homologue of the plasmid R388 type IV secretion system. *Journal of Bacteriology*. 190 (15). p.pp. 5472–5479.

Atmakuri, K., Cascales, E., Burton, O.T., Banta, L.M. & Christie, P.J. (2007). Agrobacterium ParA/MinD-like VirC1 spatially coordinates early conjugative DNA transfer reactions. *The EMBO journal*. 26 (10). p.pp. 2540–2551.

Babic, A., Lindner, A.B., Vulic, M., Stewart, E.J. & Radman, M. (2008). Direct visualization of horizontal gene transfer. *Science*. 319 (5869). p.pp. 1533–1536.

Bailey, S., Ward, D., Middleton, R., Grossmann, J.G. & Zambryski, P.C. (2006). Agrobacterium tumefaciens VirB8 structure reveals potential protein-protein interaction sites. *Proceedings of the National Academy of Sciences of the United States of America*. 103 (8). p.pp. 2582–2587.

Batchelor, R.A., Pearson, B.M., Friis, L.M., Guerry, P. & Wells, J.M. (2004). Nucleotide sequences and comparison of two large conjugative plasmids from different Campylobacter species. *Microbiology (Reading, England)*. 150 (Pt 10). p.pp. 3507–3517.

Berger, B.R. & Christie, P.J. (1994). Genetic complementation analysis of the Agrobacterium tumefaciens virB operon: virB2 through virB11 are essential virulence genes. *Journal of Bacteriology*. 176 (12). p.pp. 3646–3660.

Bolland, S., Llosa, M., Avila, P. & de la Cruz, F. (1990). General organization of the conjugal transfer genes of the IncW plasmid R388 and interactions between R388 and IncN and IncP plasmids. *Journal of Bacteriology*. 172 (10). p.pp. 5795–5802.

Bomhoff, G., Klapwijk, P.M., Kester, H.C., Schilperoort, R. a, Hernalsteens, J.P. & Schell, J. (1976). Octopine and nopaline synthesis and breakdown

genetically controlled by a plasmid of Agrobacterium tumefaciens. *Molecular & general genetics : MGG*. 145 (2). p.pp. 177–181.

Bradley, D.E. (1980). Morphological and serological relationships of conjugative pili. *Plasmid*. 4 (2). p.pp. 155–169.

Bradley, D.E. & Cohen, D.R. (1976). Basic characterization of W-pili. *Journal of general microbiology*. 97 (1). p.pp. 91–103.

Bradley, D.E. & Rutherford, E.L. (1975). Basic characterization of a lipid-containing bacteriophage specific for plasmids of the P, N, and W compatibility groups. *Canadian Journal of Microbiology*. 21 (2). p.pp. 152–163.

Buddelmeijer, N., Krehenbrink, M., Pecorari, F. & Pugsley, A.P. (2009). Type II secretion system secretin PulD localizes in clusters in the Escherichia coli outer membrane. *Journal of Bacteriology*. 191 (1). p.pp. 161–168.

Cascales, E. & Christie, P. (2004). Definition of a bacterial type IV secretion pathway for a DNA substrate. *Science*. 304 (5674). p.pp. 1170–1173.

Cellini, C., Kalogeraki, V.S. & Winans, S.C. (1997). The hydrophobic TraM protein of pKM101 is required for conjugal transfer and sensitivity to donor-specific bacteriophage. *Plasmid*. 37 (3). p.pp. 181–188.

Chandran, V., Fronzes, R., Duquerroy, S., Cronin, N., Navaza, J. & Waksman, G. (2009). Structure of the outer membrane complex of a type IV secretion system. *Nature*. 462 (7276). p.pp. 1011–1015.

Chen, I. & Dubnau, D. (2004). DNA uptake during bacterial transformation. *Nature Reviews Microbiology*. 2 (3). p.pp. 241–249.

Chiu, J., March, P.E., Lee, R. & Tillett, D. (2004). Site-directed, Ligase-Independent Mutagenesis (SLIM): a single-tube methodology approaching 100% efficiency in 4 h. *Nucleic Acids Research*. 32 (21). p.p. e174.

Clarke, M., Maddera, L., Harris, R.L. & Silverman, P.M. (2008). F-pili dynamics by live-cell imaging. *Proceedings of the National Academy of Sciences of the United States of America*. 105 (46). p.pp. 17978–81.

Cohen, S.N., Chang, A.C., Boyer, H.W. & Helling, R.B. (1973). Construction of biologically functional bacterial plasmids in vitro. *Proceedings of the National Academy of Sciences of the United States of America*. 70 (11). p.pp. 3240–3244.

Couturier, M., Bex, F., Bergquist, P.L. & Maas, W.K. (1988). Identification and classification of bacterial plasmids. *Microbiological reviews*. 52 (3). p.pp. 375–395.

Dang, T.A. & Christie, P.J. (1997). The VirB4 ATPase of Agrobacterium tumefaciens is a cytoplasmic membrane protein exposed at the periplasmic surface. *Journal of Bacteriology*. 179 (2). p.pp. 453–462.

Datsenko, K.A. & Wanner, B.L. (2000). One-step inactivation of chromosomal genes in Escherichia coli K-12 using PCR products. *Proceedings of the National Academy of Sciences of the United States of America*. 97 (12). p.pp. 6640–6645.

Datta, N. & Hedges, R. (1971). Compatibility groups among fi– R factors. *Nature*. 234. p.pp. 222–223.

Diepold, A., Amstutz, M., Abel, S., Sorg, I., Jenal, U. & Cornelis, G.R. (2010). Deciphering the assembly of the Yersinia type III secretion injectisome. *The EMBO Journal*. 29 (11). p.pp. 1928–1940.

Douard, G., Praud, K., Cloeckaert, A. & Doublet, B. (2010). The Salmonella genomic island 1 is specifically mobilized in trans by the IncA/C multidrug resistance plasmid family. *PLoS ONE*. 5 (12). p.p. e15302.

Doublet, B., Douard, G., Targant, H., Meunier, D., Madec, J.Y. & Cloeckaert, A. (2008). Antibiotic marker modifications of lambda Red and FLP helper plasmids, pKD46 and pCP20, for inactivation of chromosomal genes using PCR products in multidrug-resistant strains. *Journal of microbiological methods*. 75 (2). p.pp. 359–361.

Draper, O., César, C., Machón, C., De La Cruz, F. & Llosa, M. (2005). Site-specific recombinase and integrase activities of a conjugative relaxase in recipient cells. *Proceedings of the National Academy of Sciences of the United States of America*. 102 (45). p.pp. 16385–16390.

Durand, E., Oomen, C. & Waksman, G. (2010). Biochemical Dissection of the ATPase TraB, the VirB4 Homologue of the Escherichia coli pKM101 Conjugation Machinery. *Journal of Bacteriology*. 192 (9). p.pp. 2315–2323.

Ebersbach, G. & Gerdes, K. (2004). Bacterial mitosis: partitioning protein ParA oscillates in spiral-shaped structures and positions plasmids at mid-cell. *Molecular microbiology*. 52 (2). p.pp. 385–398.

Eisenbrandt, R., Kalkum, M. & Lai, E. (1999). Conjugative Pili of IncP Plasmids, and the Ti Plasmid T Pilus Are Composed of Cyclic Subunits. *The Journal of biological chemistry*. 274 (32). p.pp. 22548–22555.

Elledge, S.J. & Walker, G.C. (1983). The muc genes of pKM101 are induced by DNA damage. *Journal of Bacteriology*. 155 (3). p.pp. 1306–1315.

Van den Ent, F. & Löwe, J. (2006). RF cloning: a restriction-free method for inserting target genes into plasmids. *Journal of biochemical and biophysical methods*. 67 (1). p.pp. 67–74.

Fernández-González, E., de Paz, H.D., Alperi, A., Agúndez, L., Faustmann, M., Sangari, F.J., Dehio, C. & Llosa, M. (2011). Transfer of R388 derivatives by a pathogenesis-associated type IV secretion system into both bacteria and human cells. *Journal of bacteriology*. 193 (22). p.pp. 6257–6265.

Fiedler, S. & Wirth, R. (1988). Transformation of bacteria with plasmid DNA by electroporation. *Analytical biochemistry*. 170. p.pp. 38–44.

Fronzes, R., Christie, P. & Waksman, G. (2009a). The structural biology of type IV secretion systems. *Nature Reviews Microbiology*. 7 (10). p.pp. 703–714.

Fronzes, R., Schäfer, E., Wang, L., Saibil, H.R., Orlova, E. V & Waksman, G. (2009b). Structure of a type IV secretion system core complex. *Science*. 323 (5911). p.pp. 266–268.

Garcillán-Barcia, M.P., Francia, M. V & De La Cruz, F. (2009). The diversity of conjugative relaxases and its application in plasmid classification. *FEMS Microbiology Reviews*. 33 (3). p.pp. 657–687.

Garcillán-Barcia, M.P. & de la Cruz, F. (2008). Why is entry exclusion an essential feature of conjugative plasmids? *Plasmid*. 60 (1). p.pp. 1–18.

Gibson, D., Young, L. & Chuang, R. (2009). Enzymatic assembly of DNA molecules up to several hundred kilobases. *Nature Methods*. 6 (5). p.pp. 12–16.

Gigliani, F., Sporeno, E., Perri, S. & Battaglia, P. a (1989). The uvp1 gene of plasmid pR cooperates with mucAB genes in the DNA repair process. *Molecular & general genetics : MGG*. 218 (1). p.pp. 18–24.

Gomis-Rüth, F., De La Cruz, F. & Coll, M. (2002). Structure and role of coupling proteins in conjugal DNA transfer. *Research in microbiology*. 153 (4). p.pp. 199–204.

Gomis-Rüth, F.X., Moncalían, G., Perez-Luque, R., González, A., Cabezón, E., De La Cruz, F. & Coll, M. (2001). The bacterial conjugation protein TrwB resembles ring helicases and F1-ATPase. *Nature*. 409. p.pp. 1–5.

Gonzalez-Perez, B., Lucas, M., Cooke, L., Vyle, J., De La Cruz, F. & Moncalián, G. (2007). Analysis of DNA processing reactions in bacterial conjugation by using suicide oligonucleotides. *The EMBO Journal*. 26 (16). p.pp. 3847–3857.

Grant, S.G., Jessee, J., Bloom, F.R. & Hanahan, D. (1990). Differential plasmid rescue from transgenic mouse DNAs into Escherichia coli methylation-restriction mutants. *Proceedings of the National Academy of Sciences of the United States of America*. 87 (12). p.pp. 4645–4649.

Guasch, A., Lucas, M., Moncalián, G., Cabezas, M., Pérez-Luque, R., Gomis-Rüth, F., De La Cruz, F. & Coll, M. (2003). Recognition and processing of the origin of transfer DNA by conjugative relaxase TrwC. *Nature Structural Biology*. 10 (12). p.pp. 1002–1010.

Guglielmini, J., de la Cruz, F. & Rocha, E.P.C. (2013). Evolution of conjugation and type IV secretion systems. *Molecular biology and evolution*. 30 (2). p.pp. 315–331.

Guynet, C., Cuevas, A., Moncalián, G. & de la Cruz, F. (2011). The stb operon balances the requirements for vegetative stability and conjugative transfer of plasmid R388. *PLoS genetics*. 7 (5). p.p. e1002073.

Haase, J. & Lanka, E. (1997). A specific protease encoded by the conjugative DNA transfer systems of IncP and Ti plasmids is essential for pilus synthesis. *Journal of Bacteriology*. 179 (18). p.pp. 5728–5735.

Hall, R. (1987). pKM101 is an IS46-promoted deletion of R46. *Nucleic acids research*. 15 (13). p.p. 7106.

Hamilton, H.L., Domínguez, N.M., Schwartz, K.J., Hackett, K.T. & Dillard, J.P. (2005). Neisseria gonorrhoeae secretes chromosomal DNA via a novel type IV secretion system. *Molecular Microbiology*. 55 (6). p.pp. 1704–1721.

Hare, S., Bayliss, R., Baron, C. & Waksman, G. (2006). A large domain swap in the VirB11 ATPase of Brucella suis leaves the hexameric assembly intact. *Journal of molecular biology*. 360 (1). p.pp. 56–66.

Hopp, T., Prickett, K., Price, V., Libby, R., March, C., Cerretti, D., Urdal, D. & Conlon, P. (1988). A short polypeptide marker sequence useful for recombinant protein identification and purification. *Nature Biotechnology*. 6. p.pp. 1204–1210.

Jakubowski, S., Krishnamoorthy, V., Cascales, E. & Christie, P. (2004). Agrobacterium tumefaciens VirB6 domains direct the ordered export of a DNA substrate through a type IV secretion System. *Journal of molecular biology*. 341 (4). p.pp. 961–977.

Jones, A.L., Shirasu, K. & Kado, C.I. (1994). The product of the virB4 gene of Agrobacterium tumefaciens promotes accumulation of VirB3 protein. *Journal of Bacteriology*. 176 (17). p.pp. 5255–5261.

Judd, P.K., Kumar, R.B. & Das, A. (2005). The type IV secretion apparatus protein VirB6 of Agrobacterium tumefaciens localizes to a cell pole. *Molecular microbiology*. 55 (1). p.pp. 115–124.

Juhas, M., Crook, D. & Hood, D. (2008). Type IV secretion systems: tools of bacterial horizontal gene transfer and virulence. *Cellular Microbiology*. 10 (12). p.pp. 2377–2386.

Kienesberger, S., Trummler, C.S., Fauster, A., Lang, S., Sprenger, H., Gorkiewicz, G. & Zechner, E.L. (2011). Interbacterial macromolecular transfer by the Campylobacter fetus subsp. venerealis type IV secretion system. *Journal of Bacteriology*. 193 (3). p.pp. 744–758.

Kingsman, A. & Willetts, N. (1978). The requirements for conjugal DNA synthesis in the donor strain during flac transfer. *Journal of Molecular Biology*. 122 (3). p.pp. 287–300.

Koraimann, G. (2003). Lytic transglycosylases in macromolecular transport systems of Gram-negative bacteria. *Cellular and molecular life sciences : CMLS*. 60 (11). p.pp. 2371–2388.

Krause, S., Barcena, M., Pansegrau, W., Lurz, R., Carazo, J.M. & Lanka, E. (2000a). Sequence-related protein export NTPases encoded by the conjugative transfer region of RP4 and by the cag pathogenicity island of Helicobacter pylori share similar hexameric ring structures. *Proceedings of the National Academy of Sciences of the United States of America*. 97 (7). p.pp. 3067–3072.

Krause, S., Pansegrau, W., Lurz, R., de la Cruz, F. & Lanka, E. (2000b). Enzymology of type IV macromolecule secretion systems: the conjugative transfer regions of plasmids RP4 and R388 and the cag pathogenicity island of Helicobacter pylori encode structurally and functionally related nucleoside triphosphate hydrolases. *Journal of Bacteriology*. 182 (10). p.pp. 2761–2770.

Laemmli, U.K. (1970). Cleavage of structural proteins during the assembly of the head of bacteriophage T4. *Nature*. 227. p.pp. 680–685.

Lang, S., Gruber, K., Mihajlovic, S., Arnold, R., Gruber, C., Steinlechner, S., Jehl, M., Rattei, T., Fröhlich, K. & Zechner, E.L. (2010). Molecular recognition determinants for type IV secretion of diverse families of conjugative relaxases. *Molecular Microbiology*. 78 (6). p.pp. 1539–1555.

Lang, S., Kirchberger, P.C., Gruber, C.J., Redzej, A., Raffl, S., Zellnig, G., Zangger, K. & Zechner, E.L. (2011). An activation domain of plasmid R1 TraI protein delineates stages of gene transfer initiation. *Molecular microbiology*. 82 (5). p.pp. 1071–1085.

Langer, P.J. & Walker, G.C. (1981). Restriction endonuclease cleavage map of pKM101: relationship to parental plasmid R46. *Molecular & general genetics : MGG*. 182 (2). p.pp. 268–272.

Lawley, T.D., Klimke, W.A., Gubbins, M.J. & Frost, L.S. (2003). F factor conjugation is a true type IV secretion system. *FEMS Microbiology Letters*. 224 (1). p.pp. 1–15.

Lederberg, J. & Tatum, E.L. (1953). Sex in bacteria; genetic studies, 1945-1952. *Science*. 118 (3059). p.pp. 169–175.

Llosa, M., Grandoso, G., Hernando, M.A. & de la Cruz, F. (1996). Functional domains in protein TrwC of plasmid R388: dissected DNA strand transferase and DNA helicase activities reconstitute protein function. *Journal of molecular biology*. 264 (1). p.pp. 56–67.

Llosa, M., Grandoso, G. & De La Cruz, F. (1995). Nicking activity of TrwC directed against the origin of transfer of the IncW plasmid R388. *Journal of Molecular Biology*. 246 (1). p.pp. 54–62.

Llosa, M., Zunzunegui, S. & De La Cruz, F. (2003). Conjugative coupling proteins interact with cognate and heterologous VirB10-like proteins while exhibiting specificity for cognate relaxosomes. *Proceedings of the National Academy of Sciences of the United States of America*. 100 (18). p.pp. 10465–10470.

Lucas, M., González-Pérez, B., Cabezas, M., Moncalian, G., Rivas, G. & De La Cruz, F. (2010). Relaxase DNA binding and cleavage are two distinguishable steps in conjugative DNA processing that involve different sequence elements of the nic site. *Journal of Biological Chemistry*. 285 (12). p.pp. 8918–8926.

Lum, P.L., Rodgers, M.E. & Schildbach, J.F. (2002). TraY DNA recognition of its two F factor binding sites. *Journal of Molecular Biology*. 321 (4). p.pp. 563–578.

Majdalani, N. & Ippen-Ihler, K. (1996). Membrane insertion of the F-pilin subunit is Sec independent but requires leader peptidase B and the proton motive force. *Journal of Bacteriology*. 178 (13). p.pp. 3742–3747.

Mandel, M. & Higa, A. (1970). Calcium-dependent Bacteriophage DNA Infection. *Journal of molecular biology*. 53. p.pp. 159–162.

Mann, M.B., Rao, R.N. & Smith, H.O. (1978). Cloning of restriction and modification genes in E. coli: the HbaII system from Haemophilus haemolyticus. *Gene*. 3 (2). p.pp. 97–112.

McCann, J., Spingarn, N.E., Kobori, J. & Ames, B.N. (1975). Detection of carcinogens as mutagens: bacterial tester strains with R factor plasmids. *Proceedings of the National Academy of Sciences of the United States of America*. 72 (3). p.pp. 979–983.

Middleton, R., Sjölander, K., Krishnamurthy, N., Foley, J. & Zambryski, P. (2005). Predicted hexameric structure of the Agrobacterium VirB4 C terminus suggests VirB4 acts as a docking site during type IV secretion. *Proceedings of the National Academy of Sciences of the United States of America*. 102 (5). p.pp. 1685–1690.

Moncalián, G., Grandoso, G., Llosa, M. & De La Cruz, F. (1997). oriT-processing and regulatory roles of TrwA protein in plasmid R388 conjugation. *Journal of Molecular Biology*. 270 (2). p.pp. 188–200.

Moncalián, G. & de la Cruz, F. (2004). DNA binding properties of protein TrwA, a possible structural variant of the Arc repressor superfamily. *Biochimica et biophysica acta*. 1701 (1-2). p.pp. 15–23.

Moore, D., Hamilton, C.M., Maneewannakul, K., Mintz, Y., Frost, L.S. & Ippen-Ihler, K. (1993). The Escherichia coli K-12 F plasmid gene traX is required for acetylation of F pilin. *Journal of Bacteriology*. 175 (5). p.pp. 1375–1383.

Moré, M.I., Pohlman, R.F. & Winans, S.C. (1996). Genes encoding the pKM101 conjugal mating pore are negatively regulated by the plasmid-encoded KorA and KorB proteins. *Journal of Bacteriology*. 178 (15). p.pp. 4392–4399.

Mullis, K., Faloona, F., Scharf, S., Horn, G. & Erlich, H. (1986). Specific enzymatic amplification of DNA in vitro: the polymerase chain reaction. *Cold Spring Harbour Symposia on Quantitative Biology*. 51. p.pp. 263–373.

Olsen, R.H., Siak, J.S. & Gray, R.H. (1974). Characteristics of PRD1, a plasmid-dependent broad host range DNA bacteriophage. *Journal of virology*. 14 (3). p.pp. 689–699.

Pansegrau, W., Balzer, D., Kruft, V., Lurz, R. & Lanka, E. (1990a). In vitro assembly of relaxosomes at the transfer origin of plasmid RP4. *Proceedings of the National Academy of Sciences of the United States of America*. 87 (17). p.pp. 6555–6559.

Pansegrau, W., Ziegelin, G. & Lanka, E. (1990b). Covalent association of the traI gene product of plasmid RP4 with the 5′-terminal nucleotide at the relaxation nick site. *The Journal of biological chemistry*. 265 (18). p.pp. 10637–10644.

Peña, A., Matilla, I. & Martín-Benito, J. (2012). The hexameric structure of a conjugative VirB4 protein ATPase provides new insights for a functional and phylogenetic relationship with DNA translocases. *The Journal of biological chemistry*. 278 (47). p.pp. 39925–39932.

Pohlman, R., Genetti, H. & Winans, S. (1994). Common ancestry between IncN conjugal transfer genes and macromolecular export systems systems of plant and animal pathogens. *Molecular microbiology*. 14. p.pp. 655–668.

Rashkova, S., Spudich, G.M. & Christie, P.J. (1997). Characterization of membrane and protein interaction determinants of the Agrobacterium tumefaciens VirB11 ATPase. *Journal of Bacteriology*. 179 (3). p.pp. 583–591.

Redzej, A., Ilangovan, A., Lang, S., Gruber, C.J., Topf, M., Zangger, K., Zechner, E.L. & Waksman, G. (2013). Structure of a translocation signal domain mediating conjugative transfer by type IV secretion systems. *Molecular microbiology*. 89 (2). p.pp. 324–333.

Revilla, C., Garcillán-Barcia, M.P., Fernández-López, R., Thomson, N.R., Sanders, M., Cheung, M., Thomas, C.M. & de la Cruz, F. (2008). Different pathways to acquiring resistance genes illustrated by the recent evolution of IncW plasmids. *Antimicrobial agents and chemotherapy*. 52 (4). p.pp. 1472–1480.

Ripoll-Rozada, J., Zunzunegui, S., de la Cruz, F., Arechaga, I. & Cabezón, E. (2013). Functional Interactions of VirB11 Traffic ATPases with VirB4 and VirD4 Molecular Motors in Type IV Secretion Systems. *Journal of Bacteriology*. 195 (18). p.pp. 4195–4201.

Rivera-Calzada, A., Fronzes, R., Savva, C.G., Chandran, V., Lian, P.W., Laeremans, T., Pardon, E., Steyaert, J., Remaut, H., Waksman, G. & Orlova, E. V (2013). Structure of a bacterial type IV secretion core complex at subnanometre resolution. *The EMBO journal*. p.pp. 1–10.

Sanger, F., Nicklen, S. & Coulsen, A.R. (1977). DNA sequencing with chain-terminating inhibitors. *Proceedings of the National Academy of Sciences of the United States of America*. 74 (12). p.pp. 5463–5467.

Savvides, S.N., Yeo, H.J., Beck, M.R., Blaesing, F., Lurz, R., Lanka, E., Buhrdorf, R., Fischer, W., Haas, R. & Waksman, G. (2003). VirB11 ATPases are dynamic hexameric assemblies: new insights into bacterial type IV secretion. *The EMBO Journal*. 22 (9). p.pp. 1969–1980.

Shaner, N.C., Campbell, R.E., Steinbach, P. a, Giepmans, B.N.G., Palmer, A.E. & Tsien, R.Y. (2004). Improved monomeric red, orange and yellow fluorescent proteins derived from Discosoma sp. red fluorescent protein. *Nature Biotechnology*. 22 (12). p.pp. 1567–1572.

Shih, Y.-L., Le, T. & Rothfield, L. (2003). Division site selection in Escherichia coli involves dynamic redistribution of Min proteins within coiled structures that extend between the two cell poles. *Proceedings of the National Academy of Sciences of the United States of America*. 100 (13). p.pp. 7865–70.

Shih, Y.-L. & Rothfield, L. (2006). The bacterial cytoskeleton. *Microbiology and molecular biology reviews : MMBR*. 70 (3). p.pp. 729–54.

Shimomura, O., Johnson, F.H. & Saiga, Y. (1962). Extraction, purification and properties of aequorin, a bioluminescent protein from the luminous hydromedusan, Aequorea. *Journal of Cellular and Comparative Physiology*. 1353 (165). p.pp. 223–239.

Stepanenko, O. V, Stepanenko, O. V, Shcherbakova, D.M., Kuznetsova, I.M., Turoverov, K.K. & Verkhusha, V. V (2011). Modern fluorescent proteins: from chromophore formation to novel intracellular applications. *BioTechniques*. 51 (5). p.pp. 313–327.

Tato, I., Zunzunegui, S., de la Cruz, F. & Cabezon, E. (2005). TrwB, the coupling protein involved in DNA transport during bacterial conjugation, is a DNA-dependent ATPase. *Proceedings of the National Academy of Sciences of the United States of America*. 102 (23). p.pp. 8156–8161.

Terradot, L., Bayliss, R., Oomen, C., Leonard, G.A., Baron, C. & Waksman, G. (2005). Structures of two core subunits of the bacterial type IV secretion system, VirB8 from Brucella suis and ComB10 from Helicobacter pylori. *Proceedings of the National Academy of Sciences of the United States of America*. 102 (12). p.pp. 4596–4601.

Valentine, R. & Strand, M. (1965). Complexes of F-pili and RNA bacteriophage. *Science*. 148 (3669). p.pp. 511–513.

Wallden, K., Rivera-Calzada, A. & Waksman, G. (2010). Type IV secretion systems: versatility and diversity in function. *Cellular Microbiology*. 12 (9). p.pp. 1203–1212.

Walldén, K., Williams, R., Yan, J., Lian, P.W., Wang, L., Thalassinos, K., Orlova, E. V. & Waksman, G. (2012). Structure of the VirB4 ATPase, alone and bound to the core complex of a type IV secretion system. *Proceedings of the National Academy of Sciences of the United States of America*. 109 (28). p.pp. 11348–11353.

Wang, Y., Yu, X., Silverman, P., Harris, R. & Egelman, E. (2009). The structure of F-pili. *Journal of molecular biology*. 385 (1). p.pp. 22–29.

Ward, D. V, Draper, O., Zupan, J.R. & Zambryski, P.C. (2002). Peptide linkage mapping of the Agrobacterium tumefaciens vir-encoded type IV secretion system reveals protein subassemblies. *Proceedings of the National Academy of Sciences of the United States of America*. 99 (17). p.pp. 11493–11500.

Winans, S.C. & Walker, G.C. (1985a). Conjugal transfer system of the IncN plasmid pKM101. *Journal of Bacteriology*. 161 (1). p.pp. 402–410.

Winans, S.C. & Walker, G.C. (1985b). Identification of pKM101-encoded loci specifying potentially lethal gene products. *Journal of Bacteriology*. 161 (1). p.pp. 417–424.

Wozniak, R.A.F. & Waldor, M.K. (2010). Integrative and conjugative elements: mosaic mobile genetic elements enabling dynamic lateral gene flow. *Nature reviews Microbiology*. 8 (8). p.pp. 552–563.

Yeo, H.J., Savvides, S.N., Herr, A.B., Lanka, E. & Waksman, G. (2000). Crystal structure of the hexameric traffic ATPase of the Helicobacter pylori type IV secretion system. *Molecular cell*. 6 (6). p.pp. 1461–1472.

Yeo, H.J., Yuan, Q., Beck, M.R., Baron, C. & Waksman, G. (2003). Structural and functional characterization of the VirB5 protein from the type IV secretion system encoded by the conjugative plasmid pKM101. *Proceedings of the National Academy of Sciences of the United States of America*. 100 (26). p.pp. 15947–15952.

Zhang, G., Gurtu, V. & Kain, S.R. (1996). An enhanced green fluorescent protein allows sensitive detection of gene transfer in mammalian cells. *Biochemical and biophysical research communications*. 227 (3). p.pp. 707–711.

Zhu, B., Cai, G., Hall, E.O. & Freeman, G.J. (2007). In-fusion assembly: seamless engineering of multidomain fusion proteins, modular vectors, and mutations. *BioTechniques*. 43 (3). p.pp. 354–359.